CFD Analysis of Pharmaceutical Water Distribution Systems
T-Junctions

By

Salem Elmaghrum

Thesis presented at Dublin City University in fulfilment of the requirements for the Degree of Master of Engineering

Under the Supervision of
Dr. Brian G. Corcoran

School of Mechanical and Manufacturing Engineering
Dublin City University
Ireland

January 2006

Preface

Declaration

I hereby certify that the material, which I now submit for assessment on the programme of study leading to the award of Degree of Master of Engineering, is entirely my own work and has not been taken from the work of others save and to the extent that such work has been cited and acknowledged within the text of my work.

Signed: _____.

ID No: 53135121 .

Date: 08.02.2006 .

Acknowledgments

I would like to dedicate this thesis to the soul of my late father.

I gratefully express my deep and sincere gratitude to my supervisor, Dr. Brian Corcoran. His wide knowledge and his logical way of thinking have been of great value to me. His feedback, encouragement and personal guidance have contributed greatly to this thesis.

I also want to thank my parents, who taught me the value of hard work by their own example. I would like to share this moment of happiness with my mother, brothers and sisters. They rendered me enormous support during the whole tenure of my research. I will always remember their encouragement and the motivation they offered me.

During this work I have collaborated with many colleagues, friends and technicians for whom I have great regard, and I wish to extend my warmest thanks to all those who have helped me with my work.

The financial support of the Libyan government is gratefully acknowledged.

Finally, I would like to thank all whose direct and indirect support helped me complete my thesis.

Abstract

High pure water systems are used in pharmaceutical and chemical industries. Dead-legs are generally found at points of use in distribution systems. The FDA suggests that the 6D rule is sufficient to help prevent microbial contamination, due to stagnant water within the dead leg. However, more recently, industrial experts are designing systems with dead legs limited to 3D or less.

The aim of this study is to examine the effects of entry length, drop loop bends, dead-leg length and mainflow velocity on flow patterns within a branch of a 50:50 mm equal tee. A 2D CFD analysis was carried out on a range of dead-leg configurations and the resulting data presented highlight the overall flow patterns with each branch. A rig was modified to carry out the dye injection tests, to verify CFD results.

It was found that the entry length had a little effect on the flow velocity of the dead-leg branch. However, when a bend was incorporated in the system, the entry length increase improved the flow patterns of all dead-leg branches. Different combinations of mainflow velocities, dead-leg lengths and length extensions were evaluated to investigate their effect on the flow pattern. It was observed that high mainflow velocities yielded better flow patterns in 2DL and 4DL when compared with 6DL. High mainflow velocities resulted in good flow patterns at only 2DL. At low mainflow velocities, 4DL and 6DL had better flow patterns compared with 2DL. Increasing the length of the extension resulted in better flow patterns in 6DL. At both, high and low mainflow velocities, 4DL sowed a reasonable flow pattern in the branch. Flow visualization studies were performed as well as a CFD simulation. The results of both studies were in good agreement in the case of 4DL branch length. However, for 2DL, an accelerated dye dispersion was observed, suggesting a higher fluid exchange between the mainstream flow and the branch.

Table of Contents

List of Figures

List of Tables

NOMENCLATURE

CFU	Coil Forming Unit
WFI	Water For Injection
GPH	Gallons per Hour
USP	United States Pharmacopoeia
DI	Deionised Water
CFD	Computational Fluid Dynamics
LDA	Laser Doppler Anemometry
PIV	Particle Image Velocimetry
RO	Reverse Osmosis
CDI	Continuous Deionisation
LVP	Large Volume Parenterals
CFR	Code of Federal Regulations
GMP	Good Manufacturing Practice
cGMP	Current Good Manufacturing Practice
FDA	Food and Drug Administration
PI	Pressure Indicator
FCV	Fluid Control Valve
CIP	Cleaning in Place
SIP	Steam in Place
K	Turbulent Kinetic Energy
ε	Dissipation Rate
μ_t	Turbulent Viscosity
P	Pressure
Re	Renolds Number
I	Turbulent Intensity
l	Turbulent Length Scale
L	Characteristic Length
Cf	Skin Friction Coefficient
y	Distance in the y-plane
x/D	Normalised Distance in the x-direction
y/D	Normalised Distance in the y-direction
ρ	Fluid Density
$\mu_t\left(\frac{\partial u_i}{dx_j}+\frac{\partial u_j}{dx_i}\right)$	Rate of Deformation of a fluid element
$\frac{\partial}{\partial t}(\rho k)$	Rate of change of K
$\frac{\partial}{dx_i}(\rho u_i k)$	Rate of transport of K by convection
$\frac{\partial}{dx_i}\left(\frac{\mu_t}{\rho_k}\frac{\partial k}{dx_i}\right)$	Rate of transport of K by diffusion
G_k+G_b	Production terms

k	Von Kormans Constant = 0.42
E	Empirical Constant = 9.81
Up	Main Fluid Velocity at point P
kp	Turbulent Kinetic Energy at point P
yp	Distance from point P to the wall
μ	Dynamic Viscosity
τ_w	Wall Shear Stress
y_v	Viscous sublayer thickness
v	Kinetic Viscosity

Chapter One
Introduction & Literature Survey

CHAPTER 1. INTRODUCTION AND LITERATURE SURVEY

1.1- Overview of pharmaceutical waters

Modern pharmaceutical industries require high grades of purified water. While domestic consumers would consider tap water to be "pure'', this water would be considered grossly contaminated in the pharmaceutical industry. Purified water is critical in virtually all applications in today's pharmaceutical plants [1]. The "grossly contaminated" water contains impurities whose removal or reduction is required for pharmaceutical water manufacture. Certain impurities require removal or reduction in order to conform to the United States Pharmacopoeia (USP) stipulations. Others must be eliminated because their presence may be harmful to the water purification system or production process. However, various impurities may be tolerable in a specific application. An unnecessary expense can be incurred if an impurity whose presence would be acceptable for a given system is removed. As a consequence, different grades of water may be specified for pharmaceutical applications. Each is defined by the concentration limits of specific ingredients, as required for particular applications.

Understanding the process of water treatment requires knowledge of chemistry, physics, and microbiology and also fluid mechanics, materials, and instrumentation [2]. Figure 1.1 illustrates a typical pharmaceutical high purity water system.

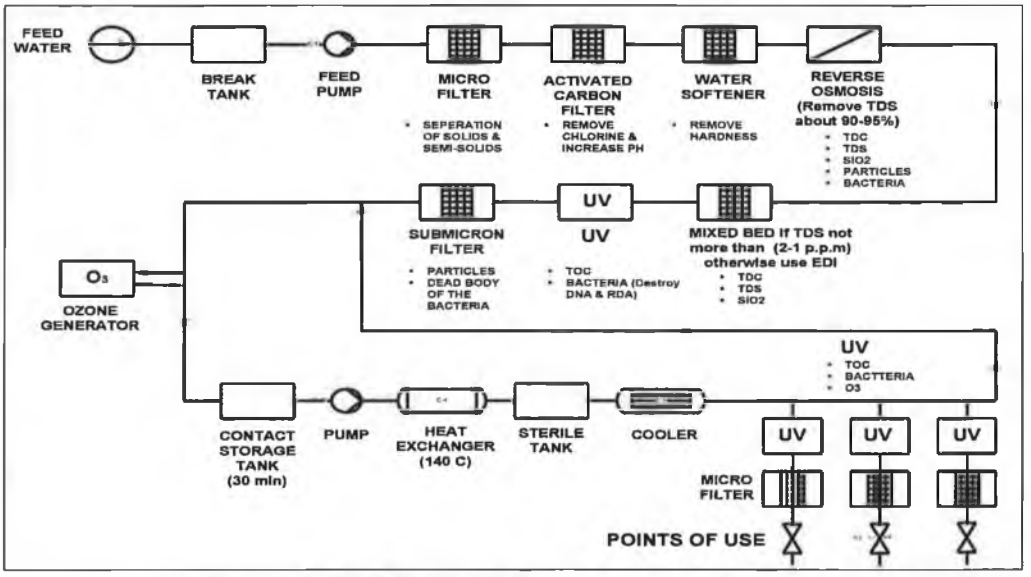

Figure 1. 1: A Typical Pharmaceutical Water Systems

1.2- Water Impurities

Waters encountered in nature are not of ultimate purity. They contain variously leached and dissolved materials and salts. For example runoffs or streams have picked up various impurities, including organic materials such as, salts, colloids, and various other soil constituents. Natural waters also nurture organisms such as bacteria and viruses [3]. Unlike other raw materials, the raw water supply varies in quality from one geographical region to another. Its chemical and physical make-up is very site specific in that it reflects the local geology and topography as modified by human activities, such as housing, agriculture, and industry. For instance, water derived from an upland source usually has a low Total Dissolved Solids (TDS) content, but a high concentration of organic contamination. It is also a relatively soft water. By contrast, water derived from an underground source generally has a high TDS content, but a low organic content. This water also has a high hardness level [3]. Due to this raw water quality variety, it can be said that there is no single water purification scheme that will cover all raw water. The treatment and equipment necessary to convert natural water to purified water is all site specific [4].

The major categories of impurities found in raw water include;

- Suspended particles
- Dissolved inorganic salts
- Dissolved organic compounds
- Micro-organisms
- Pryogens
- Dissolved gasses

Suspended matter in raw water includes silt, pipework debris, and colloids. Colloids are particles that are not truly in solution or suspension, and they may give rise to haze or turbidity. Suspended particles can foul reverse osmosis membranes and also interfere with the operation of meters and valves.

Dissolved inorganic substances include salts such as calcium, magnesium, chlorides and sulphates. Calcium and magnesium cause "temporary hardness" while chlorides and sulphates give rise to "permanent hardness".
Other dissolved inorganics include carbon dioxide, sodium salts, ferrous and ferric ions, aluminium, phosphates, and nitrites.

Organic impurities arise from the decay of vegetative matter. These include fats, oils, and solvents and residues from pesticides and herbicides. Water borne organics may also include compounds leached from pipework, tanks and purification media.

Surface water contains a variety of organisms including amoebae, bacteria, paramecia, and algae. Bacteria are kept at low levels by the introduction of chlorine or disinfectants, however once these disinfectants are moved in the purification process, the bacteria are again free to grow. Bacteria are therefore the chief micro-organism that are of concern in water purification systems.

Pryogens are the cellular fragments of bacterial cell walls, and are very dangerous in pharmaceutical waters as they can cause fever in mammals if they are contracted.

Oxygen and carbon dioxide are two gases most commonly found in natural waters [5].

1.3- Water Types

The United States Pharmacopoeia Convention (USPC) is a private non-profit organization that sets the standards for drugs, medical devices and diagnostics. It subsequently sets the standards for purified water in the pharmaceutical industry. The USP defines several types of water including; purified water, water for injection (WFI), sterile water for injection, sterile water for inhalation, and sterile water for irrigation. However there are two basic types of water preparation that we are concerned with, WFI and Purified Water. These two waters are quite similiar, except for the fact that WFI has more strict bacterial count standards than purified water, and must also pass a bacterial endotoxin test. Preparation methods are very similar.

However, WFI preparation must incorporate distillation or double pass reverse osmosis.

The source water that is supplied to the purification system for preparation of USP water must firstly comply with drinking water standards, as set out by international regulations [6]. The bacterial limits as set out by the USP in regard to colony forming units (cfu) can be seen in table 1.1.

Water Type	**USB Bacterial Limit**
Water for injection	10cfu/100ml
Purified Water	100cfu/ml
Drinking Water	500cfu/ml

Table1. 1: USP Bacterial Limits for Pharmaceutical Water [7]

Guidance on establishing specifications for purified water is provided in the USP monographs. The official monograph requirements for purified water stipulate that "Purified Water",

- Is obtained from water complying the "US Environmental Protection Agency National Primary drinking Water Regulations, or comparable regulations of the European Union or Japan, and will be referred to subsequently as Drinking Water"
- Contains no added substances
- Is obtained by a suitable process
- Meets the requirements for Water Conductivity
- Meets the requirements for TOC

The official monograph requirements for WFI stipulate that "Water For Injection",

- Meets all the requirements for purified water
- Is obtained by a suitable process and purified by distillation or reverse osmosis
- Meets the requirements of the bacterial endotoxin test and contains not more than 0.25 USP EU/ml (Endotoxin unite per ml)
- Is prepared using suitable means to minimize microbial growth [8].

1.4- CGMP, Current Good Manufacturing Practices

In addition to specifying the means of pharmaceutical water preparation to comply with USP, the FDA (Food and Drug Administration) requires that the process be carried out in conformity with current good manufacturing practices (CGMP). The CGMP requirements are intended to provide assurances that drugs are manufactured under systems and procedures such that the products will have the quality, purity, safety, identity and strength that they are labeled or supposed to possess [9]. These are more often than not referred to as Good Manufacturing Practices, GMP.

The terms "CGMP" and "GMP" are interchangeable. According to Celeste (1995) the FDA views the CGMP regulations to be very general in their nature. They require manufacturers to establish programmes to maintain the drug quality, but they generally leave the content of those programmes to the discretion of the manufacturers. Therefore there are a number of different ways in which a manufacturer may comply [10].

The FDA has established a number of CGMP's that relate to the preparation of pharmaceutical water. Listed below are examples of the types of GMP's that have to be adhered to,

A) Plumbing: drinking water shall be supplied under continuous positive pressure in a plumbing system free of defects that could contribute contamination to any drug product.

B) Filters: filters used for liquid filtration in the manufacture, processing, or packing of injectable drug products intended for human use shall not release fibres into such products.

C) Water and liquid-handling equipment

   Filters may not be used at any point in the water for manufacturing or final rinse piping system.

   Backflows of liquids shall be prevented at the interconnection points of different systems.

   Pipelines for the transmission of water for manufacturing or final rinse and other liquid components shall be sloped to provide for complete draining.

Pipelines for transmission of water for manufacturing or final rinse and other liquid components shall not have an unused portion greater in length than six diameters of the unused measured from the axis of the pipe in use. Backflows of liquids shall be prevented at points of interconnection of different systems.

The GMP's listed here are just an example in a very long list as set out by the FDA. The FDA has an ongoing and evolving understanding of what pharmaceutical water systems require and hence, since their promulgation, several GMP's have undergone some modification in practice [11].

1.5- TOC, Conductivity, and Enotoxin Levels

Total Organic Carbon (TOC) analysis is used to establish the amount of organic compounds in purified water, medical device extracts, or rinses. TOC analysis is used to determine if purified water meets the specifications according to the United States Pharmacopeia (USP). TOC is an indirect measure of organic molecules present in pharmaceutical waters measured as carbon. Organic molecules are introduced into the water from the source water, from purification and distribution system materials, and from biofilm growing in the system. Organic matter affects the biogeochemical process, nutrient cycling, biological availability, chemical transport and interactions. It also has direct implications in the planning of waste water treatment and drinking water treatment, and subsequently affects the preparation of purified water. TOC consists of thousands of components, including macroscopic particles, colloids, dissolved macromolecules, and specific compounds. The acceptable TOC level is set at 500ppb (parts per billion) as set out by the USP [12].
Conductivity is a measure of the electrical current in water that is promoted by ion formation. Gases can dissolve in water and interact to form ions. Intrinsic ions, such as those formed by carbon dioxide, affect the conductivity of the water. Extraneous ions like the chloride and ammonium ions also impact the chemical purity of water.
The combined conductivities of the intrinsic and extraneous ions act as a function of pH and are the basis for the conductivity specifications set out by the USP. As outlined in Table 1.2, conductivity testing is carried out in three stages.

Table 1.2 below describes these stages.

Stage	Method of Measurement	Acceptance Criteria
One	Use in-line or grab samples, and measure the conductivity and operating water temperature	Use the stage 1 Table 1.3 to determine the conductivity limit
Two	Re-test at least 100ml of the stage 1 grab sample for conductivity after vigorous mixing and temperature normalization to 25◦C	When the change does not exceed a net of 0.1 µS/cm over 5 minutes, measure the conductivity. Again use Table 1.3 to determine the conductivity limit
Three	If stage 2 test does not meet the requirements, re-test the sample within 5 minutes while maintaining temperature. Add 0.3ml per 100ml of saturated potassium chloride solution and determine the pH to the nearest 0.1pH unit.	Use the stage 3 Table 1.4 to determine the conductivity limit

Table1. 2 : Three-Stage Conductivity Testing [13]

If the best conditions and conductivity limits are met at either of the preliminary stages, the water meets the requirements of the test and the third stage in which the pH is measured is unnecessary. Tables 1.3&1.4 show the specifications for water conductivity.

Temperature	**Conductivity (µS/cm)**
0	0.6
10	0.9
20	1.1
30	1.4
40	1.7
50	1.9
60	2.2
70	2.5
80	2.7
90	2.7
100	3.1

Table1. 3: Temp &Conductivity requirements [8].

pH	**Conductivity (µS/cm)**
5	4.7
5.2	3.6
5.4	3
5.6	2.6
5.8	2.4
6.0	2.4
6.2	2.5
6.4	2.3
6.6	2.1
6.8	3.1
7	4.6

Table1. 4: pH & Conductivity requirements [8].

An endotoxin is a poisonous substance or toxin produced by micro-organisms that is not secreted into the surrounding medium but confined within the microbial cell and released when the micro-organism dis-integrates. An endotoxin is quite stable both physically and chemically and is not destroyed by temperatures used to kill the bacteria themselves. Endotoxin is present in municipal water in the range of 10 to 50 EU/ml. The USP sets the requirements for endotoxin levels to be ≤ 0.25 EU/ml.

1.6- Pre-Treatment of Water

The preparation of water for the pharmaceutical industry is generally carried out in three steps; pre-treatment, principle purification, and polishing or point-of-use treatment.

In order for the principle purification process to be rendered practical in the economic sense, pre-treatment of source water is always required. In fact, the pre-treatment stage enhances and improves the service life of the principle purification equipment. Pre-treatments generally deal with higher levels or quantities of impurities. The USP stipulates that pharmaceutical waters must be derived from sources suitable in their quality for drinking water. There is no unique or definite pre-treatment process that is suitable for all locations. As already stated, the treatment and equipment necessary to convert natural water to purified water is all site specific. The following process may be used in pharmaceutical water pre-treatment [**Error! Reference source not found.**].

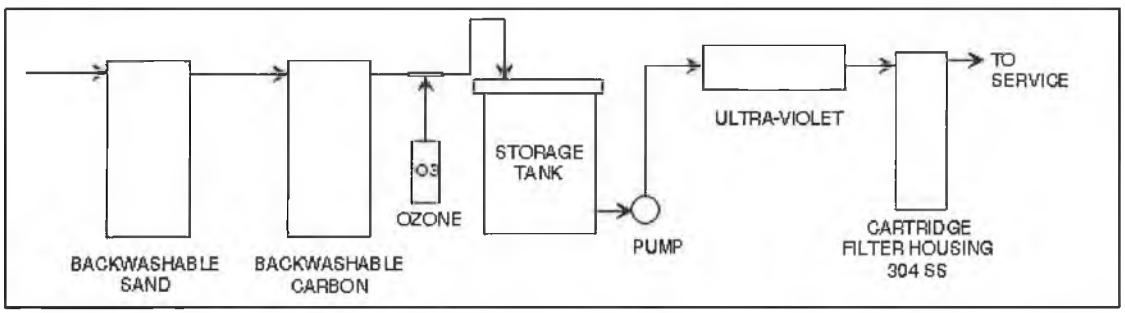

Figure 1. 2: Pre-Treatment Process [15].

1.6.1- Chlorine Treatment

Water is chlorinated to control the microbial growth. Where municipal water supplies are used, the water is usually already chlorinated. However, it is often common practice to add more chlorine to bring the water up to the plant's stipulated level. Chlorine is usually added to the water supply until a residual concentration of 0.5 to 2ppm (parts per million) is achieved [16]. However, on occasion an initial chlorine quantity of 50ppm can be added as a shock treatment. This process is referred to as hyperchlorination.

For larger installations, chlorine is generally added to water as a gas, stored in cylinders under pressure. Smaller chlorination relies on 'active' chlorine to be added to the water either by metering pumps or by being periodically batch-fed. The presence of the chlorine residual is usually retained as long as possible within the water stream as it undergoes processing. In order to provide a bacteriostatic umbrella against the ever present threat of microbial growth it is then treated to get rid of its suspended solids [**Error! Reference source not found.**].

1.6.2- Deep Bed Filtration

Sand bed filters are used to remove the total suspended solids in the preparation of pharmaceutical waters. Deep bed filters must prevent the passage of the suspended matter and must also be capable of accommodating a reasonable volume of suspended materials. The deep bed filters are contained within a steel pressure vessel and are coated to withstand the corrosive effects of the water and resist the abrasive effects of the sand particles that constitute the bed. The coating is usually epoxy resin or PVC. The sand overlies a layer of gravel, which usually consist of several layers of different sizes. Deep bed filters themselves serve as havens where organisms can proliferate. Water is therefore always chlorinated before it enters the deep beds, and this in turn ensures that the beds are sanitized [**Error! Reference source not found.**].

Figure 1. 3: Deep Bed Filter [19]

Deep bed filters have a finite capacity for removing contaminants from water and therefore require periodic regeneration. There are four stages in the regeneration process; backwash, brine injection, slow rinse and fast rinse. At the backwash stage, feed water passes in the opposite direction through the resin of sand.

The resin becomes fluidized and expands, releasing any contaminants. After the resin has settled, the brine injection (sodium chloride) takes places. It passes through the resin in the normal service flow direction but passes to the drain. This removes the contaminants exchanged by the resin during normal service and replaces them with fresh chlorides. During the slow rinse stage water again passes through the resin in the normal service flow direction. This displaces most of the brine in the vessel. The fast rinse then follows, where water passes though the resin but at a greater flow rate. This removes any traces of the brine and again flows to the drain.

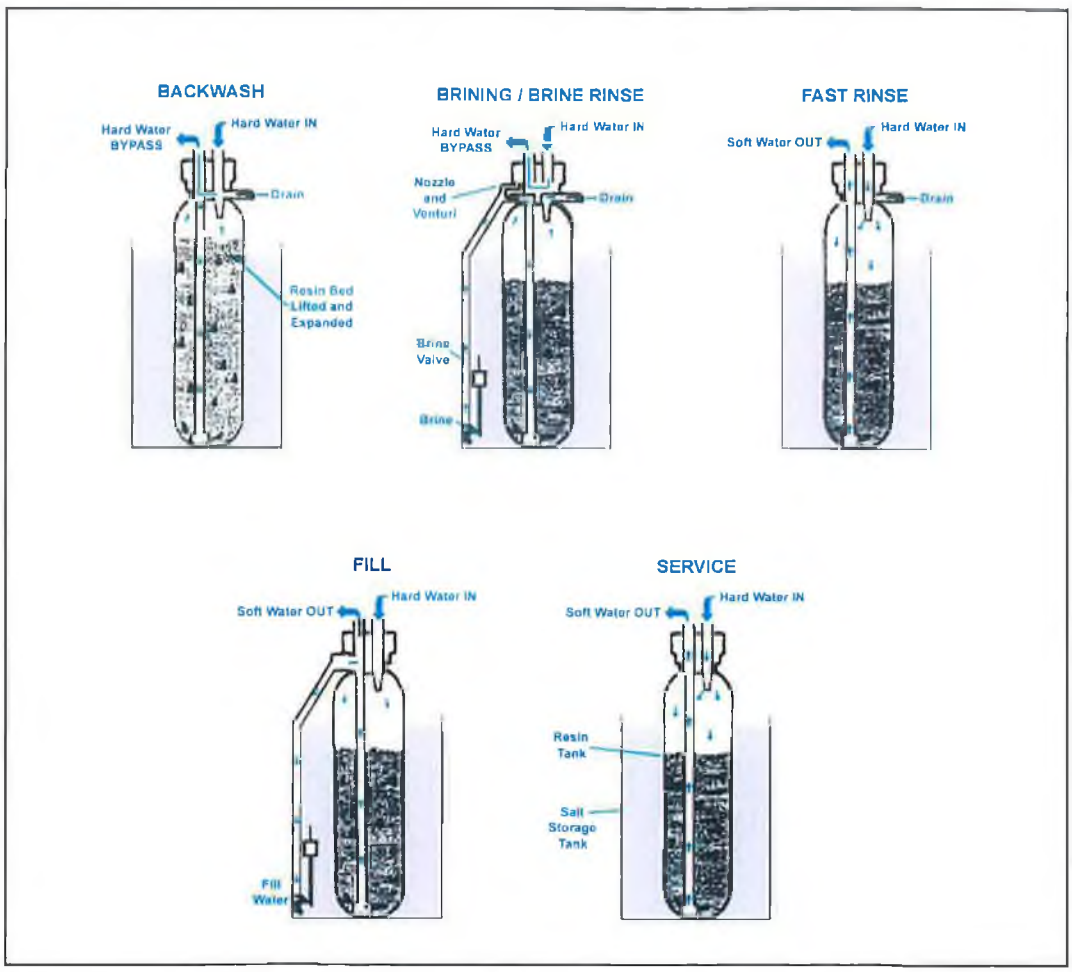

Figure 1. 4: Regeneration Process [20].

1.6.3- Water Softening

Water softening re-treatment generally precedes de-chlorination of feed-water in order to extend the biological action of chlorine throughout the softening process. However there are some that prefer to remove the chlorine prior to water softening in order to avoid a resin loss through reaction with chlorine.

Softening is a way of removing calcium and the other elements that creates hardness of water, which can scale up reverse osmosis membrane. It also removes aluminium, copper, and other troublesome trace metals.

There are two general methods of water softening. The first involves the precipitation of calcium and magnesium in their carbonate and hydroxide forms, respectively, by the use of calcium hydroxide and sodium carbonate. This is called the lime-soda process and it reduces the water hardness by about one third. The addition of lime (calcium hydroxide) and soda ash (sodium carbonate) reduces water hardness. However, despite the economy of this operation, the lime-soda process of hardness removal by precipitation is declining in use. Overall it increases the TDS content of the water, and it requires much floor space. The second method is by the removal of the objectionable ions by ion exchange. The objectionable calcium and magnesium ions can be removed by ion exchange reactions. The softeners contain a strong cation exchange resin in its sodium form and as the water passes through it, the calcium and magnesium ions are replaced by sodium ions, thereby removing the water hardness [**Error! Reference source not found.**].

The TDS remains unchanged with this process. As with the deep bed filters the water softeners have a finite capacity and therefore undergo the same regeneration process.

1.6.4- Chlorine Removal

The chlorine residue is retained as long as possible in order to discourage organism growth. However, it must be eventually removed as it can be harmful to RO (reverse osmosis) membranes and it can corrode and stress-crack stainless steel stills. Beds of activated carbon are widely used to remove chlorine from the water by the process of adsorption. In pharmaceutical usage, carbon beds are replaced when they experience excessive particle shedding, or when the bacterial counts in the effluent from the beds cannot be controlled by appropriate means of sanitizing (hot water or steam). Carbon beds inevitably nurture bacteria in the bed regions below those where the chlorine is absorbed. The deep carbon beds are, in effect, depth-type filters. Thus they accumulate particulate matter and in time develop increasing pressure drops. This necessitates their being cleansed by backwashing. [22] Chlorine can also be eliminated by reduction reactions involving sulphites, bisulphites, or metabisulphites. This action is often recommended as an avoidance of the problems associated with carbon beds, particularly with their sanitization. Injection of a

reducing agent in the water stream requires very little equipment, usually a pulse-speed metering pump. The capital cost of this de-chlorination method is therefore extremely low. However there is an ongoing expense of chemical procurement.
Also, the mixing of reducing agents in water produces hazardous gasses. Another disadvantage of utilization of reducing agents for de-chlorination is the promotion of growth of certain organisms that thrive in a reduced environment. Therefore, when utilizing a reducing agent, the dose must be kept as low as possible to minimize proliferation of these organisms [22]. As an overview it can be stated that the installation of a carbon bed to remove chlorine requires an initial capital expenditure, while the cost of bisulphate addition lies in its maintenance. Presently about 30% of chlorine removal is accomplished by using sodium bisulphate or one of like-acting chemical relations.

1.6.5- Acidification/Degasification

Acidification and degasification are methods used for removing scale forming components in the pre-treated water. The acidification/degasification process occurs when the incoming water is acidified before the reverse osmosis units and degasifier is then used to remove residual carbon dioxide created by the acidification process. In this pre-treatment process the pH of the incoming water is adjusted with the addition of sulphuric acid. This acidified water is then sent to the degasifier where the carbon dioxide is removed. A problem associated with the degasification process is that the potential for increasing microbial contamination is high. The degasifier should therefore be located where bacterial control measures are still available. It is therefore suggested to locate the degasifier between stages of a double pass reverse osmosis unit [**Error! Reference source not found.**].

1.7- Principle Purification

The principle purification stage includes processes such as ion exchange, reverse osmosis and distillation. In the case of WFI, distillation is seen as wasteful of energy costs, while osmosis is higher than ion exchange in its capital costs, but lower in chemical costs. Reverse osmosis is more demanding on feedwater pre-treatment than

ion exchange. Each process is described below so as to give a better understanding of its operation.

1.7.1- Ion exchange

Ion exchange ensures that purified water systems satisfy the conductivity requirements set out by USP. The use of de-ionising (DI) ion exchange beds may result in the bacterial contamination of their effluent waters. The beds are havens for the growth of organisms that enter with the feedwater. Thus DI beds can also serve as sources of endotoxins derived from waterborne organisms. Ion exchange therefore is not a USP approved methods for preparing WFI. It is instead used for the preparation of USP purified water. Typically the ion exchange process uses cation and anion ions in exchange for sodium, calcium and magnesium ions.

The individual cation exchange resin bed is the first ion exchange unit the water encounters. The cations, such as sodium and calcium are removed by exchange with hydrogen ions from the resin. The emerging solution is consequently acidic. The solution that emerges from the anion resin is basic [**Error! Reference source not found.**]. Use of separate beds for cation and anion resin provides extreme pH in the beds that helps retard bacterial growth. However, a single cation bed followed by a single anion bed does not provide very low conductivity water, due primary to sodium leakage. The addition of second cation bed (cation – anion - cation) can instead greatly reduce conductivity [22].

Figure 1. 5: Ion Exchange Equipment [24].

1.7.2- Reverse osmosis

Reverse osmosis offers a means of removing ionic components from their aqueous solutions. It also serves to remove most soluble organic compounds and to restrain the passage of insoluble particles, both viable and otherwise. In the pharmaceutical industry, reverse osmosis is designated by the USP as one of the methods permissible in the preparation of WFI.

Osmosis is the process that takes place when a solution is separated from a less concentrated solution by semi-permeable membrane. The membrane will allow water molecules to pass through, but not larger molecules, so that it can act effectively as a molecular filter. During osmosis the water molecules in the more diluted solution will migrate into the more concentrated solution equalizing concentration on both sides of the membrane. This migration can be stopped and reserved, by the application of a pressure gradient in opposition to the natural direction of flow. Thus, water molecules can be forced to immigrate from the more concentrated solution to the less concentrated solution. [25]

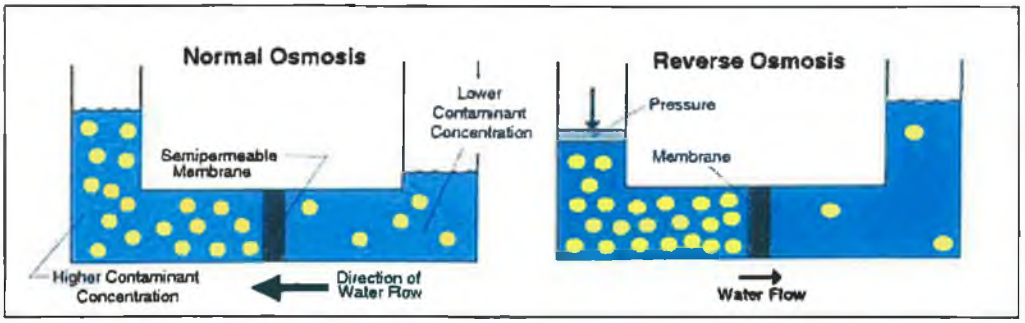

Figure 1. 6 : The Reverse Osmosis Processes [25]

Single stage systems are only capable of reducing contaminants by 90 to 95%, which does not meet the requirements for purified water treatment. Instead double pass reverse osmosis units are capable of producing water that meets the requirements of the USP for both TOC and conductivity [26]. The FDA requires that WFI being

prepared by reverse osmosis be the result of double pass units. The product water effluent from the first stage is used as the feed stream for the second stage. In such arrangements there is almost never a need to clean the second stage, and they can therefore be smaller. However if it is of the same size it can be used independently as a single stage if necessary. Figure 1.7 below shows a typical reverse osmosis system found in industry.

Figure 1. 7: Reverse Osmosis Equipment [27]

1.7.2- Distillation

Distillation is a process that relies on evaporation to purify water. The water is heated to form steam. In-organic compounds and large non-volatile organic molecules do not evaporate with the water and are left behind. The steam then cools and condenses to form purified water. This distillation equipment in its simplest form consists of a boiler within which the water is vaporized and a condenser in which the water vapour is condensed. The water is changed from a liquid to a gas by being heated, and reverts from gas to liquid through the application of cooling or heat removal. By undergoing the changes in its states of matter, water becomes separated from its non-volatile contents that cannot vaporize, and from its volatile components that cannot condense. [**Error! Reference source not found.**]

The water vapour is converted to the liquid state by encountering the cooling surface of the condenser. However, to permit the separation of the water in its gaseous state

from accompanying volatile contaminants, the cooling must be adequate but minimal. Higher degrees of cooling would encourage condensation of the volatiles as well. This means that the water exiting the condenser is still quite hot. This heat can be used to preheat the incoming feedwater to the still. Still design focuses on the economic reuse of this residual heat. The cost of heating the water is an important consideration in the distillation process [**Error! Reference source not found.**].

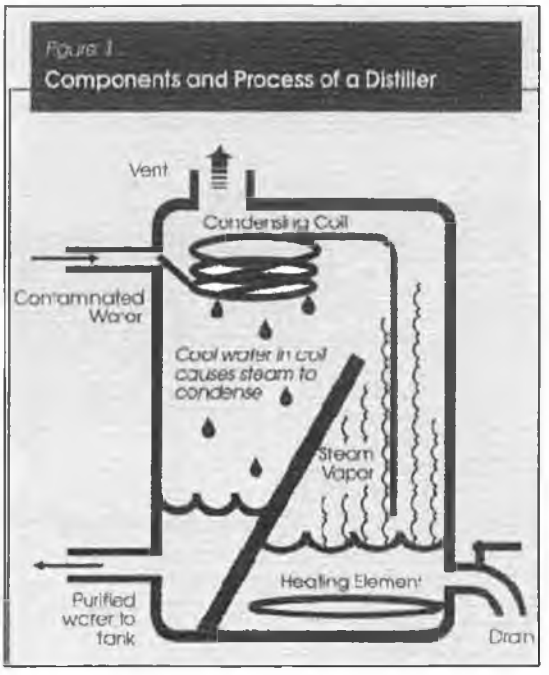

Figure 1. 8: The Distillation Process [29].

Neither reverse osmosis nor distillation can be relied upon automatically to guarantee the desired product quality independent of maintenance-free operation. Distillation is the favoured method because it involves evaporating the water. As a result the threat of organisms is eliminated, or at least sharply reduced. Distillation is seen as a self-sanitising process. Most thermophiles will not grow above **73° C** and most waterborne organisms are killed at **60° to 80° C**. Most pathogens will not grow above 50° to 60° C and vegetative organisms do not grow above 60° C. The FDA recognizes that water emanating from stills can be bacterial endotoxin free. However, still operations can be mismanaged and bacterial endotoxin may become entrained into the distillate [30].

In some cases where the bacterial endotoxin has been found downstream from stills, it was found to have been caused by carry-over in the water vapour. Although WFI needs to be sterile, it is accepted that use of stills according to manufacturer's instructions will yield sterile water. The finding of organisms or endotoxins in the water exiting from the still will be taken as evidence of a serious disfunction, irrespective of adherence to relevant good manufacturing practice (GMP) [**Error! Reference source not found.**].

1.8- Ozone and UV Radiation

The application of ozone to high purity water system offers advantages over chlorine as a disinfectant in that the removal of its residues do not depend upon the use of carbon beds. Instead ozone is readily destroyed by exposure to 254-nm UV light. The presence of ozone stored in waters may offer an alternative to storage at elevated temperatures (80°C). Also, being a strong oxidant it is useful in endotoxin destruction.

Additionally, ozone has a higher lethality co-efficient than chlorine against most organisms and readily destroys viruses. Ozone has a very short life span, and is referred to as a "half-life". The half-life of ozone is approximately 7 to 20 minutes. This means that half of the ozone created will break down and re-combine as oxygen each 7 to 20 minutes until all the Ozone is gone, depending upon temperature and the amount of contaminants in the water.

Inevitably, ozone comes to be compared with chlorine because of its use as a dis-infectant. The relatively short half-life of ozone means that significant concentrations of dissolved residuals may not endure over the reach of an extensive water distribution system. The micro-organism population, which was controlled up to that point, may begin to flourish again. On the other hand, long-lived chlorine may not be as fugitive as ozone. Chlorine is a stable compound and hence is not described by any half-life characteristic. However, once chlorine has served its purpose it is difficult to remove. Adsorptions by activated carbon or reaction with bisulphate (reducing) solutions are the usual means as described above, but each method has its complications. Because ozone can be easily removed by UV light, the application of

ozone can be found in-line. Multiple feed points can reinforce the ozone concentration throughout the system. The short half-life of ozone means that upon discharge, treated waters are less likely to be toxic to aquatic life. The decomposition of the ozone actually serves to increase the dissolved oxygen levels of the water. This is usually desirable, however increased corrosion may result [**Error! Reference source not found.**].

UV light is widely used in water purification systems for disinfections and TOC reduction. Use of UV for dechlorination is a relatively new process. UV light has long been known as a good energy source for breaking chemical bonds.

The capital cost of UV light for dechlorination is very close to that of properly designed carbon filtration system. There is an ongoing electrical cost with UV dechlorination. However, there is an extreme benefit in elimination of bacterial colonization ground. Furthermore, the water is given a very strong disinfection dosage that benefits downstream treatment systems [22]. The devising of effective UV systems requires careful engineering, however, more than a radiation source is needed. Removal of the UV-killed microbes is required by filtration. Placement of UV lights at numerous points in the water purification system is appropriate. Often UV placement on both the inlet and discharge of treatment device will significantly prolong the time between periodic sanitizations.

1.9- Storage and Distribution System

Generally a storage system is used to accommodate peak flow requirements against usage rates. It must maintain the quality of the feedwater and ensure that the quality remains constant at the points of use. Some purified water systems do not contain storage tanks, and instead run straight to the distribution loop. However, the presence of a storage tank is a better option as it allows a smaller and less costly pre-treatment system to be able to meet with peak demand. The main disadvantage of a storage tank is in the capital cost that is incurred, and also the costs associated with pumps, vent filters and instrumentation. Storage tanks also introduce a region of slow moving water, which can promote microbial growth [13].

Achieving an acceptable purified water distribution systems design is critical to success of the total project. Great expense is incurred in the purchase, installation and validation of purification equipment. The distribution system must therefore be capable of maintaining the generated water quality. Crucial design parameters include continuous recirculation at an adequate velocity, continuous sanitization and the absence of stagnant areas [33].

1.10- Sanitisation

Biofilm can be removed and/or destroyed by chemical and physical treatments. Chemical biocides can be divided into two major groups, oxidising and non-oxidising. Physical treatments include mechanical scrubbing and hot water. Unless water contains a continuous biocide like chlorine, a biofilm will develop on wetted piping surfaces in an automated watering system and high numbers of bacteria and may become present. Regular flushing will limit bacterial accumulation in an automated watering system, but no amount of flushing alone will totally eliminate biofilm [33].

There are two basic approaches for controlling bacterial growth in a water system. One is to maintain a residual level of biocidal agent within the system. This method is known as continuous dosing. This is similar to the common technique where municipal water treatment facilities inject enough chlorine into their treated water to provide a residual throughout the distribution system. In purified water systems, however, continuous sanitization is not permitted. These systems must therefore employ periodic cleaning and sanitizing instead of continuous dosing of a biostatic chemical.

The main physical sanitization treatment is heat treatment. WFI systems use recirculating hot water loops, greater then 80°C, to kill bacteria. According to Mittelman (1986), when these systems are used on continuous basis, planktonic bacteria are killed and biofilm development is reduced. However, biofilms are even found in hot water and periodic hot water sanitization can also be used to destroy bacteria in biofilm.

Bacteria associated with biofilms are much more difficult to kill and remove from surfaces than planktonic organisms. According to Characklis (1990), numerous investigators observed "a rapid resumption of biofouling immediately following chlorine treatment". Incomplete removal of the biofilm will allow it to quickly return to its equilibrium state, causing a rebound in total plate counts following sanitisation. Figure 1.5 below shows typical re-growth of bacteria following sanitization [34]. Initially, the bulk water bacteria count dropped to zero after sanitization, but this was followed by a gradual increase in numbers to levels at or below the pre-treatment levels.

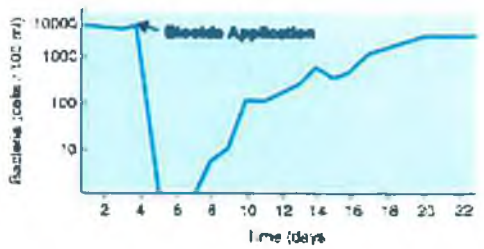

Figure 1. 9: Sanitization Followed By Biofilm Recovery [33].

1.11- Validation – URS, IQ, OQ, and PQ

Validation of a water system involves three distinct specifications, a user requirement specification (URS), a functional requirements specification and a design requirement specification. The URS defies the quality of water required and the type of pharmaceutical production process available, while the functional requirement specification describes how the water system operates.

Functional requirement specifications are used to identify the system capacity and whether or not it meets the specified chemical and microbial limits. Design requirement specifications detail how the system is built, and includes system components and materials of construction.

Each of the specification requirements mentioned here is linked to a validation qualification document. The design specification requirement is linked to an

installation qualification (IQ) document and details the physical configuration of the installed system. The operational qualification (OQ) document is developed from the functional requirement specification and details that system can operate within the design parameters. After successful completion of the IQ's and OQ's, the system's specified water quality is tested during a performance qualification (PQ). The URS serves as the basis for the development of the PQ [35]. Figure 1.10 below should give a better understanding of how the basis framework for the validation of water purification system actually works.

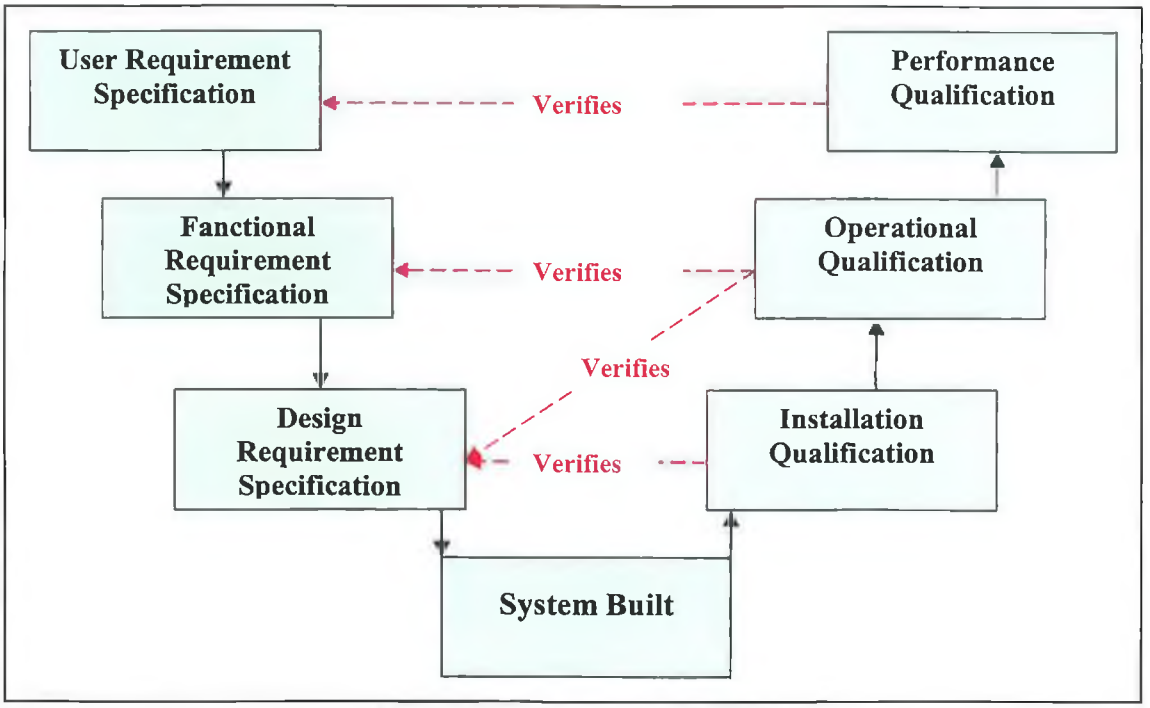

Figure 1. 10: Basic Framework Validation

1.12- Biofilm Development

Biofilm refers to a layer of living and dead micro-organisms, surrounded by the slime they secrete, that are attached to an inert or living surface. Simple examples of biofilm include plaque found on teeth, the gel-like film found on the inside of a flower vase, or the slime found on river stones. The presence of biofilm threatens the sufficiency of WFI or Purified Water. Biofilm development occurs in the following steps.

1.12.1- Surface Conditioning

Almost immediately after a clean pipe surface comes into contact with water, an organic layer deposits on the water/solid interface. These organics form a 'conditioning layer' that neutralizes the surface charge, which may repel approaching bacteria. The absorbed organic molecules may also often serve as a nutrient source for bacteria.

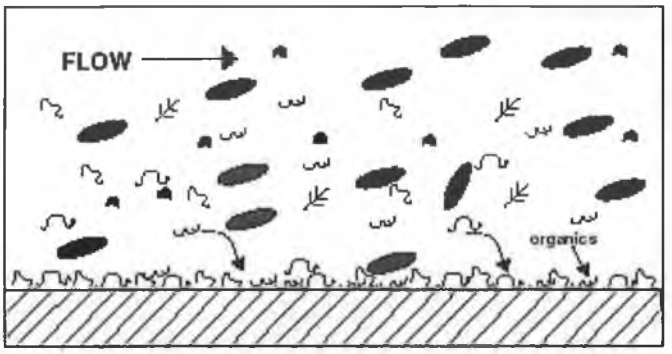

Figure 1. 11: Adsorption of organic molecules on a clean surface forms a conditioning film[36].

1.12.2- Adhesion of 'Pioneer' Bacteria

In a pipe of flowing water, some of planktonic (free floating) bacteria approach the pipe wall and become entrained within the boundary layer. The boundary layer refers to the laminar quiescent zone as the pipe wall flow velocity falls to zero. Some of these cells will collide and adsorb to the surface for some time, and will then become unadsorbed. This is referred to as reversible adsorption. Some of the reversibly adsorbed cells may then permanently adhere to the surface, and are then referred to as irreversibly adsorbed cells (Figure 1.12).

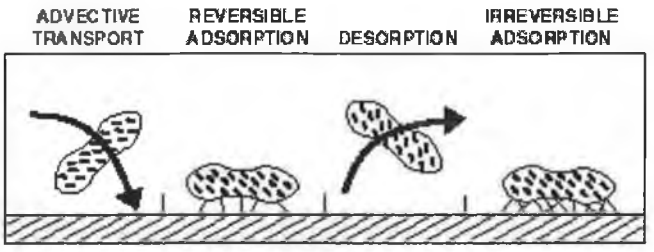

Figure 1. 12: Transport of bacteria cells to the conditioned surface, adsorption, desorption, and irreversible adsorption[36].

1.12.3- Glycocalyx or Slime' Formation

Biofilm bacteria excrete a sticky substance, which hold the biofilm together and cement it to the pipe wall. The biofilm also acts as an ion-exchange system that traps trace nutrients from the water. As nutrients accumulate, the pioneer cells reproduce. This process continues, which greatly increases the volume of the ion exchange surface and a thriving colony of bacteria is soon established.

Figure 1. 13: Biofilm is made up microbes and "spiders web" of extracellular polymers [36].

The mature biofilm is like a living tissue on the pipe surface. It is a complex metabolically co-operative community made up of different species. As the film grows to thickness that allows it to extend through the quiescent zone at the pipe wall into zones of more turbulent flow, some cells will be sloughed off. These cells can then colonise downstream [36].

1.13- Organisms and Their Control

The need to avoid the presence of impurities or microbes in pharmaceutical waters is quite obvious. Their presence in oral or topical formulations can cause infections, while their presence in injectable formulations can be fatal.

It is therefore necessary to design a purification system that will alleviate the problem of biofilm build-up in order to fulfill the requirements set out by the USP. The following considerations should be taken into account in the design of such a system;

- Pipe surface smoothness
- Water velocity
- Dead leg effects

1.13.1- Pipe Surface Smoothness

No surfaces are exempt from biofouling. In general, smooth surfaces foul at a slower initial rate than rough ones but biofilm formation is inevitable within a period of days. Smoother surfaces delay the initial build up of attached bacteria but they do not reduce the total number attached.

There is no universally accepted standard for surface finishing of stainless steel. Electropolishing is considered to be the best method for finishing for high purity water systems. Shown below are the roughness profiles of various stainless steel finishes used in water systems.

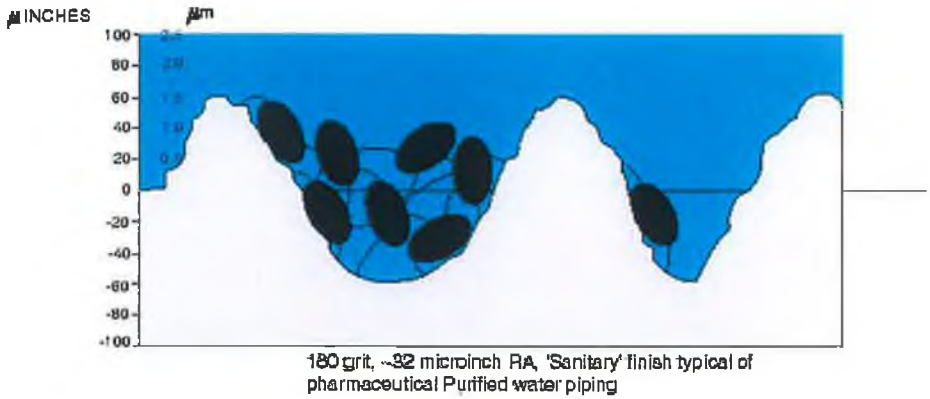

Figure 1. 14: Typical Finish for Purified Water [37].

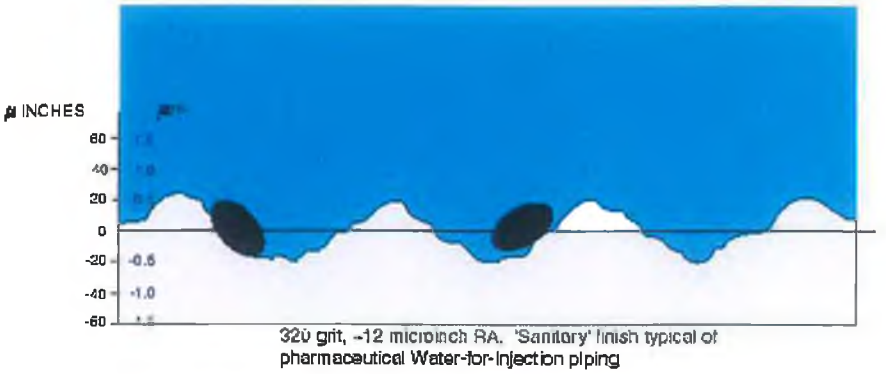

Figure 1. 15: Typical Finish for Water for Injection Piping [37].

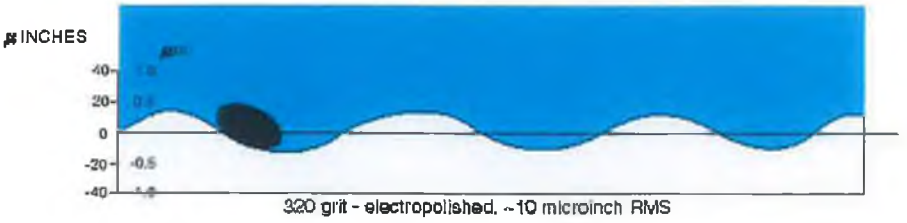

Figure 1. 16: Electro-Polished Finish [37].

1.13.2- Water Velocity

High water flow may alter biofilm growth but will not prevent the attachment of bacteria to pipe surfaces because of the following reasons:

1- Low flow in the boundary layer

Regardless of the water velocity, it flows slowest in the layer adjacent to pipe surfaces. Even when water flow in the center of the pipe is turbulent, the flow velocity falls to zero at the pipe wall. The distance out from the pipe wall in which flow rate is not turbulent is called the boundary layer or laminar sublayer. The thickness of the laminar sublayer was calculated by Pittner (1988) [38] for various flow velocities and for 5 size pipes (see following table). Pittner calculated that the shear forces within the laminar sublayer are much less than that required to dislodge a bacteria cell.

Laminar Sublayer Thickness (microns)[Pittner 1988]

Pipe Size	Velocity (ft/sec)					
	0.2	1.0	2.0	5.0	8.0	12.0
E.I. RDS 0.428"ID	*	*	125	55	37	26

1/2" Sch.80	*	*	136	60	40	28
1" Sch.80	*	265	146	65	43	30
2" Sch.80	537	291	158	69	46	32
3" Sch.80	563	305	165	74	48	33
4" Sch.80	582	312	170	75	50	34

* Flow may or may not be turbulent at these conditions
Current E.I. RDS flush velocity is approximately 2 ft/sec.

Table1. 5: Laminar Sublayer Thickness

2- Strong adhesion by exopolymers

In water systems with continuous high-velocity flow, the bacteria that accumulate in biofilm tend to be filamentous varities (like Pseudomonas) especially suited for attachment by filaments. The bacteria anchor themselves to the surface with their 'sticky' exopolymers.

The effects of fluid velocities on biofilm and their formation are still somewhat uncertain. However both the structure and induction time for biofilm formation have been found to be influenced by fluid velocity [McCoy&Costerton 1982; Corcoran 1996] [39&40]. For the test carried out, it was found that the induction phase for low velocity conditions was much lower than that of the high velocity conditions. At the lower velocities less shear forces permitted filamentous bacteria attachments to grow on a cleaner surface, while at the higher velocities the filamentous baceria became a permanent part of the biofilm only after the surface had acquired large amounts of extra-cellular material.

Although high flow velocity will not prevent the attachment of bacteria to pipe surfaces, it does have the following effects on biofilm structure.

1- Denser biofilm

According to Mittelman (1985) [41], "at higher rate flow rates, a denser, somewhat more tenacious biofilm is formed. As a result, these surfaces often appear to be free from foulants, since they are not slimy to the touch."

2- Limited biofilm thickness

The maximum thickness of the biofilm can be considered to be the thickness of the laminar flow layer. In a constant flow system, "an equilibrium thickness is reached which is dependent on water velocity and nutrients. Growth of the biofilm beyond the laminar layer will result in the release of blanktonic 'pioneer' cells that will, conditions permitting, establish the biofilm in another section of pipe."(Patterson 1991)[42] In systems that have fluctuating water flow, such as automated watering systems with periodic flushing, bacteria will be sloughed off during the flush. This results in random 'particle showers' of bacteria which can explain day-to-day fluctuations seen in total bacteria count results.

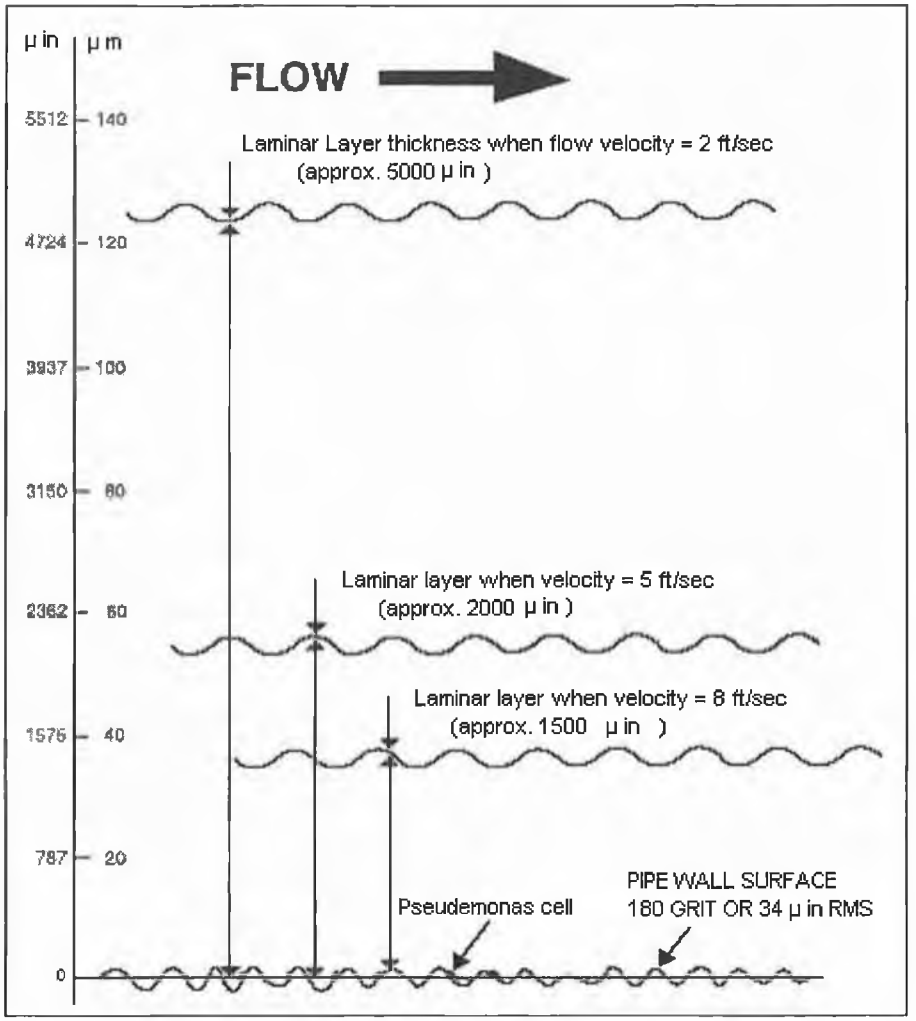

Figure 1. 17: The effect of flow velocity on the biofilm thickness of the pipe

1.13.3- Dead Leg Effects

A dead leg is any area in a piping system where water can become stagnant and where water is not exchangeable during flushing. Bacteria in dead-end pipe lengths and crevices are protected from flushing and sanitization procedures and can re-contaminate the piping system.

The formal definition of a pipe dead-leg as given by the FDA is; "Pipelines for the transmission of purified water for manufacturing or final rinse should not have an unused portion greater in length than 6 diameters (the 6D rule) of the unused portion of pipe measured from the axis of the pipe in use". The FDA suggests that the 6D rule is sufficient to help prevent microbial contamination, due to stagnant water within the dead leg. However, more recently, industrial experts are designing systems with dead legs limited to 3D or less [43].

Figure1.18 below illustrates a classic dead leg, e.g. configuration.

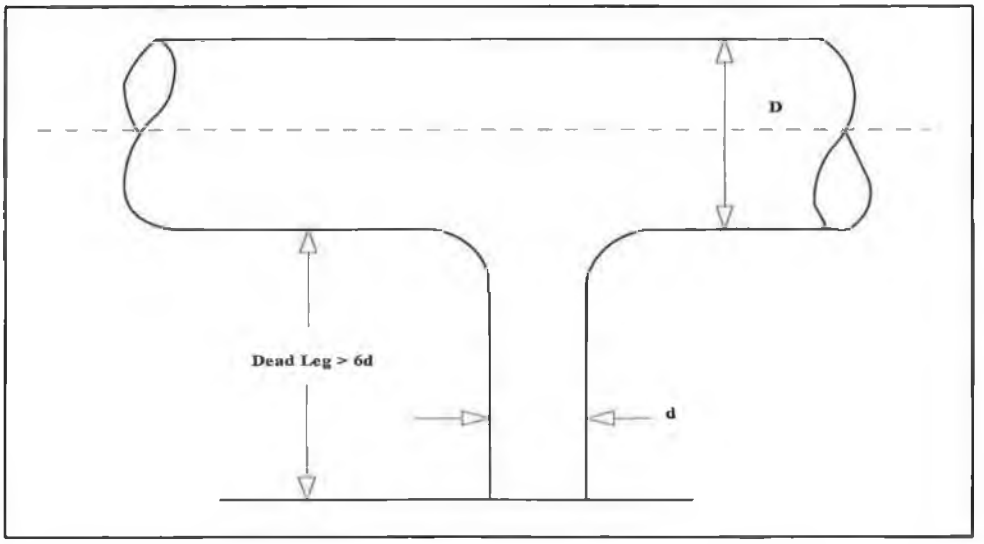

Figure 1. 18: Classic Dead Leg Configuration

Dead legs can occur in a number of areas in water purification systems. Filter housing, and various other fittings and instruments are susceptible to dead legs. However, the problem is most common in the distribution loop at the points-of-use. To overcome this, systems fittings have been designed with 'zero dead legs'. These are expensive pieces of equipment and it is not yet fully known if their inclusion in a

water purification system properly addresses the problem of microbial contamination.

Limited information is available on the effect of location of dead-legs within a rig main / distribution loop. The objective of this thesis is, through the use of 2D CFD modeling and flow visualization studies, to:

1) Examine flow patterns within a 50mm equal branch dead-leg.

2) Examine the effect of increased entry length on branch flow patterns.

3) Examine the effect of introducing a bend immediately before the dead-leg branch.

4) Examine the effect of a combined bend and entry length configuration.

5) Carry out flow-visualization studies on a glass tee dead-leg of 2D and 4D dead-leg length.

Chapter Two
CFD & Flow Theory

CHAPTER 2. COMPUTATIONAL FLUID DYNAMICS AND FLUID FLOW THEORY

2.1 Computational Fluid Dynamics and Computing

Computational Fluid Dynamics or CFD is the analysis of systems involving fluid flow, heat transfer and associated phenomena by means of computer based simulation. The technique is very powerful and spans a wide range of industrial and non-industrial applications from lift and drag on aircraft to blood flow is arteries. From the early 1960's the aerospace industry had integrated CFD techniques into the design and manufacture of aircraft and jet engines. More recently these methods have been applied to design of internal combustion engines, gas turbines etc and CFD has become a vital tool in the design of industrial products and processes [44]

All CFD codes are structured around a numerical algorithm used to model fluid flow problems [45]. These codes irrespective of supplier contain three main elements: a pre-processor, a solver and a post processor.

1) Pre-processor: The pre-processor consists of the input of a flow problem to the CFD program by means of a user-friendly interface and the subsequent transformation of this input into a form suitable for the solver Activities at the pre-processing stage include definition of the geometry (the computational domain), grid generation, definition of fluid properties and specification of boundary conditions.

2) Solver: This is numerical method used to solve the flow problem. The solver is used to approximate the unknown variables by means of simple functions, to discretise by substitution these approximations into the governing equations and to solve the algebraic equations.

One of the best understood and most highly validated techniques is the Finite Volume Method [46] which is used by four of the five commercially available CFD codes namely FLUENT, PHOENICE, FLOW3D and STAR-CD. This numerical algorithm consists of the following steps:

- Integration of the governing equations of the flow field over the control volume of the solution domain.
- Discretisation of these integral equations into a system of algebraic equations.
- Solution of the algebraic equations by an iterative method.

3) Post-processor: This is a method of analyzing and presenting data computed by the solver. Modern post-processing may include grid display, velocity plots, contour plots, particle and animation.

2.2 Turbulence and CFD.

Turbulent flow is a highly complex phenomenon. Although researchers have studied the phenomenon for many years, it is not yet possible to characterize turbulence from a purely theoretical standpoint. Many important characteristics of turbulence are well-known and these include,

- Turbulence is time-dependent, three-dimensional, and highly non-linear.
- Fully-developed turbulent motion is characterized by entangled eddies of various sizes. The largest eddies arise from hydrodynamic instabilities in the mean flow field
- The largest eddies break down into smaller eddies which, in turn, break down into even smaller eddies. This process of eddy break-down transfers kinetic energy from the mean flow to progressively smaller scales of motion. At the smallest scales of turbulent motion, the kinetic energy is converted to heat by means of *viscous dissipation*
- The dynamic and geometrical properties of the largest eddies are closely related o the corresponding properties of the mean flow field.
- The time and length scales of the smallest turbulent eddies are many orders of magnitude greater than the time scales and free paths of molecular motion. As a result, the process of viscous dissipation are statistically independent of molecular motion.

- Turbulent motion is not a random phenomenon. As a consequence, turbulent fields posses definite spatial and temporal structures.

For computers to provide accurate and realistic simulations of flow processes they must be supplied with a set of instruction which embody the implications of the conservation laws of momentum, mass and energy. While reliable computer programs are available for two dimensional and some three dimensional flows particularly for laminar flow situations, the same is not generally true turbulent flow [47].

In principle there is no reason to adopt special practice for turbulent flow processes over laminar as the Navier-Stokes equations apply equally in both cases. The reason why this is not possible is that important details related to turbulent flow are small scale in character e.g. eddies responsible for the decay of turbulence in some flow problems are typically 0.1 mm. To accurately calculate the equations of motion for such eddies is beyond the capacity of existing computers. Speziale (1991)[48] states that the direct simulation of turbulent pipe flow at a Reynolds number of 500,000 requires a computer which is 10 million times faster than current generation supercomputers.

Fortunately there is no need for an engineer to consider the details of such eddies. They are primarily concerned with time-averaged effects even when the mean flow is unsteady. By predicting turbulent flow only on the time averaged properties of turbulence and since these vary gradually in space, no excessively fine grids are necessary. This avoids the need to predict the effects of each and every eddy in the flow field. Engineers and CFD users are almost always satisfied with information about the time averaged properties of the flow (mean velocities, mean pressures and mean stresses). The process of time averaging is not without its problems as it causes statistical correlation's involving fluctuating velocities to appear in the conservation equations. There is no direct way of knowing the magnitude of these terms and we must therefore approximate or 'model' their effects. The result of this approach has been the development and use of various 'models of turbulence'.

2.3 Turbulence Modeling

The crucial difference between visualization of laminar and turbulent flow is the appearance of eddying motions of a wide variety of length scales in turbulent flows. A typical flow domain of 0.1 by 0.1 m with a high Reynolds number turbulent flow may contain eddies down to 10 to 100um. Such eddies would require computing meshes of 10^9 to10^{12} points to accurately describe processes at all length scales [48].

The computing requirements for direct solutions of time averaged Navier-Stokes equations of fully developed turbulent flow must await major development in computer hardware. Meanwhile engineering require computational procedures which can supply adequate information about turbulent processes without the need to predict the effect of each and every eddy in the flow field [49]. They are almost always satisfied with information about time-averaged properties of the flow (mean velocity, mean pressure etc). In performing time averaging six additional unknowns are obtained, namely the Reynolds Stresses. The main task of turbulence modeling is to determine of the Reynolds Stress and other scalar transport terms.

A turbulence model is a computational procedure used to close the system of mean flow equations so that a variety of flow problems may be calculated. For a turbulence model to be useful in a general purpose CFD code it must have a wide field of use, be accurate, simple and economical to run. Large eddy simulations are turbulence models where the time-dependent flow equations are solved for the mean flow and the largest eddies and where the effects of the smaller eddies are modeled. This approach result in a good model of the main effects of turbulence, however the calculations are very costly and seldom used on industrial applications [50]. Of the classical turbulence models the Mixing length and k-ε models are presently by far the most widely used and validated. These models are based on the assumption that an analogy exist between the action of the viscous stresses and the Reynolds stresses on the mean flow [51].

2.3 The k-ε Eddy Models

In the *k*-ε eddy-viscosity models, the turbulence field is characterized in terms of two variables:

- Turbulent kinetic energy
- Viscous dissipation rate of turbulent kinetic energy, ε

The k-ε model is an eddy-viscosity model in which the Reynolds stresses are assumed to be proportional to the mean velocity gradient with the constant of proportionality being the Turbulent Viscosity μ_t [52]. This assumption, known as the Boussinesq hypothesis, provides the following expression for the Reynolds stresses

$$\rho u_i' u_j' = \rho \frac{2}{3} k \delta_{ij} - \mu_t \left(\frac{\partial u_i}{dx_j} + \frac{\partial u_j}{dx_i} \right) + \frac{2}{3} \mu_t \frac{\partial u_i}{dx_i} \delta_{ij}$$

Where '*k*' is the turbulent kinetic energy. The turbulent viscosity μ_t is obtained by assuming that it is proportional to the product of a turbulent velocity scale and a length scale. In the *k*-ε model, these velocity and length scales are obtained from two parameters: *k* the turbulent kinetic energy and ε the dissipation rate of *k*. The velocity scale is taken to be the $\sqrt{k}$ and the length scale to be $\frac{\sqrt{k^3}}{\varepsilon}$. Hence, μ_t is given by

$$\mu_t = \rho C_\mu \frac{k^2}{\varepsilon}$$

where C_μ is an empirically derived constant of proportionality (typically set to 0.09).

The value of *k and* ε are obtained by solution of the conservation equations:

$$\frac{\partial}{\partial t}(\rho k) + \frac{\partial}{dx_i}(\rho u_i k) = \frac{\partial}{dx_i}\left(\frac{\mu_t}{\rho_k} \frac{\partial k}{dx_i} \right) + G_k + G_b - \rho\varepsilon$$

$$\frac{\partial}{\partial t}(\rho \varepsilon) + \frac{\partial}{dx_i}(\rho u_i \varepsilon) = \frac{\partial}{dx_i}\left(\frac{\mu_t}{\rho_k} \frac{\partial \varepsilon}{dx_i} \right) + C_{1\varepsilon} \frac{\varepsilon}{k}\left(G_k + (1 - C_{3\varepsilon}) G_b \right) - C_{2\varepsilon t} \rho \frac{\varepsilon^2}{k}$$

In words these equations are:

The 'Rate of change of *k or ε*' plus 'Transport of *k or ε* by conduction' equals 'Transport of *k or ε* by diffusion' plus 'Rate of production of *k or ε* ' minus the 'Rate of destruction of *k or ε*'. The equations contain five empirical constants and the standard '*k-ε* model' employs values for these constant arrived at via comprehensive data fitting over a wide range of turbulent flows [53]:

$$C_{1\varepsilon} = 1.44 \qquad C_{2\varepsilon} = 1.92 \qquad C_{\mu} = 0.09 \qquad \sigma_k = 1.0 \qquad \sigma_e = 1.3$$

The *k-ε* model is the most widely used and validated turbulent model. It has achieved considerable success in modeling a wide variety flows without the need for case adjustment of the model constant. The model performs particularly well for confined flows which embrace a wide variety of industrial engineering applications.

ADVANTAGES

- Simplest turbulence model for which only initial and/or boundary conditions need to be supplied
- Excellent performance for a range of industrial applications
- Well established and the most widely validated of all models
- Economical.

DISADVANTAGES

- More expensive to implement than simpler mixing length models
- Poor performance in a variety of important cases
  1) Complex flows with large strains (swirling flows)
  2) Rotating flows
  3) Unconfined flows
- Isotropic description of turbulence

2.4 Standard Wall Functions

The standard wall functions available in FLUENT, are based on the work of Launder and Spalding [54]. These are the most widely used of wall functions and have been

validated on numerous industrial flows. The law-of-the-wall for mean velocities yields:

$$U^* = \frac{1}{k}\ln\left(Ey^*\right)$$

Where

$$U^* = \frac{U_P C_\mu^{\frac{1}{4}} k_P^{\frac{1}{2}}}{\frac{\tau_w}{\rho}}$$

$$y^* = \frac{\rho C_\mu^{\frac{1}{4}} k_P^{\frac{1}{2}} y_P}{\mu}$$

The logarithmic law for mean velocity is known to be valid for y^*>30-60. In FLUENT the log-law is employed when y^*> 11.225. When the mesh is such that y^*< 1.225 at the wall adjacent cells FLUENT applies the laminar stress-strain relationship,

$$U^* = y^*$$

2.5 Non-Equilibrium Wall Functions

In addition to the standard wall function a two-layer based non-equilibrium wall function is also available. The key differences between this and the standard wall functions are:

- Launder and Spalding's lag-law for mean velocity is sensitised to pressure gradient effects.
- The two-layer based concept is adopted to compute the turbulent kinetic energy in the wall neighboring cells.

The log-law for mean velocity sensitized to pressure gradient is given by:

$$\frac{\tilde{U}C_{\mu}^{\frac{1}{4}}K^{\frac{1}{2}}}{\frac{\tau_w}{\rho}} = \frac{1}{k}\ln\left(E\frac{\rho C_{\mu}^{\frac{1}{4}}K^{\frac{1}{2}}y}{\mu}\right)$$

Where

$$\tilde{U} = U - \frac{1}{2}\frac{dp}{dx}\left[\frac{y_v}{\rho k^{*}k^{\frac{1}{2}}}\ln\left(\frac{y}{y_v}\right) + \frac{y - y_v}{\rho k^{*}k^{\frac{1}{2}}} + \frac{y_v^2}{\mu}\right]$$

Where y_v is the physical viscous sublayer thickness and is computed from:

$$y_v \equiv \frac{\mu y_v^{*}}{\rho C_{\mu}^{\frac{1}{4}}K_p^{\frac{1}{2}}}$$

Where $y_v^{*} = 11.225$.

A summary of the performance of the *standard and non-equilibrium wall functions* is given in table 2.1 below.

Type of Function	Strengths	Weaknesses
Standard Wall Function	Robust Economical Reasonably Accurate Well Validated	Poor for low *Re* flows Does not account for pressure gradient
Non-equilibrium Wall Function	Pressure Gradient sensitive Accurate for -separation -reattachment -impignment	Poor for low *Re* flows Limited advantages with severe pressure gradients

Table2. 1 : Performance of the standard and non-equilibrium wall functions

2.6.1 Fluent CFD Software

FLUENT has become one of the market leaders in commercial CFD software. Its broad spectrum of modeling capabilities has been applied to various disciplines, from chemical, biomedical to even meteorological analysis.

Fluent Inc., describe their package as a "finite volume method based solver for compressible/ incompressible and laminar/ turbulent flows that include chemical reactions, multiple phases and that transfer" [55]. The finite volume method is a numerical algorithm consisting of the following steps [56]:

- Integration of governing equations of fluid flow over all control volumes of the solutions domain.
- Conversion of integrals into algebraic equations by substitution of finite-difference approximations for the terms of the integrated equations representing flow parameters such as convection, diffusion and flow sources.
- Solving the algebraic equations by an iterative method.

Figure 2.1 describes the architecture of fluid analysis modelling using CFD simulation.

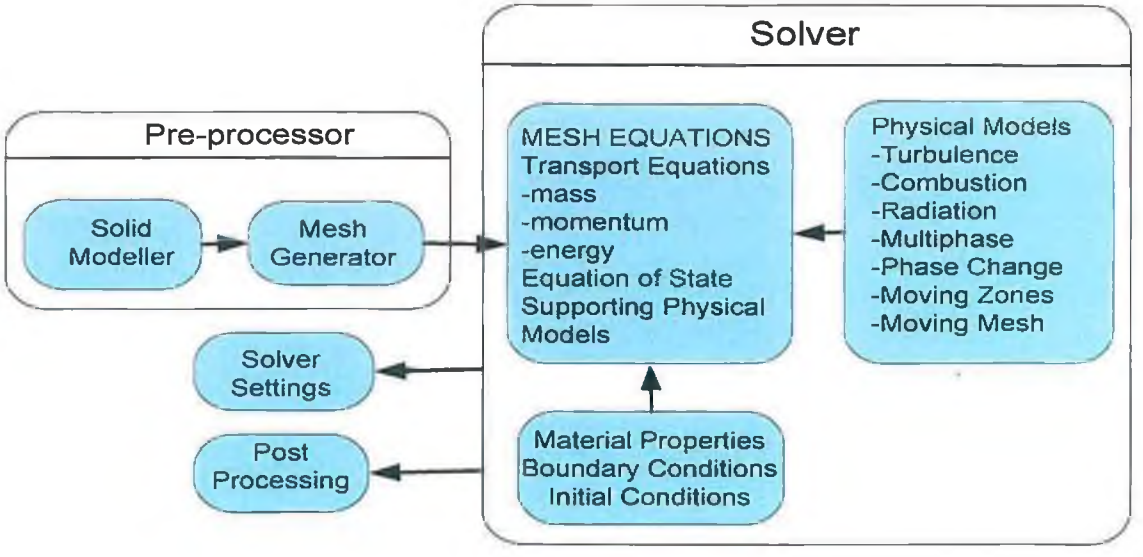

Figure 2. 1:CFD Modeling Overview

2.6.2 Gambit: Fluent Pre-Processor Software

Gambit is an integrated pre-processor package for CFD analysis. The package allows geometry to be constructed using bottom-up or top-down techniques or geometry to be imported from alternate package. Its capabilities include:
ACIS solid modeling capabilities.
IGES import, cleanup and modification.

Gambit allows the construction and meshing of models by means of its graphical user interface. It's used to generate meshes for all fluents solvers and it offers a wide range of elements and schemes including structured and unstructured hexahedral, tetrahedral, pyramid and prisms. Once generated the mesh quality may be analysed and modified if necessary. The general sequence of operations for geometry construction and meshing is as follows:

1. Initial set-up: this includes solver selection; mesh size specification and defaults settings.
2. Geometry creation: Full geometry creation or decomposition into meshable sections.
3. Meshing: Edge and boundary local meshing or face and volume global meshing.
4. Mesh examination: Mesh quality analysis and modification.
5. Zone assignment and mesh export.

Pre-processing is the first step for building and analyzing a flow scenario. FLUENT software supports three pre-processors; GAMBIT, G/TURBO and T-Grid packages. GAMBIT v2.1.6 was used in this analysis. The operations involved in creating a 2D tee-section model in GAMBIT are:

1- Initial set-up: before building the tee-section in GAMBIT, initial settings are specified. Assigning a new project heading and altering setting creates a new modeling session. GAMBIT v2.1.6 supports several pre-processors/ solvers, thus at

the beginning of each modeling of each session the solver type must be set. CFD simulation was created using the following steps:

a) The Fluent 5/6 solver has been chosen to run CFD calculation.
b) Created the geometry of the tee pipe.
c) Created the faces of the pipe.
d) Specify the edges of the faces for meshing operation by use reverse option and double-sided grading.

2- Geometry creation: the 2-D model of the tee-section is built in the GAMBIT Graphical User Interface (GUI). All model geometry is created using the GAMBIT operational toolpad. Shown in figure 2.2, the toolpad is based upon a series of command buttons grouped together according to their heirarchy and purpose in the overall scheme of creating and meshing the model [57]. Using the 'Geometry' subpad, the model was created as a series of edges, lines and faces. The geometry of the tee section was created in the following stages:

a) Specify the node distribution to the edges of the face to define the grid density on the edges of the geometry, assigned the number of nodes, and specified the distribution of nodes of the edge. Select the interval count option (the interval length ratio, R, is a function of both the edge length, L, and the number of intervals). The spacing geometry was 1.0
b) Created structured meshes of the face by using QUAD-element option-high quality hex mesh in order to reduce discritization errors. (Specifies that the mesh includes only quadrilateral mesh elements meshing) to specify the meshing elements, then specifying scheme type by use Map option to creates a regular, structured grid of mesh element. When applying the Quad-map meshing scheme to a face, gambit meshes the face using regular grid of quadrilateral face mesh elements, as seen in figures 2.3, 2.4 and 2.5. Meshing geometry spacing used is 2.5

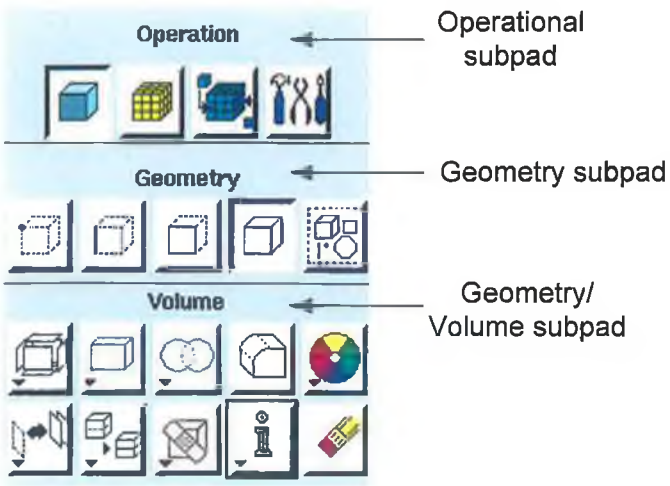

Figure 2. 2: Screenshot of Modeling toolpad

3- Mesh and Quality

a) Select boundary types (the inflow and the outflow pipe) to define the spacing of mesh node rows in regions immediately adjacent to edge and / or face. They are used primarily to control mesh density, and, thereby, to control the amount of information available from the computational model in specific regions of interest.

b) Export the mesh and save case file.

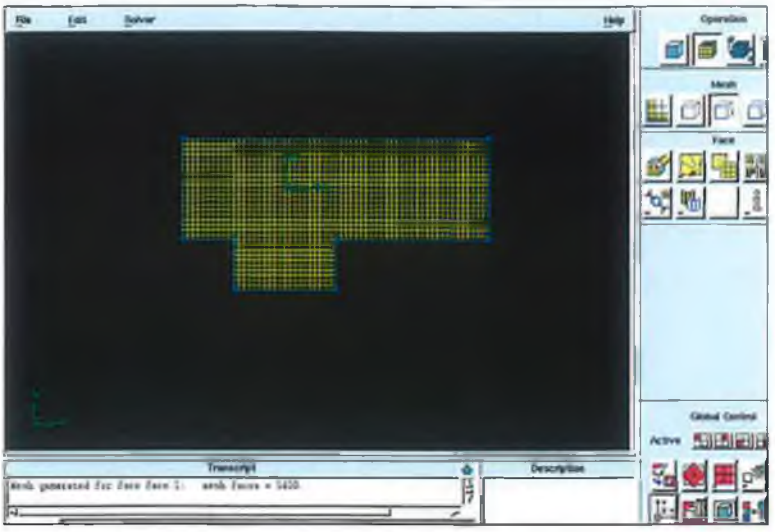

Figure 2. 3: Short entry tee

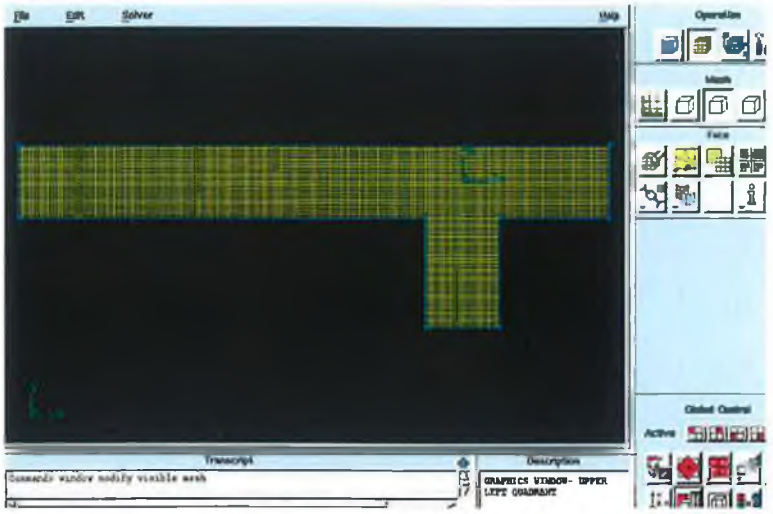

Figure 2. 4: Long entry tee

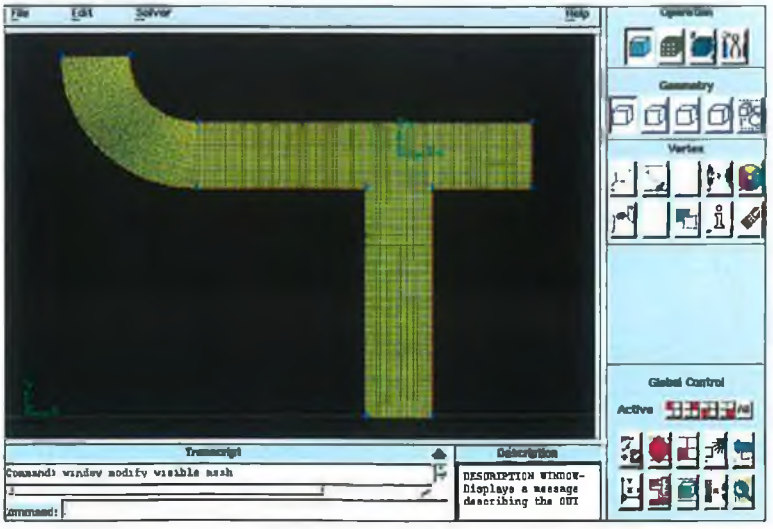

Figure 2. 5: Long entry tee with bend

2.6.3 Fluent Set-up

1- Import

Following a series of meshes with Gambit, the mesh case file for each configuration was imported into Fluent.

2- Modeling

Each mesh was the read into Fluent and checked to ensure the quality domain. The mesh was then adjusted using Fluents smooth and swop, which can be used to improve the quality of an imported mesh. Any cells that may cause problems during solving within Fluent are adjacent in order to aid convergence. Once problem cells have been adjusted the mesh may then be scaled and units applied. The mesh may then have a model applied.

The standard k-ε model was used in this thesis for the turbulent fluid flow modelling. The simplest "complete model" of turbulence are two-equation models in which the solution of two separate transport equations allows the turbulent velocity and length scales to be independently determined. The standard k-ε model was used for all studies.

Robustness, economy, and reasonable accuracy for a wide range of turbulent flows explain its popularity in industrial flow and heat transfer simulations. It is a semi-empirical model, and has achieved considerable success in modelling a wide variety of flows without need for case-by-case adjustment the model constants.

3- Material definition

An important step in the set-up of the model is the definition of the material and this material is then assigned as a boundary conditions for zones. In this problem the fluid was water. Standard temperature and pressure condition were applied over the range of models investigated.

4-Boundary Conditions

Boundary conditions specify the flow variables on the boundaries of the physical model. They are, therefore, a critical component of our fluent simulations and it is

important that they are specified appropriately. Boundary conditions were applied to the inlet, outlet and the wall of the pipe. The boundary types used in this model were:

- Flow inlet and exit boundaries: velocity inlet, outflow.
- Wall boundary conditions: standard wall function.

Initialization controls and monitoring of residuals was used to check progression of the models (figure 2.6). At the end of each solver iteration the residual sum for each of the conserved variables was computed and stored thus recording the convergence history. This history was saved in the data file.

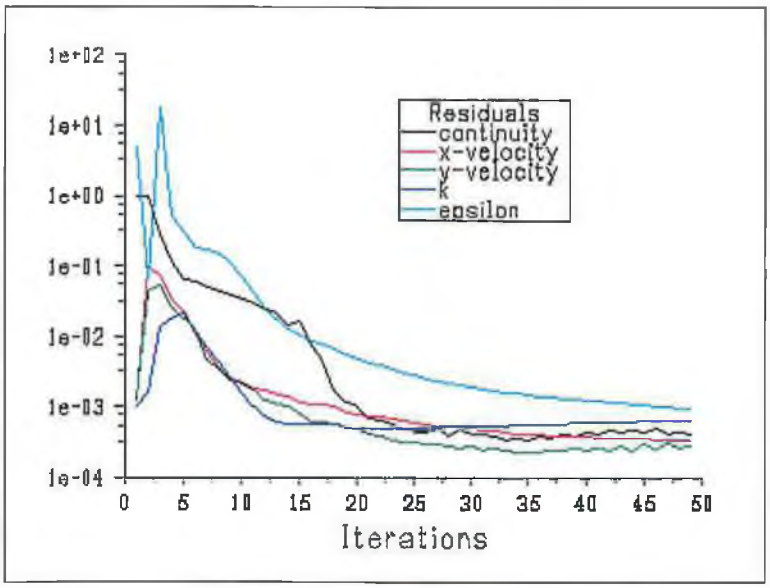

Figure 2. 6: Typical Residuals Graph

Chapter Three
Results and Discussion

CHAPTER 3. RESULTS AND DISCUSSION

3.1 Introduction of the Sharp Tee

Most of the tees used in high purity water distribution networks are sharp entry tees. These tees are cheap to manufacture as they eliminate the need for complicated welding of the joint between the distribution loop and the branch. The data presented in this section is based on a 50mm equal tee (the most common tee found in high purity water systems) of various dead-leg lengths from 1D to 6D.

This initial study examined the effect of the length of tee pipe entrance on the branch flow. The shortest entrance examined was 1D while the longest is 9D. Different velocities have been applied (0.5m/s,1m/s,1.5m/s and 2m/s) to a 1D,2D,4Dand 6D dead-legs to study the changes of flow patterns in the branch. Finally a 50mm bend was added in the entrance of the flow to examine its effect on the branch flow. So this work can be divided into two stages:

1. **Tee-junction without a bend**

   This part studying the flow of pipe tees using different entrance lengths from 1D-9D.

2. **Tee-junction with a bend**

   Adding a 50mm 90° bend and analysing the effect of this change on branch flow patterns.

3.2 Dead Leg Flow Profiles for A 50mm Equal Tee

Dead leg contours of velocity magnitude are presented in the following work for a sharp tee 50mm equal tee. This configuration was achieved by preventing flow into the branch. This is common set up which regularly occurs in pharmaceutical and semi-conductor plants when the branch valve is in closed position.

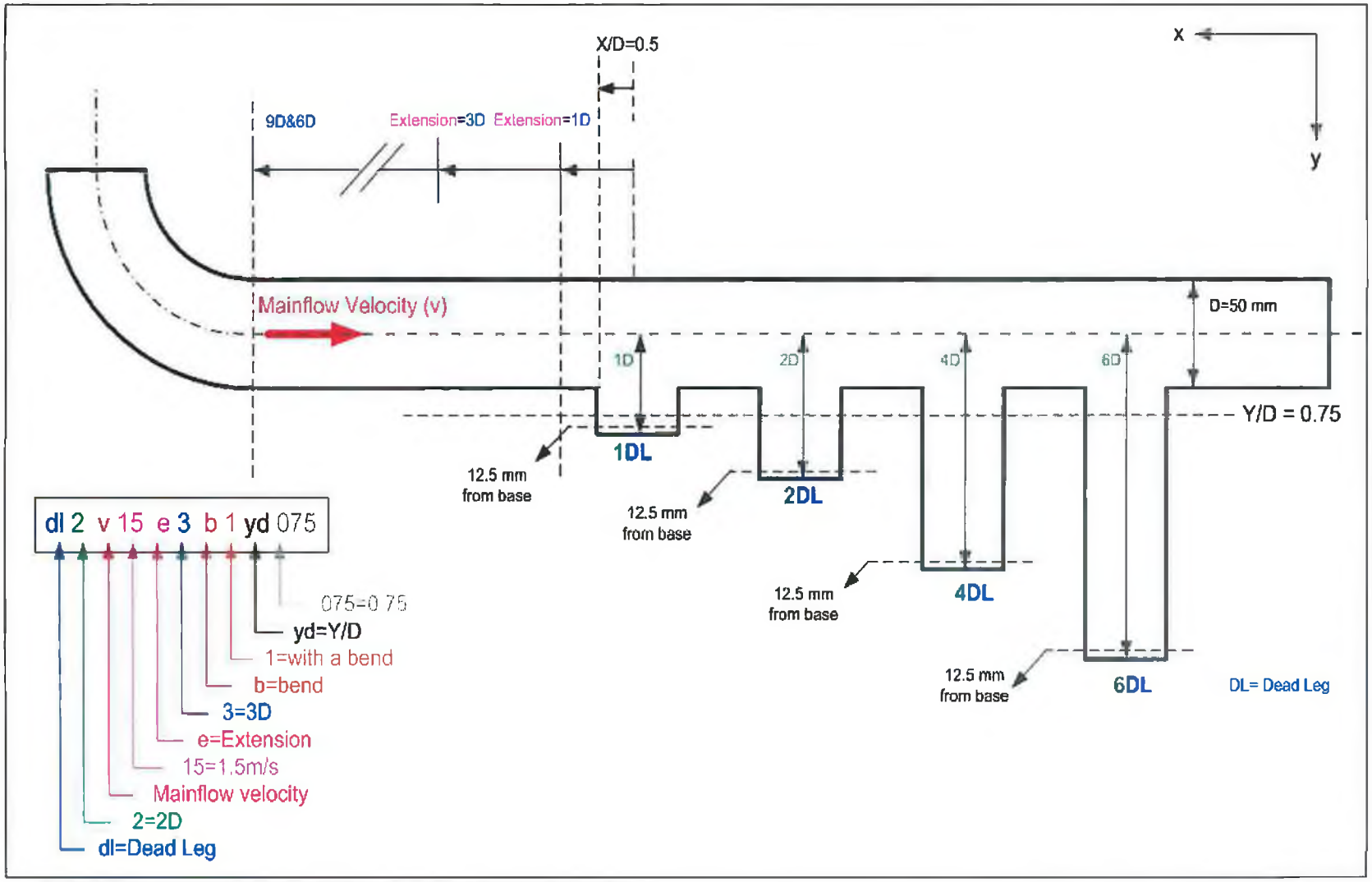

Figure 3. 1: Schematic of pipe dead-leg

3.3 Tee-Junction without a Bend

The following section examines the effect of varying velocity on a range of dead-legs with no bend upstream of the tee section.
Sections 3.3.1 to 3.3.4 highlight the velocity contours for 0.5 to 2m/s.

3.3.1 Tee-junction with 1D extension and velocity of 0.5m/s

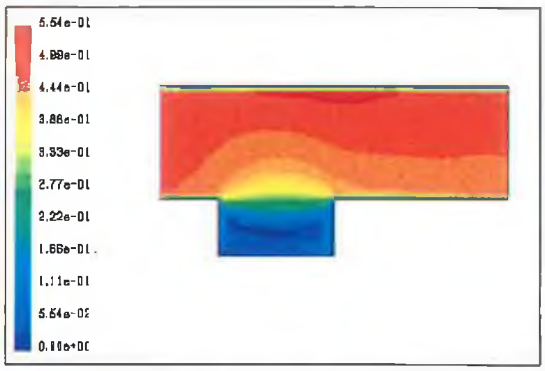

Figure 3. 2:Velocity contours for a 1D sharp tee at 0.5m/s

- Mainstream contours disturbed
- Compact contours across top of branch
- Stagnation in the middle of the branch

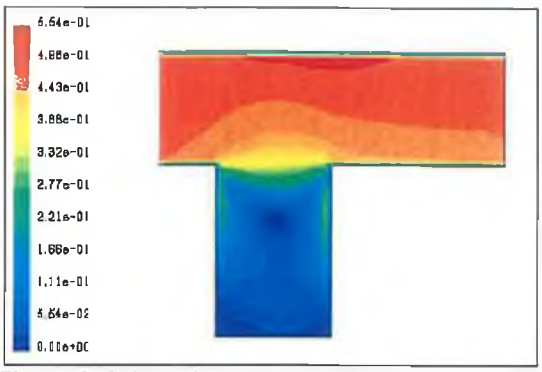

Figure 3. 3:Velocity contours for a 2D sharp tee at 0.5m/s

- Mainstream contours disturbed
- Flow patterns extended beyond 1D
- Motion noted in the branch to a depth of 1.5D. Beyond this velocity is very slow

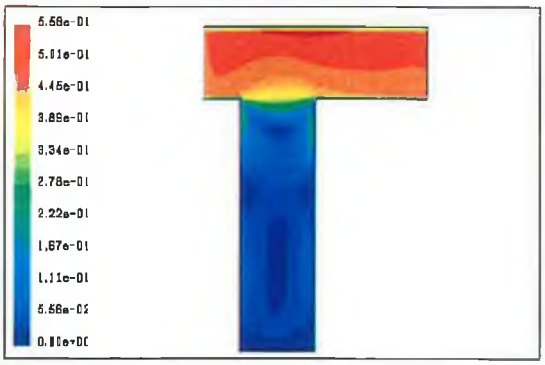

Figure 3. 4:Velocity contours for a 4D sharp tee at 0.5m/s

- Little disturbance of the main stream flow.
- Beyond 3.5D little motion of the fluid and at 4D velocity is zero.

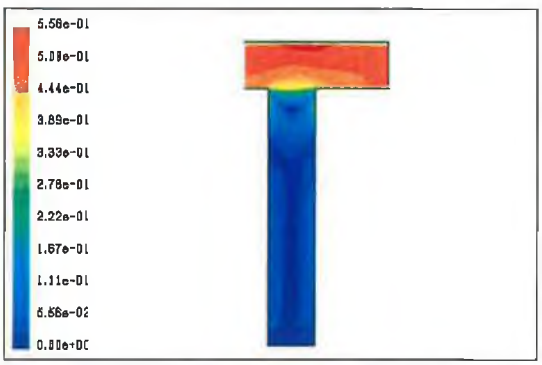

Figure 3. 5:Velocity contours for a 6D sharp tee at 0.5m/s

- Little disturbance of the main stream flow.
- Motion noted in the branch to a depth of 5.5D beyond velocity is very slow

3.3.2 Tee-junction with 1D extension and velocity of 1m/s

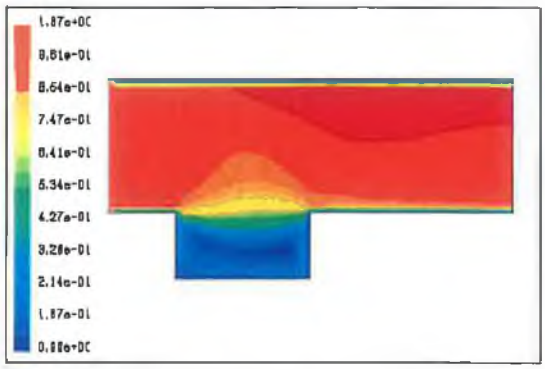

Figure 3. 6:Velocity contours for a 1D sharp tee at 1m/s

- Little disturbance of the main stream flow.
- Increased flow in the branch
- Improvement in velocity along the upstream wall of the branch

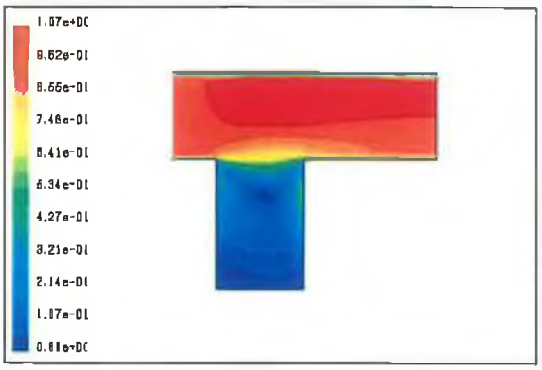

Figure 3. 7:Velocity contours for a 2D sharp tee at 1m/s

- Slight acceleration of main stream flow across the top of branch
- Stagnant noted to a depth 2D
- Minor improvement in penetration into the branch

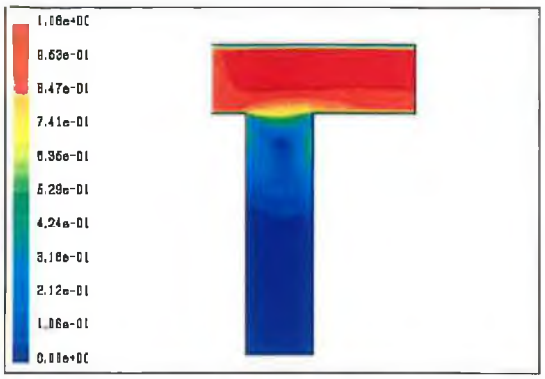

Figure 3. 8:Velocity contours for a 4D sharp tee at 1m/s

- Little disturbance of the main stream flow.
- Motion noted in the branch to a depth of 2.5D beyond velocity is zero

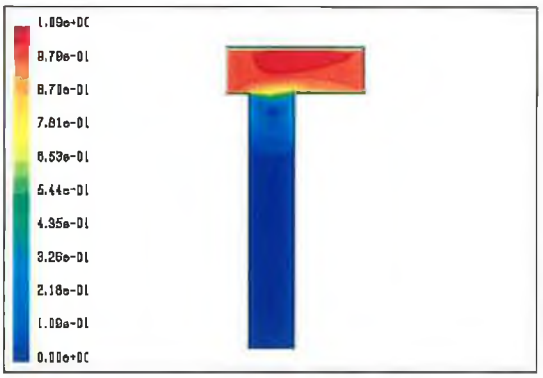

Figure 3. 9:Velocity contours for a 6D sharp tee at 1m/s

- Similar trend to that of 4D configuration.
- Very little change throughout.

3.3.3 Tee-junction with 1D extension and velocity of 1.5m/s

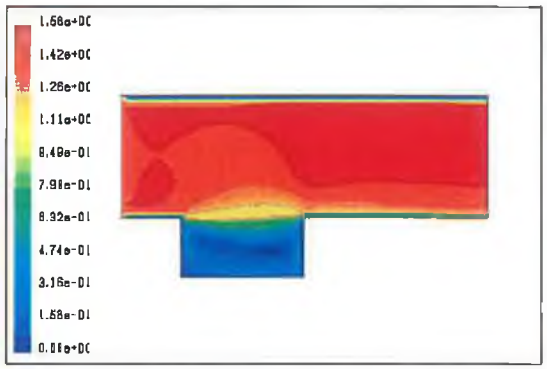

Figure 3. 10:Velocity contours for a 1D sharp tee at 1.5m/s

- Little disturbance of the main stream flow.
- Increased velocities surrounding a rotating vortex

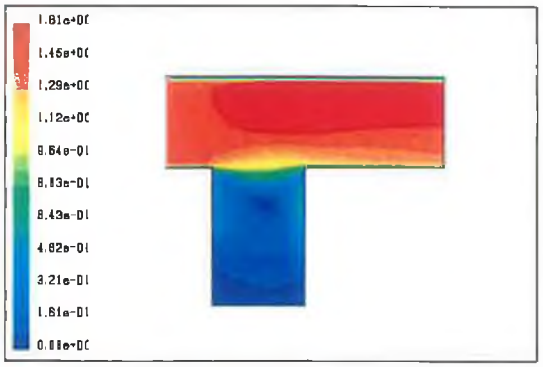

Figure 3. 11:Velocity contours for a 2D sharp tee at 1.5m/s

- Similar trend to that of 1 m/s configuration
- Stagnation at the base of the branch

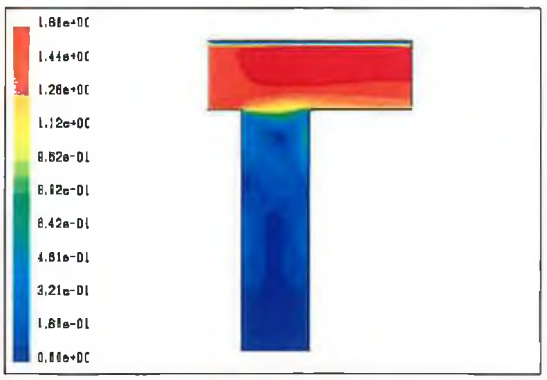

Figure 3. 12:Velocity contours for a 4D sharp tee at 1.5m/s

- Improved velocity throughout the branch to a depth of 3D
- No motion of the fluid in the branch beyond 3D

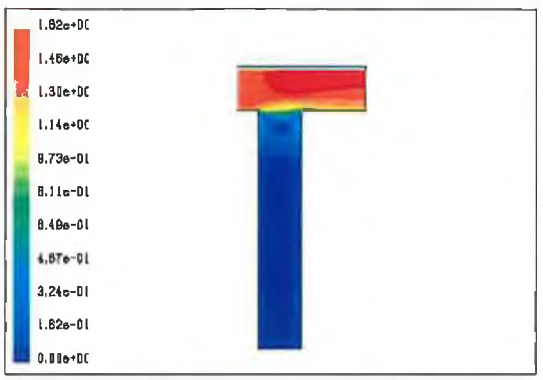

Figure 3. 13:Velocity contours for a 6D sharp tee at 1.5m/s

- Flow pattern established to depth of 2D of the branch
- Motion noted in the branch to a depth of 2D beyond velocity is very slow

3.3.4 Tee-junction with 1D extension and velocity of 2m/s

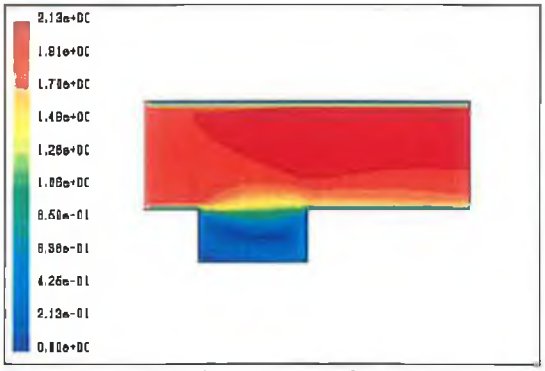

Figure 3. 14:Velocity contours for a 1D sharp tee at 2m/s

- Flow patterns extended further into the branch
- Motion noted throughout the branch and along the base of the dead leg

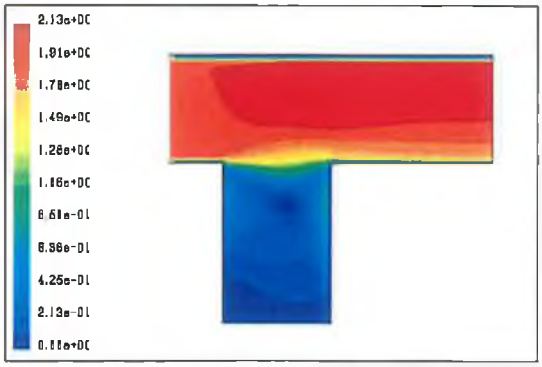

Figure 3. 15:Velocity contours for a 2D sharp tee at 2m/s

- Little disturbance of the mainstream flow
- Base of the branch has low velocities
- Drop off in velocity around the rotating vortex

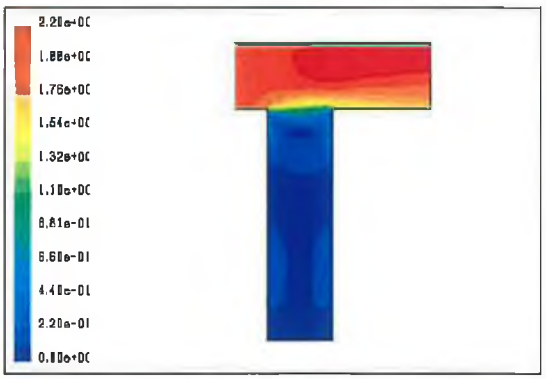

Figure 3. 16:Velocity contours for a 4D sharp tee at 2m/s

- No change in mainstream configurations
- Beyond 2D little motion of the fluid and at 4D velocity is zero.

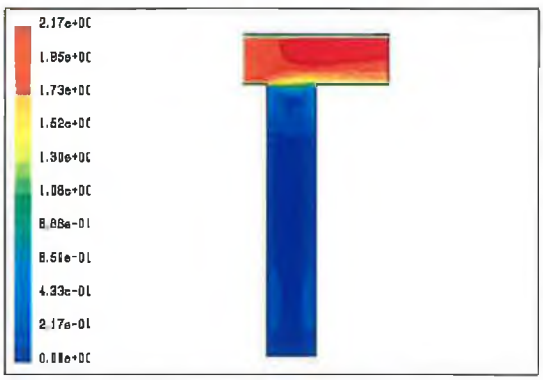

Figure 3. 17:Velocity contours for a 6D sharp tee at 2m/s

- Beyond 2D little motion of the fluid
- Vortex isolated between 1D and 2D

3.3.5 Velocity plots for 1DL, 2DL, 4DL and 6DL with 1D extension 0.5-2m/s velocity

Flow profiles are similar throughout the range of graphs. An increase in mainstream velocity results in an increase in both upstream & downstream velocity within the 1D branch. The lowest velocity was noted at the base of the branch for all configurations.

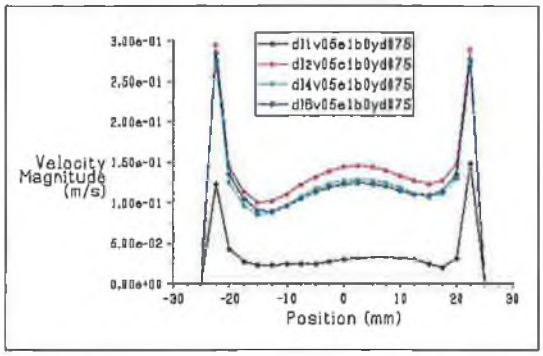

Figure 3. 18: y-Velocity plots at y/D=0.75, 1D extension and 0.5m/s for1D, 2D, 4Dand6D

- Max Velocity at 2D
- Min Velocity at 6D
- Upstream max velocity at 0.3m/s
- Downstream max velocity at 0.3m/s

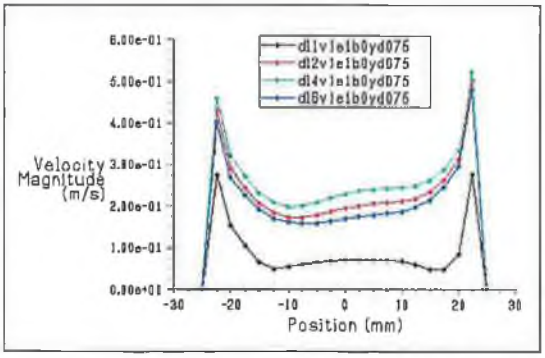

Figure 3. 19: y-Velocity plots at y/D=0.75, 1D extension and 1m/s for1D, 2D, 4Dand6D

- Max Velocity at 4D
- Min Velocity at 1D
- Upstream max velocity at 0.47m/s
- Downstream max velocity at 0.55m/s

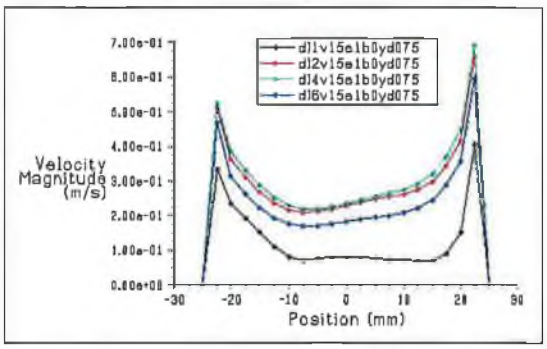

Figure 3. 20: y-Velocity plots at y/D=0.75, 1D extension and 1.5m/s for1D, 2D, 4Dand6D

- Max Velocity at 4D
- Min Velocity at 1D
- Upstream max velocity at 0.53m/s
- Downstream max velocity at 0.7m/s

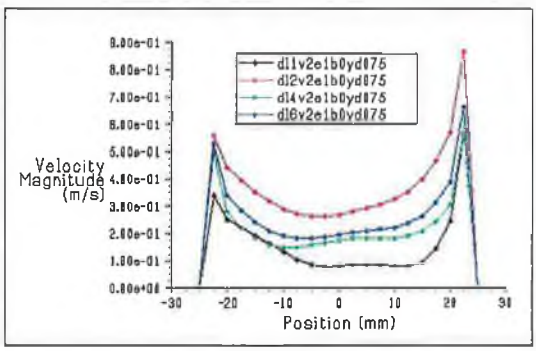

Figure 3. 21: y-Velocity plots at y/D=0.75, 1D extension and 2m/s for1D, 2D, 4Dand6D

- Max Velocity at 2D
- Min Velocity at 1D
- Upstream max velocity at 0.57m/s
- Downstream max velocity at 0.88m/s

3.3.6 Velocity plots for 1DL, 2DL, 4DL and 6DL with 1D extension and 0.5-2m/s velocity at 12.5 mm from Base

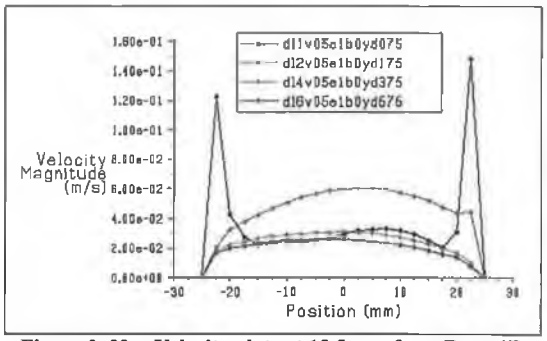

Figure 3. 22:y-Velocity plots at 12.5 mm from Base, 1D extension and 0.5m/s for1D, 2D, 4Dand6D

- 1D max 0.15m/s and min 0.02m/s
- 2D max 0.06m/s and min 0.02m/s
- 4D max 0.03m/s and min 0.01m/s
- 6D max 0.025m/s and min 0.01m/s

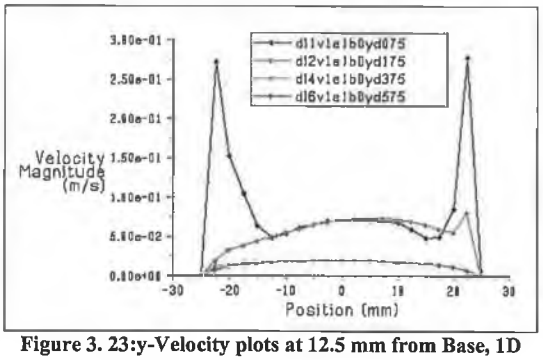

Figure 3. 23:y-Velocity plots at 12.5 mm from Base, 1D extension and 1m/s for1D, 2D, 4Dand6D

- 1D max 0.255m/s and min 0.05m/s
- 2D max 0.055m/s and min 0.005m/s
- 4D max 0.005m/s and min 0.001m/s
- 6D max 0.005m/s and min 0.001m/s

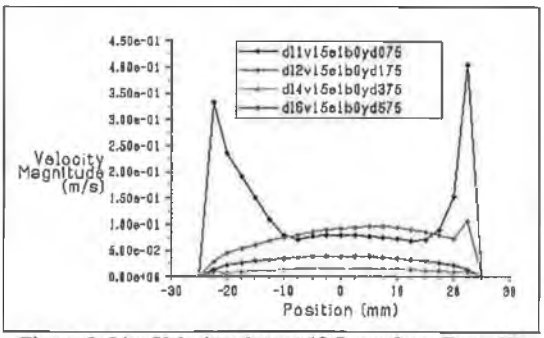

Figure 3. 24:y-Velocity plots at 12.5 mm from Base, 1D extension and 2m/s for1D, 2D, 4Dand6D

- 1D max 0.4m/s and min 0.055m/s
- 2D max 0.1m/s and min 0.025m/s
- 4D max 0.02m/s and min 0.005m/s
- 6D max 0.027m/s and min 0.01m/s

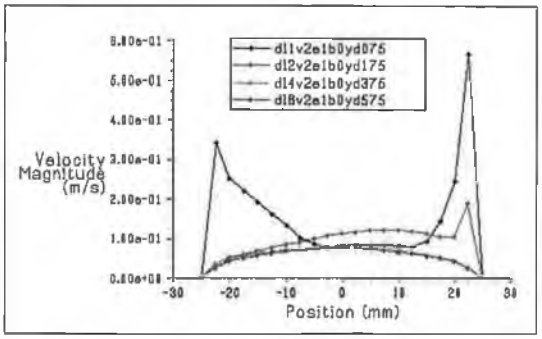

Figure 3. 25:y-Velocity plots at 12.5 mm from Base, 1D extension and 2m/s for1D, 2D, 4Dand6D

- 1D max 0.58m/s and min 0.08m/s
- 2D max 0.2m/s and min 0.03m/s
- 4D max 0.08m/s and min 0.025m/s
- 6D max 0.08m/s and min 0.025m/s

3.3.7 Velocity plots for 1DL, 2DL, 4DL and 6DL with 1D extension and 0.5&2m/s velocity at x/D=0.5.

Figure 3.22 and 3.23 highlight the effect of a long entry length on the mainstream velocity profile to the branch. Apart from a slight readjustment of the profile at high velocity there is little effect due to entry length.

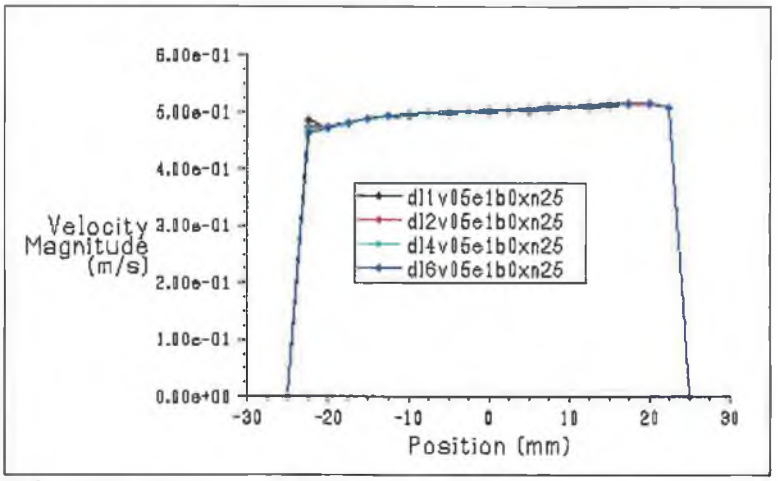

Figure 3. 26: y-Velocity plots at x/D=0.5, 1D extension and 0.5m/s for1D, 2D, 4Dand6D

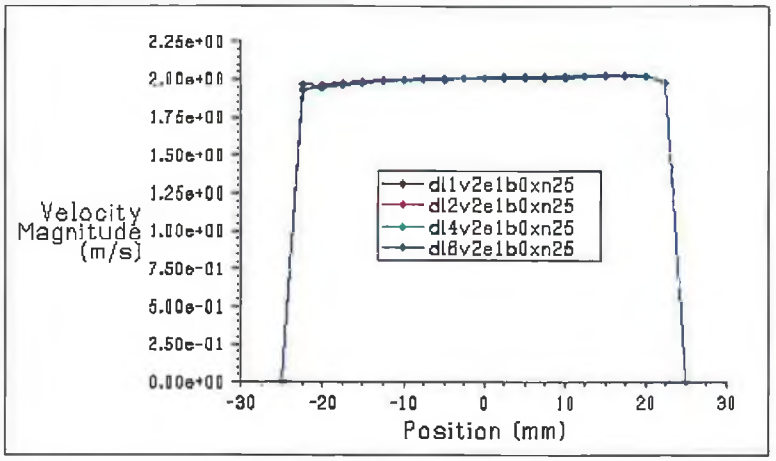

Figure 3. 27: y-Velocity plots at x/D=0.5, 1D extension and 2m/s for1D, 2D, 4Dand6D

- increase in velocity results in uniform turbulent profile
- increase in entry length (extension) has no effect on inlet profile irrespective of dead-leg length

3.3.8 Tee-junction with 9D extension and velocity of 0.5m/s

Velocity contours for a 9D extension upstream of a dead-leg for 0.5 to 2m/s mainstream velocities are presented in figures 3.28 and 3.35.

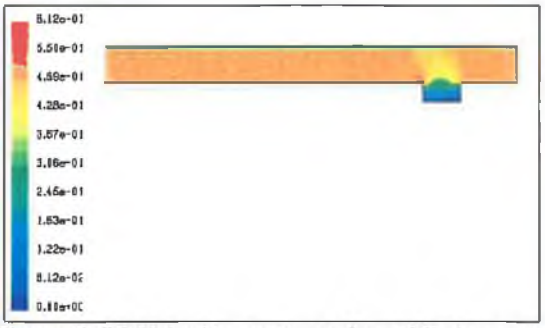

Figure 3. 28:Velocity contours for a 1D sharp tee at 0.5m/s

- Little disturbance in the mainstream flow
- Pattern well defined
- Motion noted into the all branch

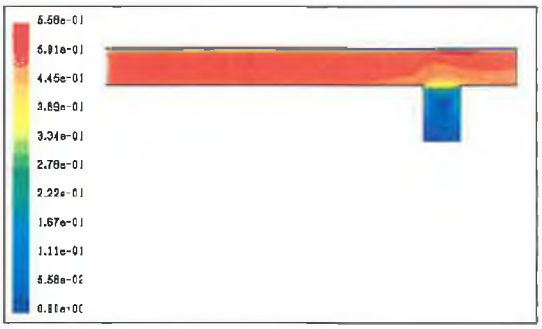

Figure 3. 29:Velocity contours for a 2D sharp tee at 0.5m/s

- Little disturbance of the mainstream flow.
- Base of the branch has low velocities.
- Movement on downstream wall.

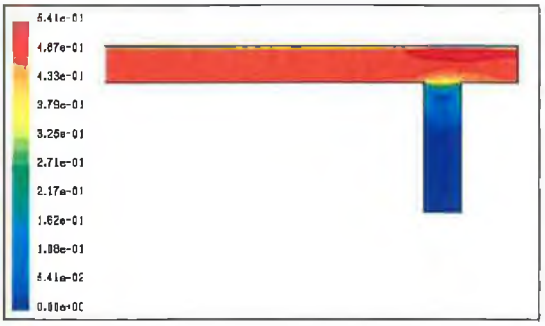

Figure 3. 30:Velocity contours for a 4D sharp tee at 0.5m/s

- Beyond 2D is stagnant.
- Stagnant zone towards base.
- Primary & secondary zone developed.

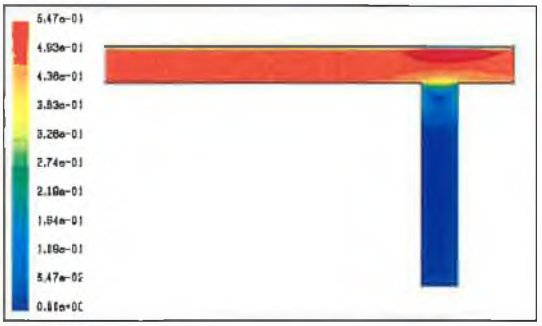

Figure 3. 31:Velocity contours for a 6D sharp tee at 0.5m/s

- Beyond 2D little motion of the fluid and at 4D velocity is zero.
- Secondary zone extended.

3.3.9 Tee-junction with 9D extension and velocity of 2m/s

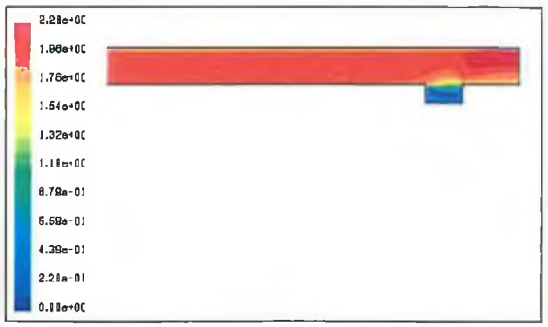

Figure 3. 32:Velocity contours for a 1D sharp tee at 2m/s

- Higher velocities noted within the dead-leg.
- Movement noted throughout the branch.

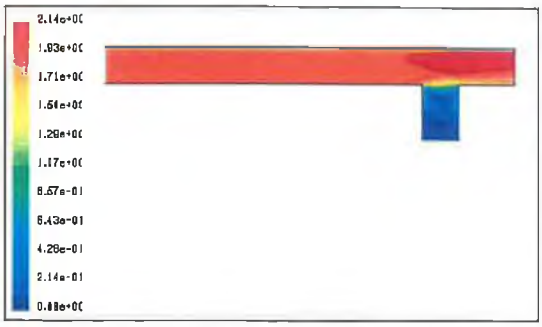

Figure 3. 33:Velocity contours for a 2D sharp tee at 2m/s

- Increased velocity of the mainstream flow
- Motion noted in 1.5D of the branch and beyond the velocity is very slow

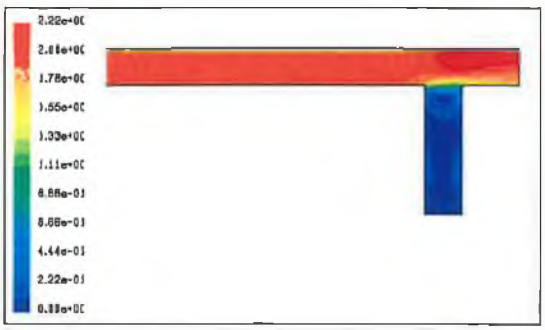

Figure 3. 34:Velocity contours for a 4D sharp tee at 2m/s

- Mainstream configuration similar to 2D
- Flow is very slow beyond 1.5D
- Little motion at the base of branch

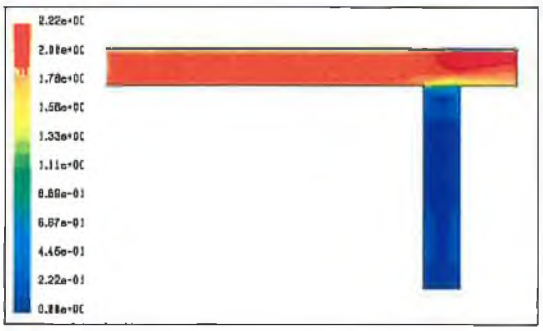

Figure 3. 35:Velocity contours for a 6D sharp tee at 2m/s

- Flow is very slow beyond 1.5D
- Remainder branch considered as slow flowing region.
- Secondary zone beyond 1.5D.

3.3.10 Velocity plots for 1DL, 2DL, 4DL and 6DL with 9D extension and 0.5-2m/s velocity at y/D=0.75

Figures 3.36 to 3.39 highlight the velocities found at various points throughout a range of dead-legs with a 9D extension upstream of the branch.

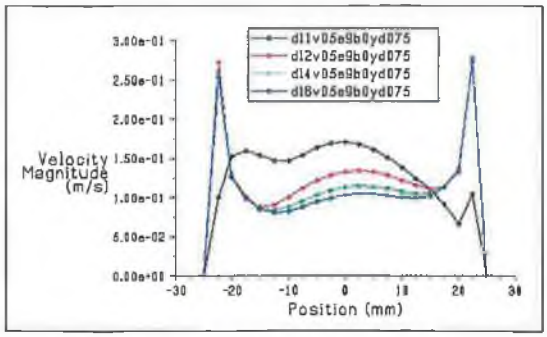

Figure 3. 36: y-Velocity plots at y/D=0.75, 9D extension and 0.5m/s for 1D, 2D, 4Dand6D

- Max Velocity at 2D
- Min Velocity at 6D
- Upstream max velocity at 0.255m/s
- Downstream max velocity at 0.255m/s

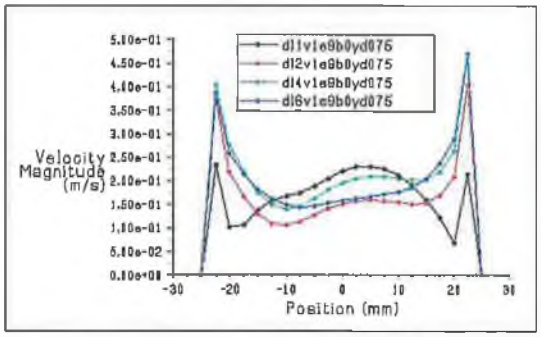

Figure 3. 37: y-Velocity plots at y/D=0.75, 9D extension and 1m/s for 1D, 2D, 4Dand6D

- Max Velocity at 4D
- Min Velocity at 1D
- Upstream max velocity at 0.42m/s
- Downstream max velocity at 0.455m/s

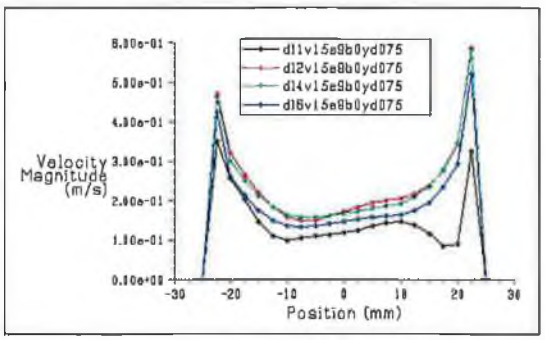

Figure 3. 38: y-Velocity plots at y/D=0.75, 9D extension and 1.5m/s for 1D, 2D, 4Dand6D

- Max Velocity at 2D
- Min Velocity at 1D
- Upstream max velocity at 0.48m/s
- Downstream max velocity at 0.59m/s

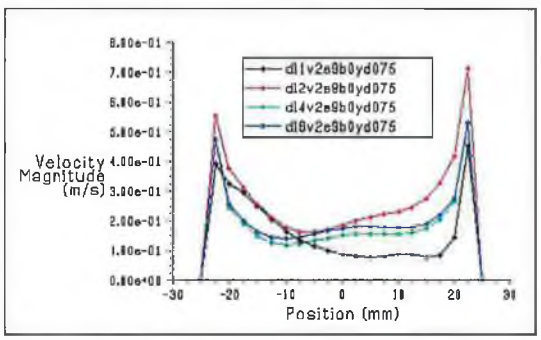

Figure 3. 39: y-Velocity plots at y/D=0.75, 9D extension and 2m/s for 1D, 2D, 4Dand6D

- Max Velocity at 2D
- Min Velocity at 1D
- Upstream max velocity at 0.57m/s
- Downstream max velocity at 0.74m/s

From previous work it is obvious the motion of fluid in the branch is very slow. There is no improvement by extending the entrance length while there is a slight different in flow velocity by changing the dead leg length.

In the next step a 90° bend effect will be examined. The following table shows the manufactured and dimensions of the bend used in this study.

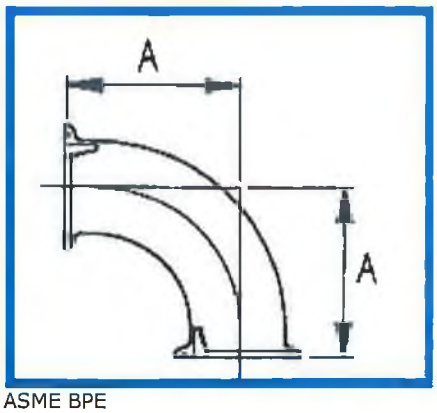

ASME BPE

90° Bend CC Table DT-16

Size (ins)	Part Code	A (mm)
0.25	90B02CC	41.3
0.375	90B04CC	41.3
0.5	90B05CC	41.3
0.75	90B07CC	41.3
[redacted]	[redacted]	[redacted]
1.5	90B15CC	69.9
2.0	90B20CC	88.9
2.5	90B25CC	108.0
3.0	90B30CC	127.0
4.0	90B40CC	168.3
6.0	90B60CC	266.7

Figure 3. 40:Biobore Bends

While some industrial layouts allow long entry length before dead-leg tee sections, the majority require a drop-loop configuration. This results in a drop from high elevation pipework down to a reaction vessel and a sharp return back to high elevation. It is therefore common to introduce a bend immediately before and after the dead-leg tee section.

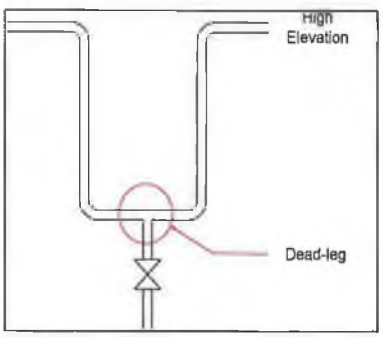

Figure 3. 41: Drop loop dead-leg configuration.

3.4 Tee-Junction with a Bend

3.4.1 Tee-junction with a bend, 1D extension and velocity of 0.5m/s

Thee introduction of a bend upstream of a dead-leg is now analysed for a range of velocities from 0.5 to 2m/s. figures 3.46, 3.54, 3.57 and 3.62 highlight the effect of dead-leg length on flow pattern with the branch and show areas of stagnation within the dead-leg.

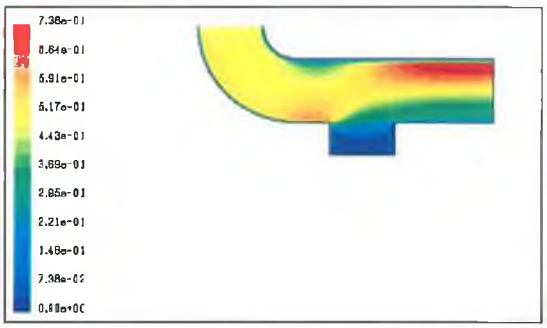

Figure 3. 42:Velocity contours for a 1D sharp tee at 0.5m/s

- Little disturbance of the main stream flow
- Stagnant beyond 0.5D

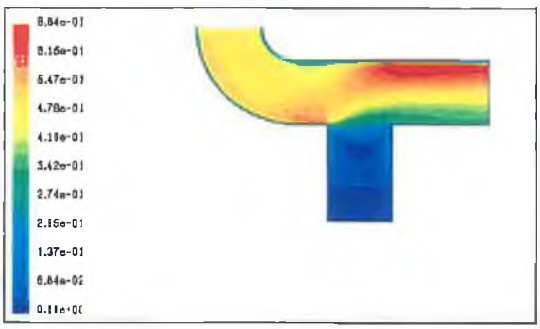

Figure 3. 43:Velocity contours for a 2D sharp tee at 0.5m/s

- Little disturbance of the main stream flow
- Motion noted in the branch to a depth of 1.5D beyond which velocity is zero.

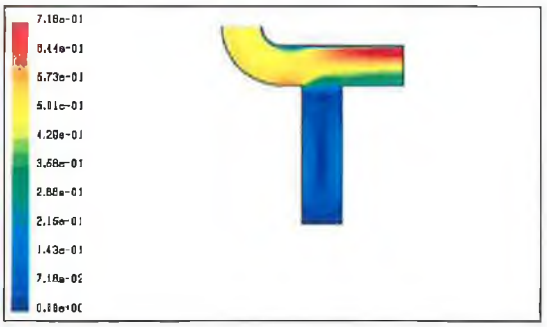

Figure 3. 44:Velocity contours for a 4D sharp tee at 0.5m/s

- Little disturbance of the main stream flow
- Flow pattern established to a depth of 3.5D
- Beyond 3.5D little motion of the fluid

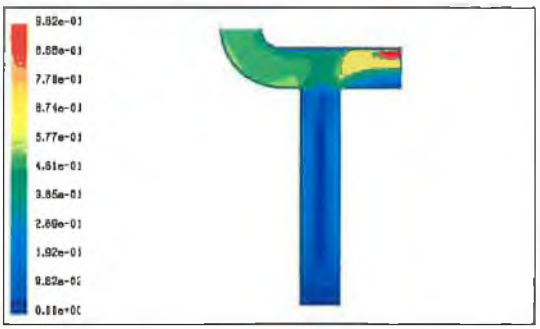

Figure 3. 45:Velocity contours for a 6D sharp tee at 0.5m/s

- Little disturbance of the main stream flow
- Flow pattern established to a depth of more than 5.5D
- Motion noted to a depth of 5.5D with the remainder of the branch stagnant

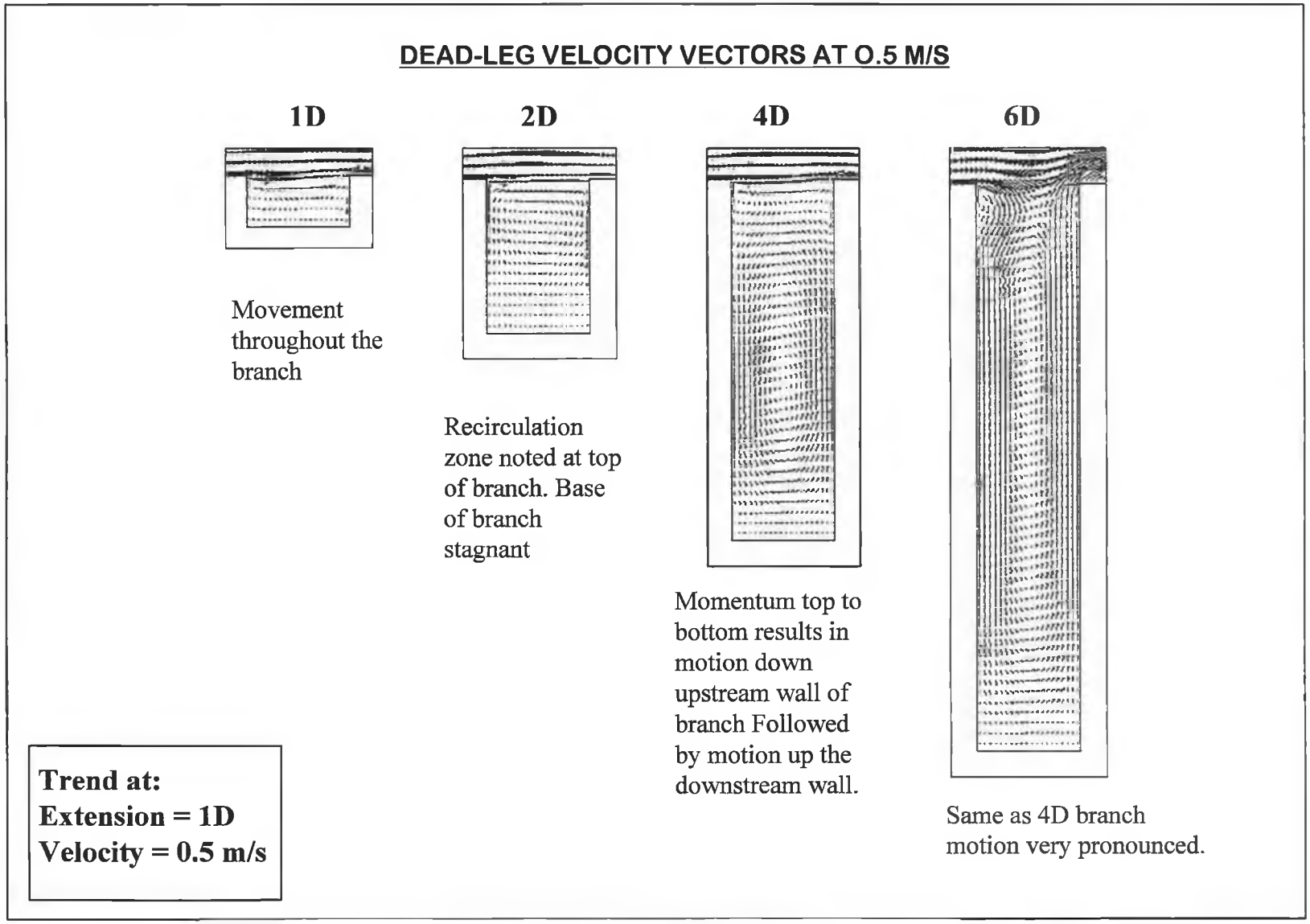

Figure 3. 46: Velocity Vectors for a 50mm sharp tee with various dead-leg drop

3.4.2 Tee-junction with a bend, 1D extension and velocity of 1m/s

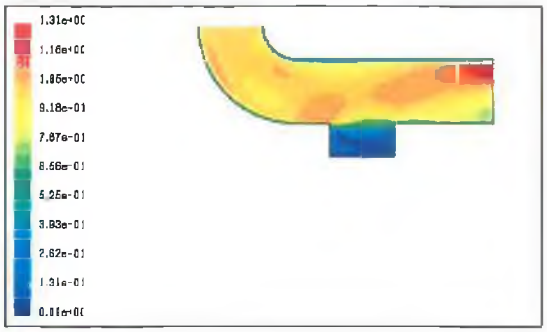

Figure 3. 48:Velocity contours for a 1D sharp tee at 1m/s

- Little disturbance of the main stream flow
- Increased flow in the branch over 0.5m/s
- Improved velocity along the upstream of the branch

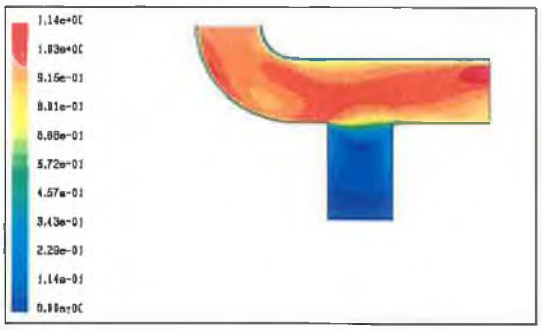

Figure 3. 49:Velocity contours for a 2D sharp tee at 1m/s

- Slight acceleration of main stream flow across the top of the branch
- Minor improvement in penetration into the branch

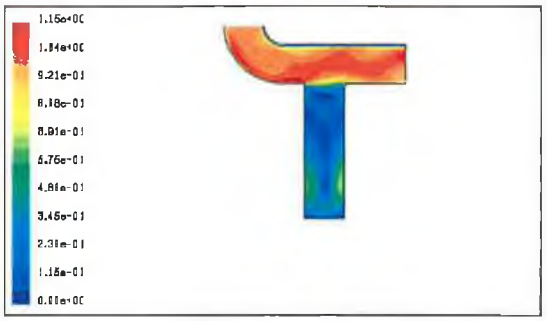

Figure 3. 50:Velocity contours for a 4D sharp tee at 1m/s

- Good improvement in penetration into the branch
- Motion noted in the whole branch
- Increased flow in the branch obviously beyond 2D

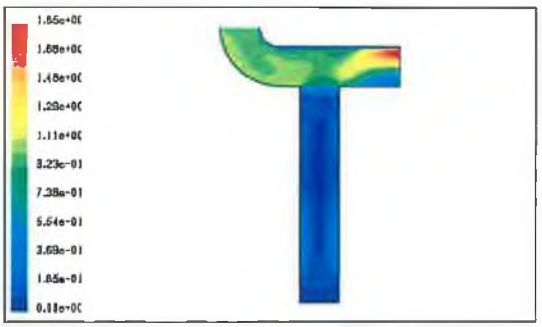

Figure 3. 51:Velocity contours for a 6D sharp tee at 1m/s

- Flow pattern established to depth of 5.5D
- Stagnant beyond 5.5D

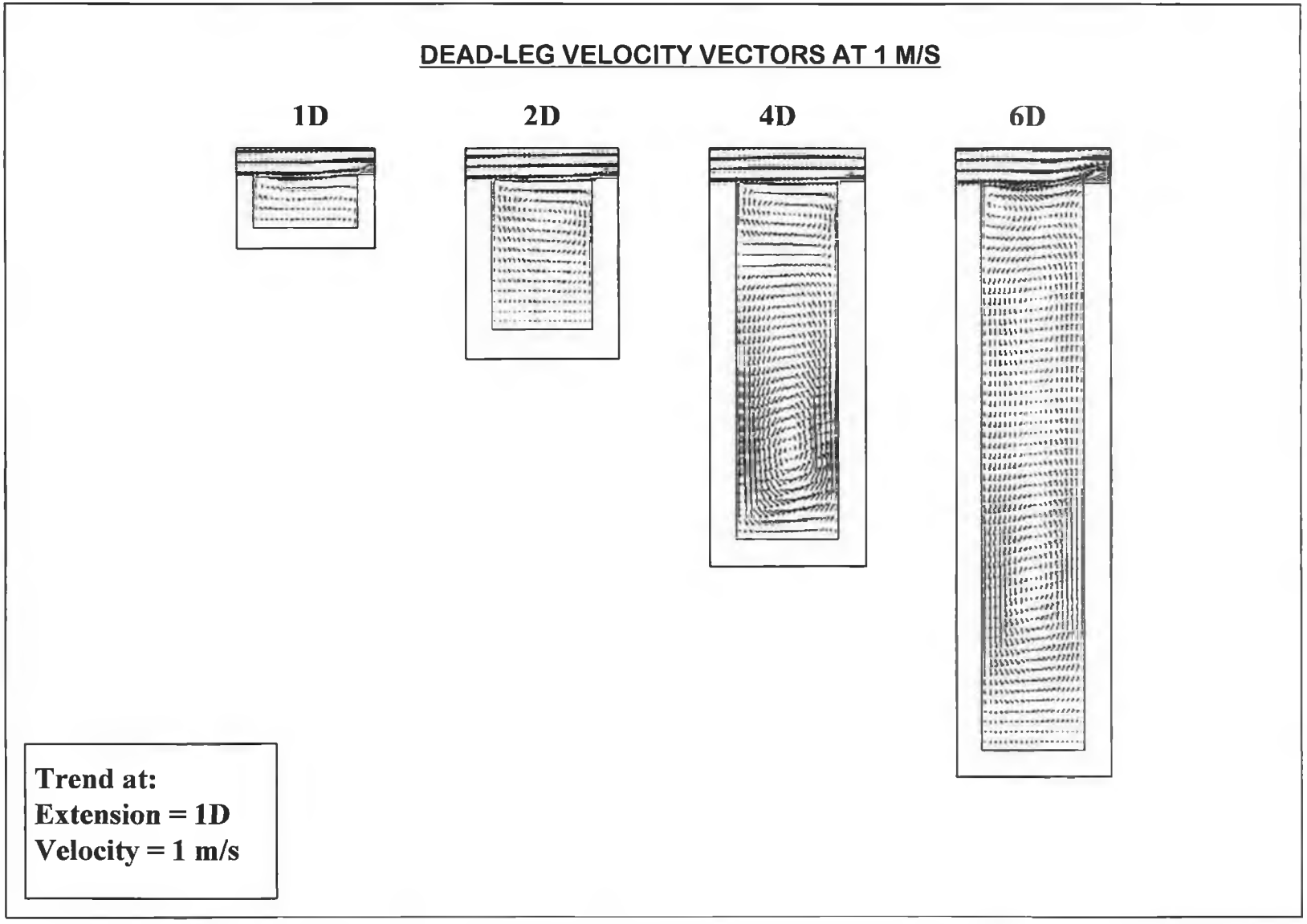

Figure 3. 52: Velocity Vectors for a 50mm sharp tee with various dead-leg drop

3.4.3 Tee-junction with a bend, 1D extension and velocity of 1.5 m/s

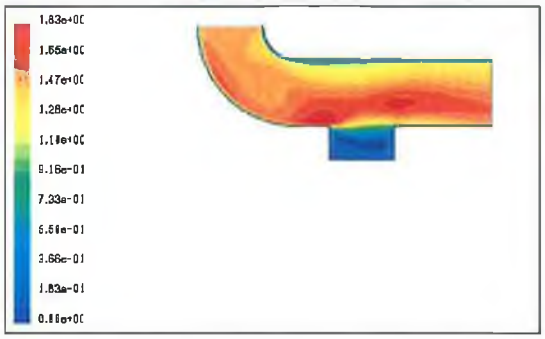

Figure 3. 53:Velocity contours for a 1D sharp tee at 1.5m/s

- Main stream flow similar to 1m/s
- Improved penetration into the branch
- Improved velocity in the branch

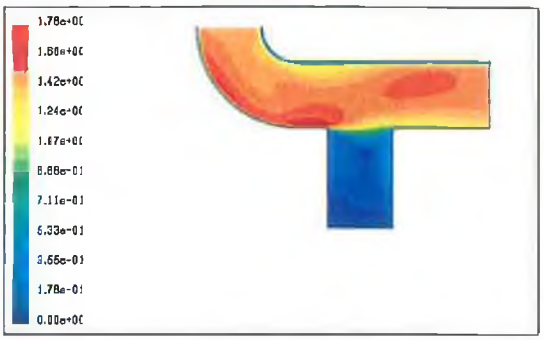

Figure 3. 54:Velocity contours for a 2D sharp tee at 1.5m/s

- Little disturbance of the main stream flow
- Flow pattern extended beyond 1D
- Motion noted in the branch to a depth of 1.5D beyond which velocity is very slow

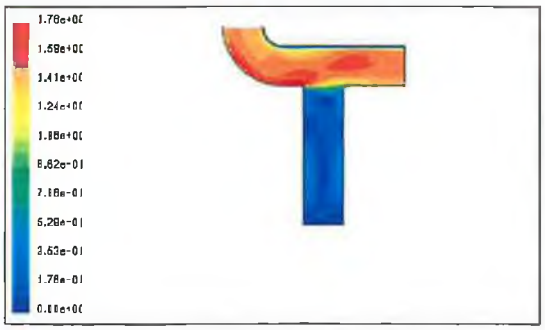

Figure 3. 55:Velocity contours for a 4D sharp tee at 1.5m/s

- Flow pattern established to a depth of 3.5D
- Beyond 3.5D little motion of the flow and at 4D velocity is zero
-

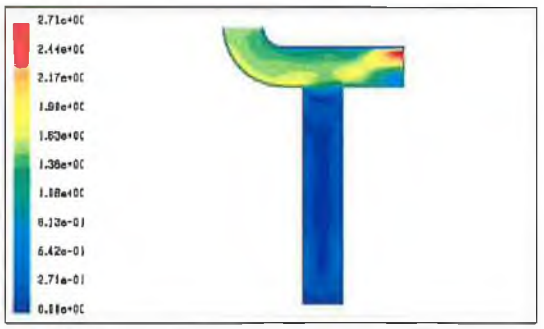

Figure 3. 56:Velocity contours for a 6D sharp tee at 1.5m/s

- Little disturbance of the main stream flow
- Flow pattern established in the upstream and downstream walls to depth of 5.5D
- The center and base of the branch are stagnant

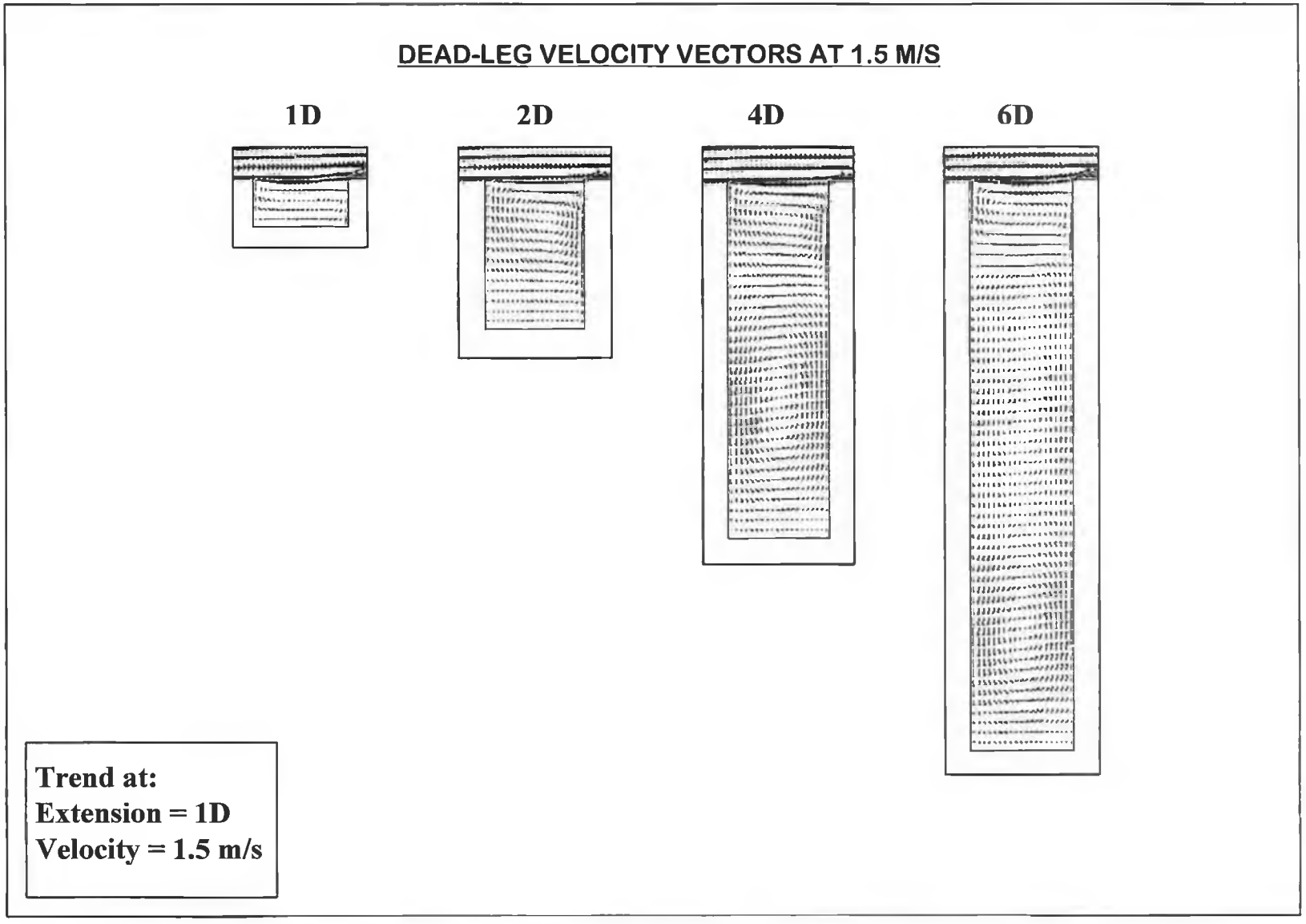

Figure 3. 57: Velocity Vectors for a 50mm sharp tee with various dead-leg drop

3.4.4 Tee-junction with a bend, 1D extension and velocity of 2m/s

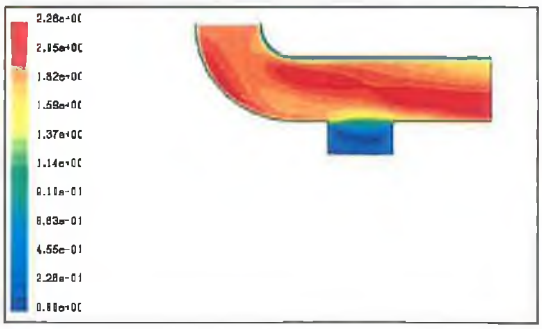

Figure 3. 58:Velocity contours for a 1D sharp tee at 2m/s

- Flow pattern in the branch similar to 1.5m/s
-

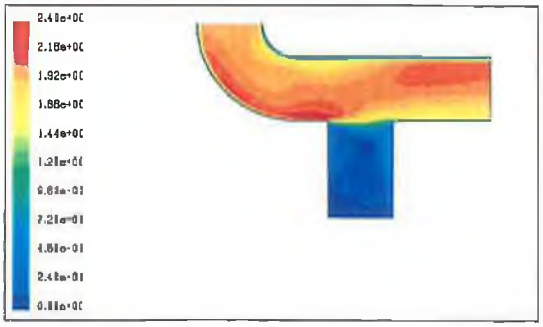

Figure 3. 59:Velocity contours for a 2D sharp tee at 2m/s

- Similar trend to 1.5m/s
- Flow pattern extended further into the branch
- Base of the branch has low velocity

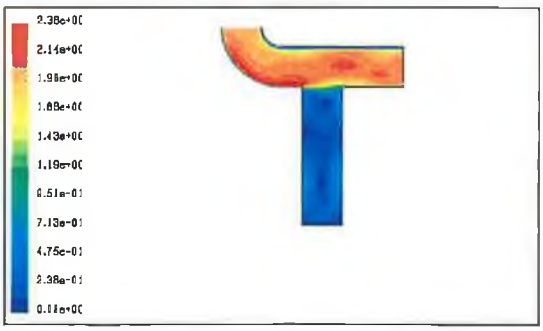

Figure 3. 60:Velocity contours for a 4D sharp tee at 2m/s

- No change in mainstream configuration
- Improved penetration into the branch
- Low velocity on the base of branch

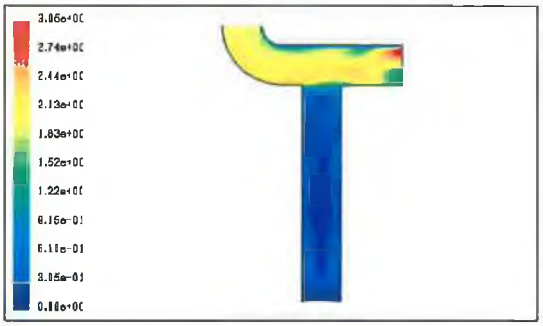

Figure 3. 61:Velocity contours for a 6D sharp tee at 2m/s

- Increased flow pattern
- Less stagnant in the center of branch
- Flow pattern extended further into the branch

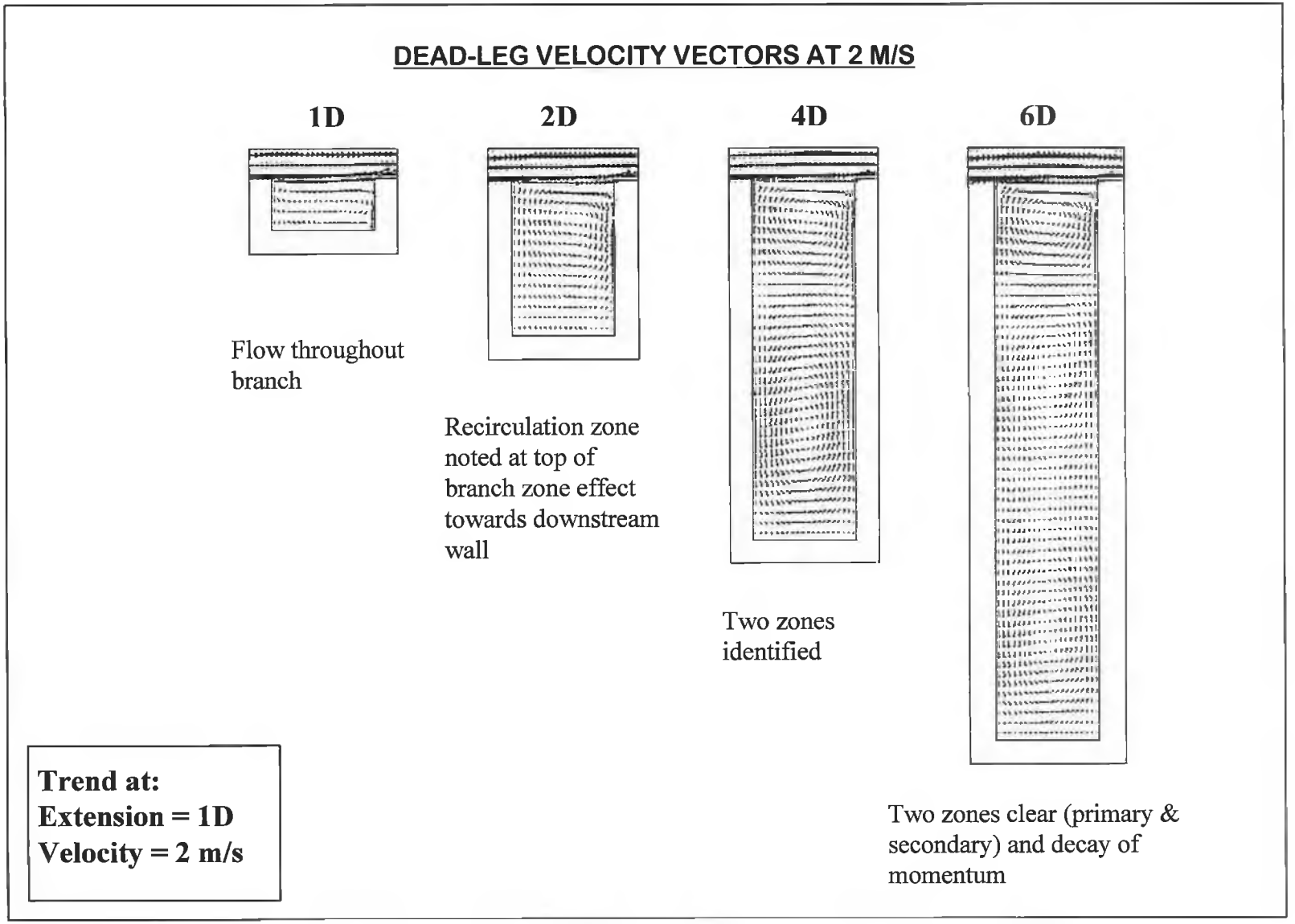

Figure 3. 62: Velocity Victors for a 50mm sharp tee with various dead-leg drop

3.4.5 Velocity plots for 1DL, 2DL, 4DL and 6DL with 1D extension and velocity of 0.5&2 m/s

Increase in mainstream velocity results in a variation in branch flow patterns. Addition of the branch at low velocity was found to disturb flow patterns within the 1D branch. However at high velocity a similar flow pattern was found to that of straight entry highest velocity were found along the upstream and downstream walls at 2m/s.

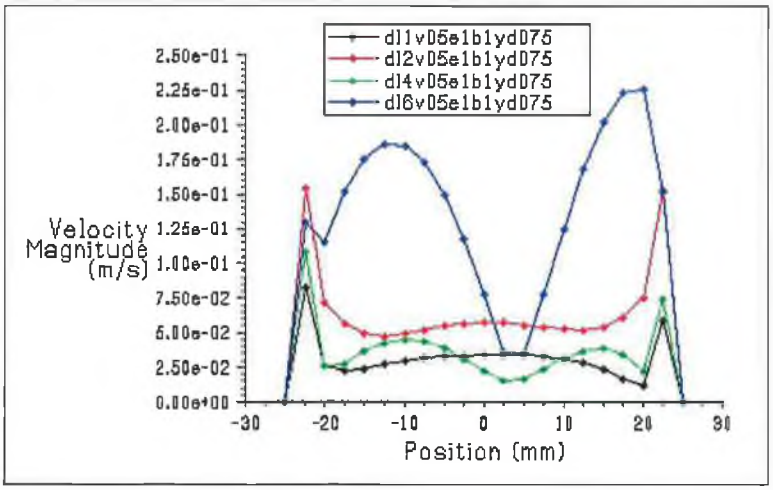

Figure 3. 63:y-Velocity plots at y/D=0.75, 1D extension and 0.5m/s for1D, 2D, 4Dand6D dead-leg length

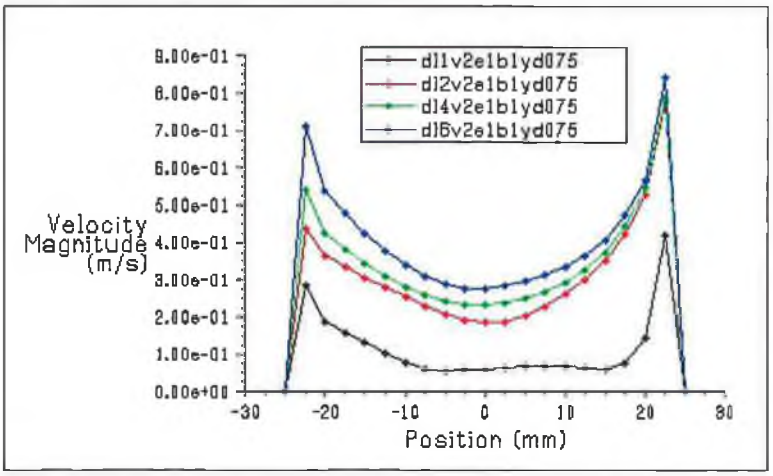

Figure 3. 64:y-Velocity plots at y/D=0.75, 1D extension and 2m/s for1D, 2D, 4Dand6D dead-leg length

3.4.6 Tee-junction with a bend, 1D extension and 2D dead-leg

It is clear that the introduction of a bend upstream of the branch had an effect on a flow patterns within the dead-leg. In order to investigate the effect of the position of the bend upstream of the branch a series of simulations were carried out. These include positioning the bend 1D and 3D upstream of a 2D, 4D and 6D dead-leg.

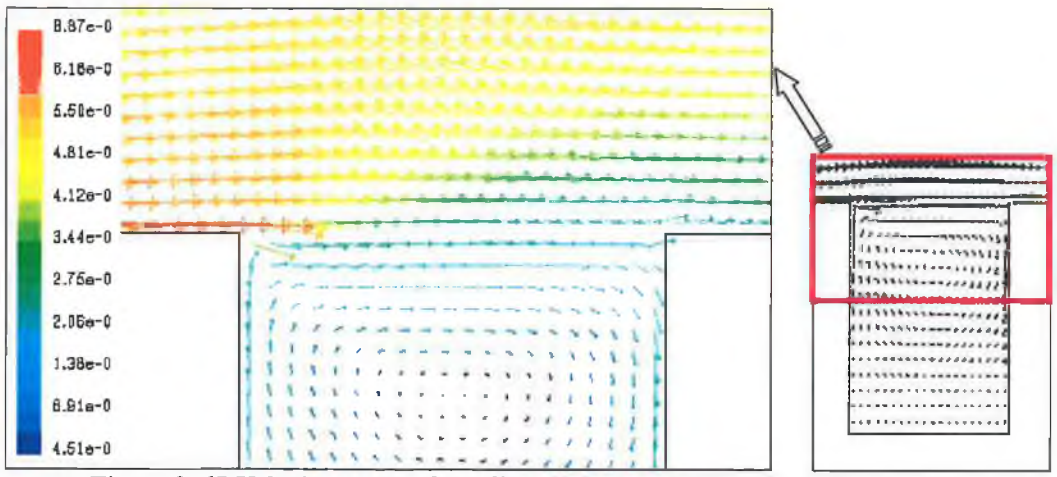

Figure 3. 65:Velocity vectors for a 2DL sharp tee at 0.5m/s and 1D extension

Circulation noted around the branch. This circulation was driven by flow across the top of the branch inducing motion in the dead-leg.

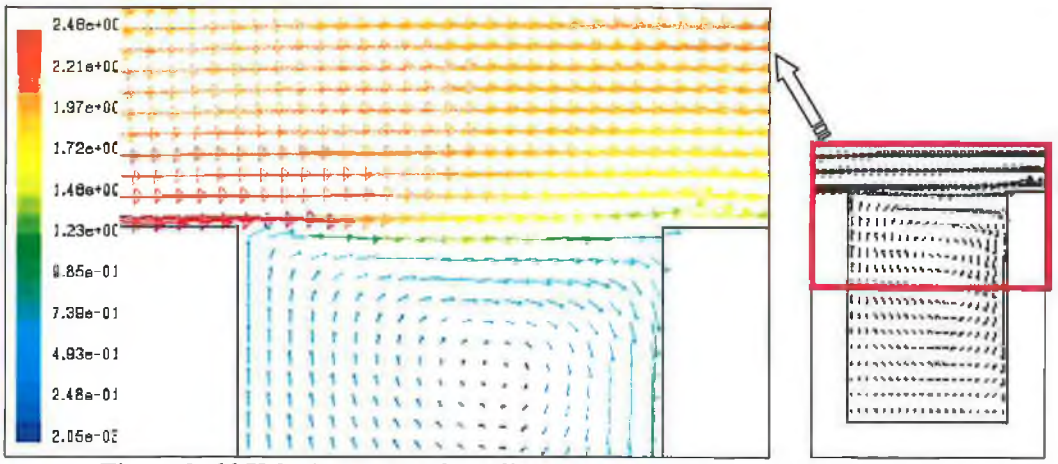

Figure 3. 66:Velocity vectors for a 2DL sharp tee at 2m/s and 1D extension

With increasing mainstream velocity higher flowrate on downstream wall. Only one primary region visible. Rotating cavity noted off-set towards downstream wall. Trends for both high and low velocities similar to there noted without the bend.

3.4.7 Tee-junction with a bend, 1D extension and 4D dead-leg

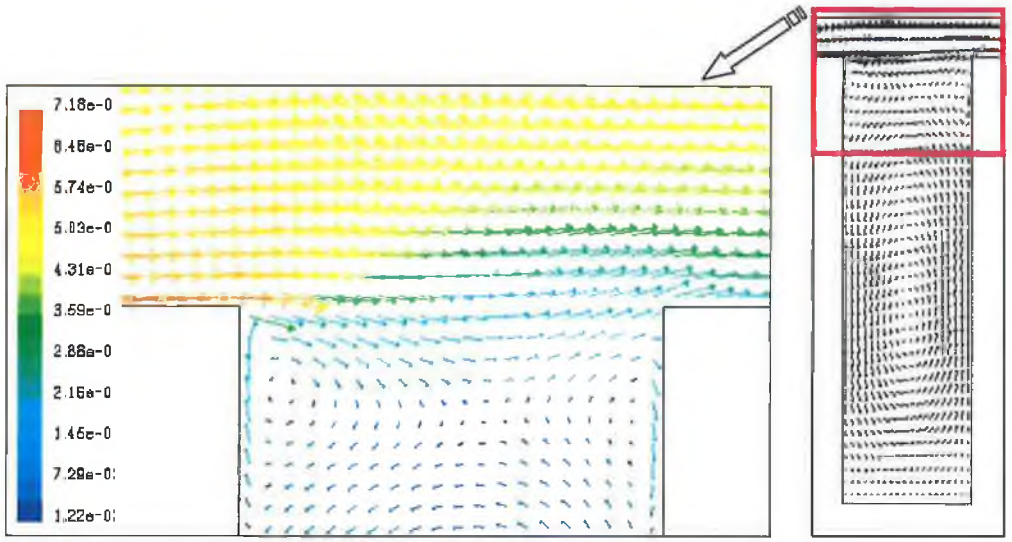

Figure 3. 67:Velocity vectors for a 4DL sharp tee at 0.5m/s and 1D extension

Increased length of the dead-leg results in separation of flow. Three re-circulating zones noted. Two high up the branch and one large zone further into the dead-leg.

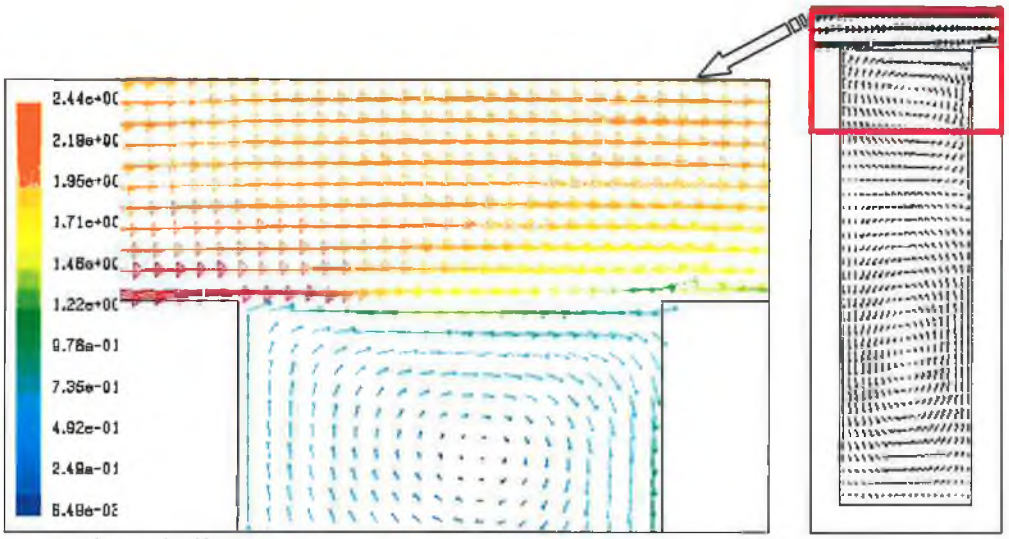

Figure 3. 68:Velocity vectors for a 4DL sharp tee at 2m/s and 1D extension

Similar to 2D in primary zone however secondary zone also visible further into branch. Flow pattern revert to these seen at similar velocities without a bend.

3.4.8 Tee-junction with a bend, 1D extension and 6D dead-leg

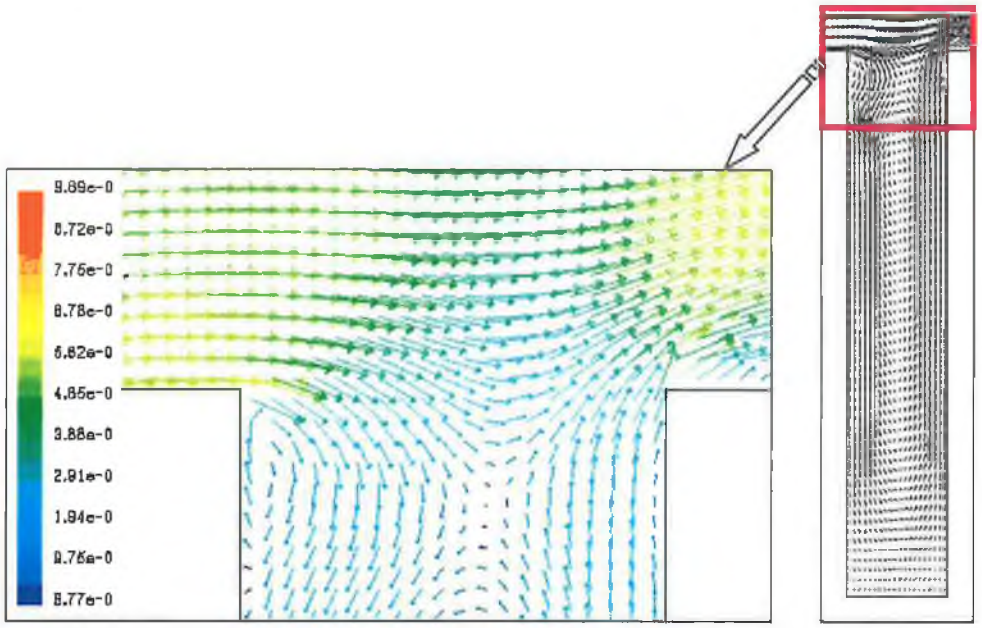

Figure 3. 69:Velocity vectors for a 6DL sharp tee at 0.5m/s and 1D extension

6D dead-leg resulted in complex flow pattern in primary zero. 3 zones still present however there was further penetration into the branch. The additional length of the dead-leg contributes to the increased penetration in the primary zone.

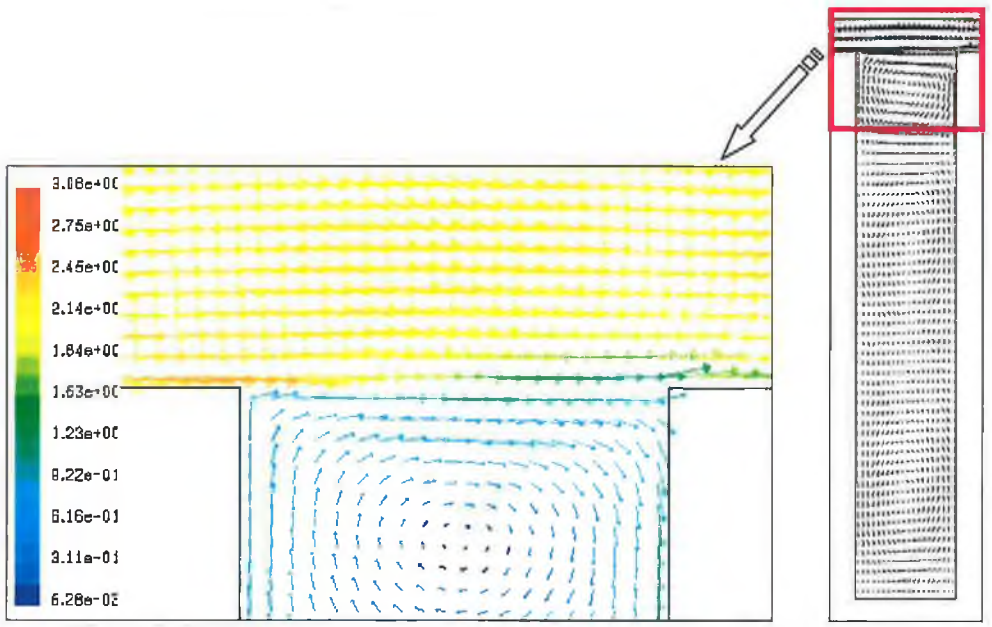

Figure 3. 70:Velocity vectors for a 6DL sharp tee at 2m/s and 1D extension

Primary re-circulating zone centered within the branch and not off-set towards the downstream wall. Very little penetration into the branch.

3.4.9 Tee-junction with a bend, 3D extension and 1D dead-leg

Velocity vectors for 3D extensions upstream of the branch are now presented in figures 3.71 to 3.78 for 1D, 2D, 4D and 6D branch lengths.

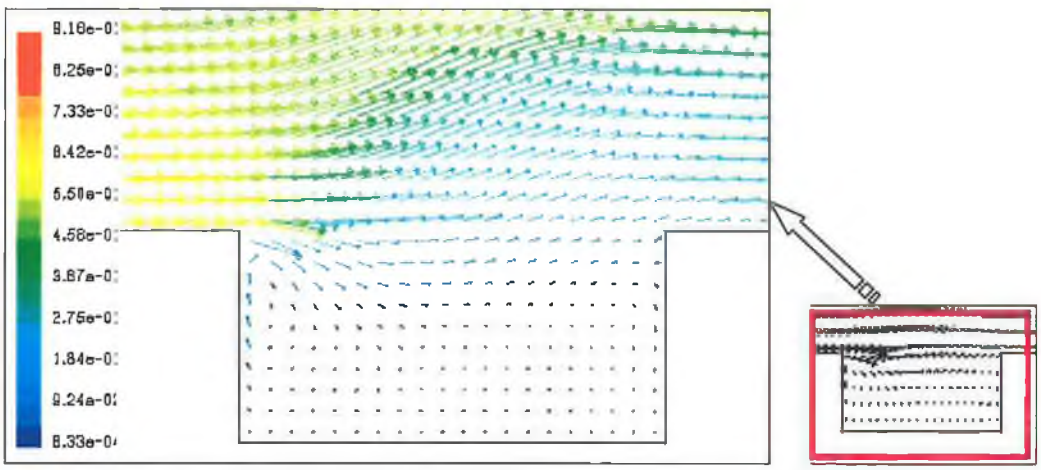

Figure 3. 71:Velocity vectors for a 1DL sharp tee at 0.5m/s and 3D extension

Little change and little motion within the dead-leg. Although a small re-circulation zone was noted on the upstream wall of the branch. Very little movement within the branch.

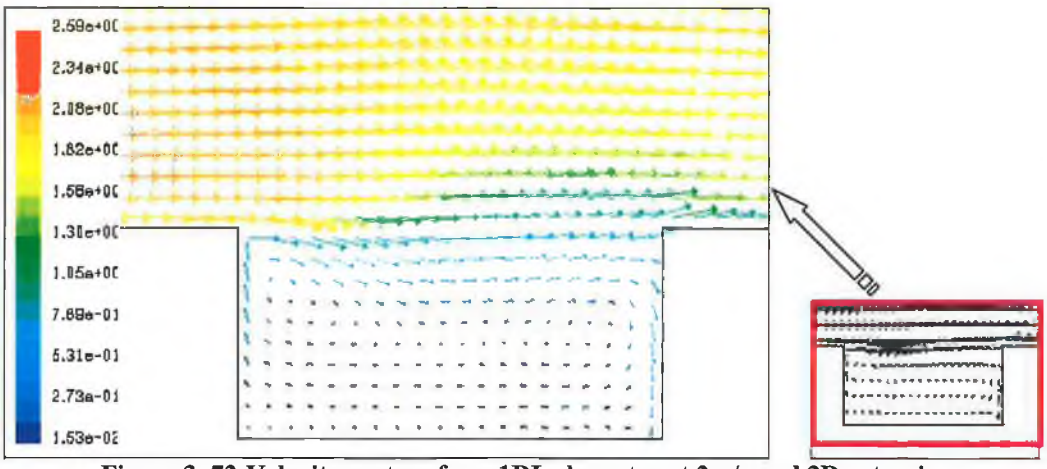

Figure 3. 72:Velocity vectors for a 1DL sharp tee at 2m/s and 3D extension

Same penetration into branch along the upstream wall. Penetration of the mainstream flow into the dead-leg is evident although towards the base of the dead-leg little escalating of fluid occurs

3.4.10 Tee-junction with a bend, 3D extension and 2D dead-leg

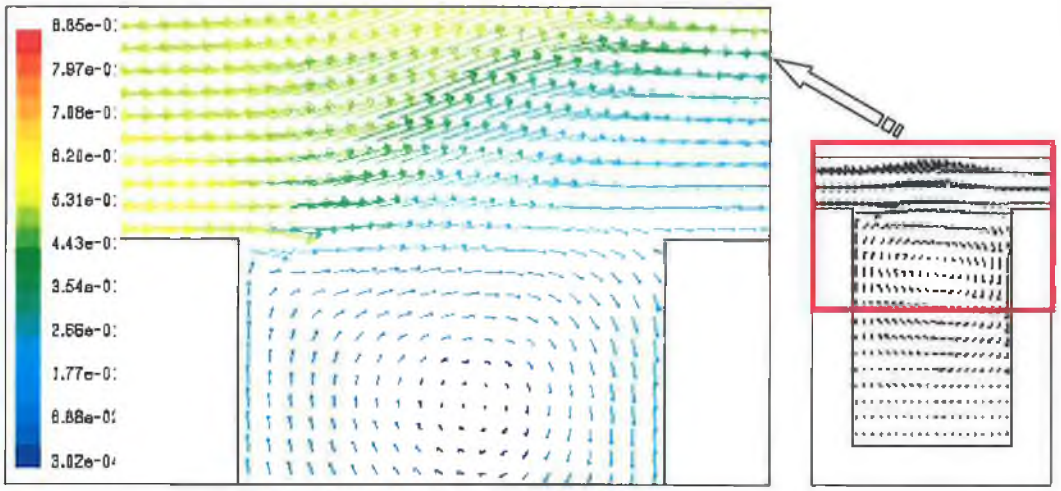

Figure 3. 73:Velocity vectors for a 2DL sharp tee at 0.5m/s and 3D extension

The introduction of a 2D dead-leg results in the development of a primary re-circulation zone within the branch

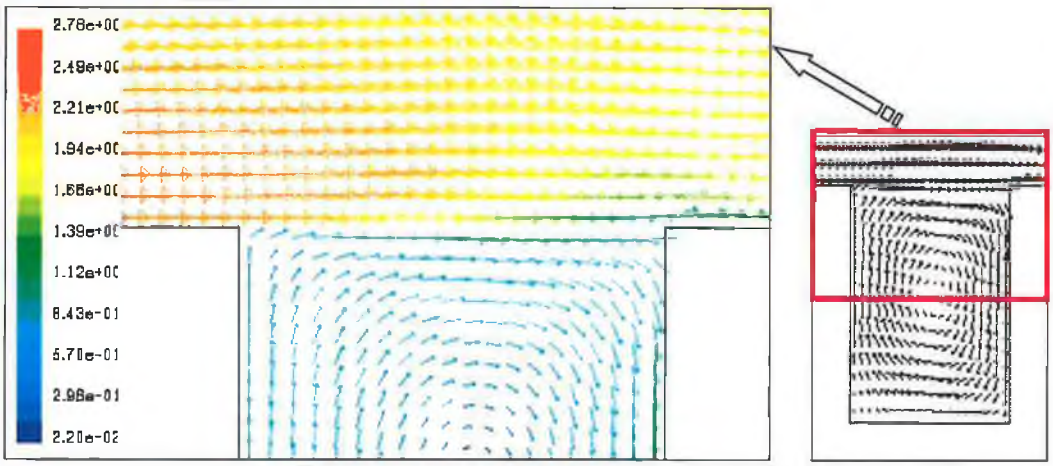

Figure 3. 74:Velocity vectors for a 2DL sharp tee at 2m/s and 3D extension

Similar flow patterns to these noted a low velocity. However higher velocities noted within the dead-leg zone. Motion is noted down into the branch along the downstream wall into the branch.

3.4.11 Tee-junction with a bend, 3D extension and 4D dead-leg

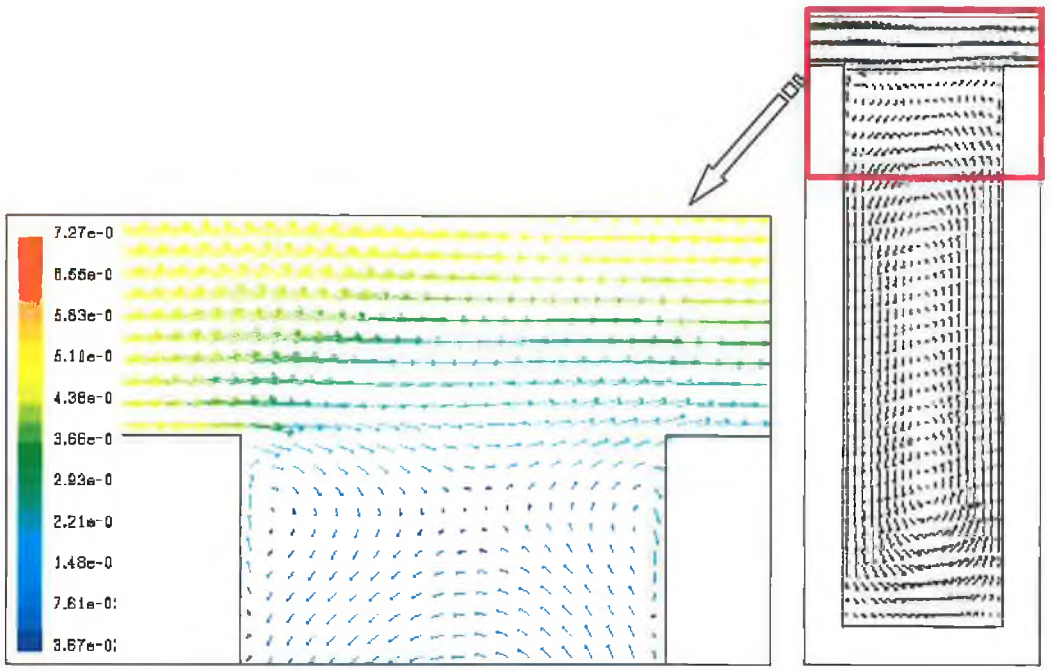

Figure 3. 75:Velocity vectors for a 4DL sharp tee at 0.5m/s and 3D extension

3D section downstream of the bend results in similar flow patterns to that of 1D extension in fig 3.67.

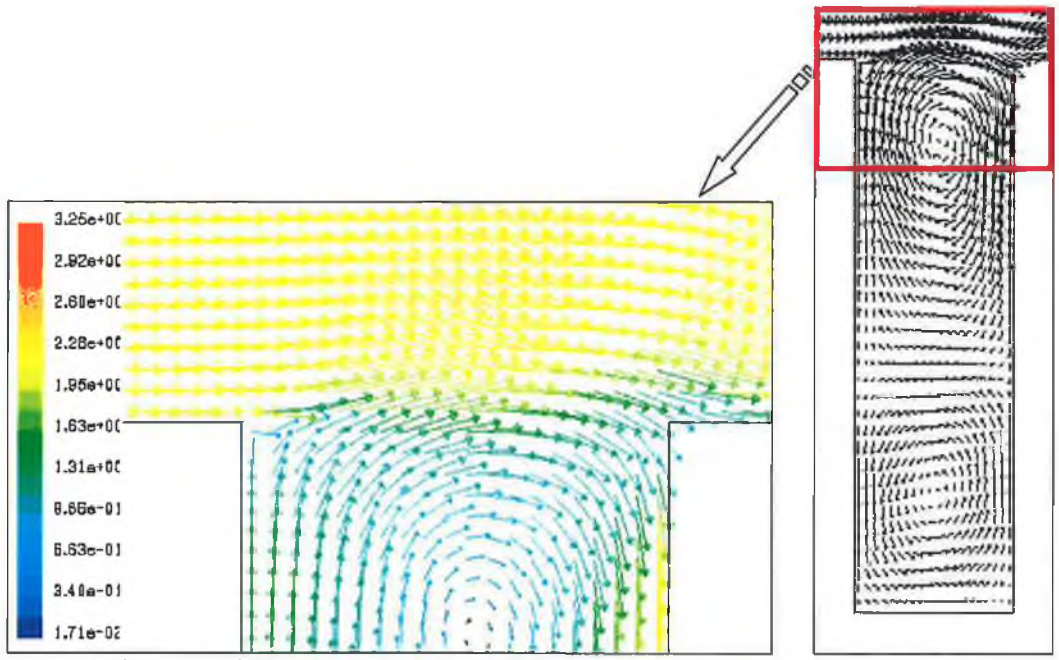

Figure 3. 76:Velocity vectors for a 4DL sharp tee at 2m/s and 3D extension

The primary recirculation zone had disturbed the mainstream flow. The result is a moving of the rotating cavity out of the dead-leg branch and the formation of a secondary zone deep into the dead-leg. This important development could improve penetration ….. way into the 4D zone.

3.4.12 Tee-junction with a bend, 3D extension and 6D dead-leg

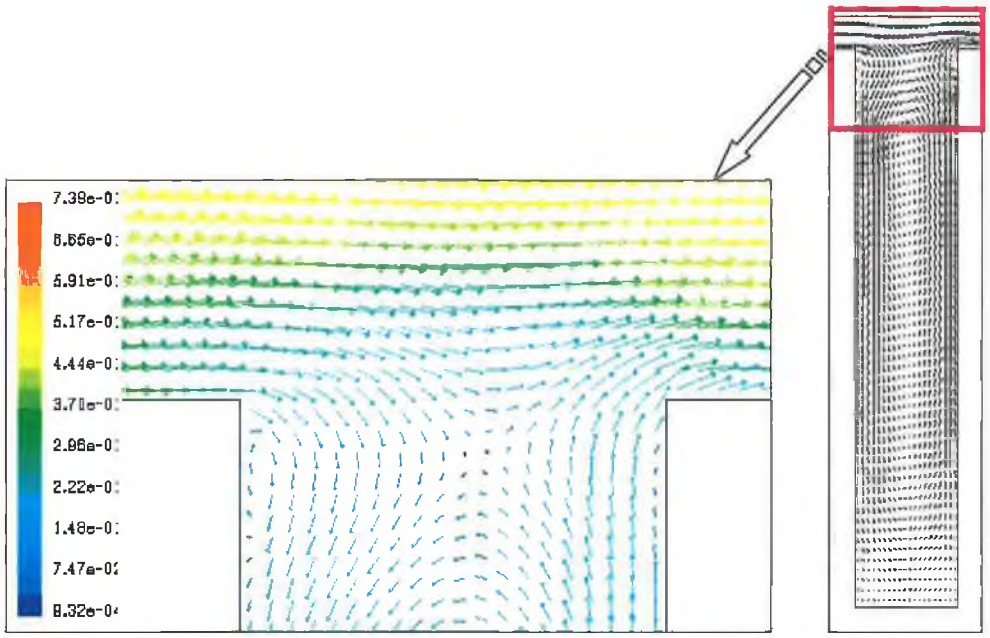

Figure 3. 77:Velocity vectors for a 6DL sharp tee at 0.5m/s and 3D extension

No significant change when compared to 1D extension data.

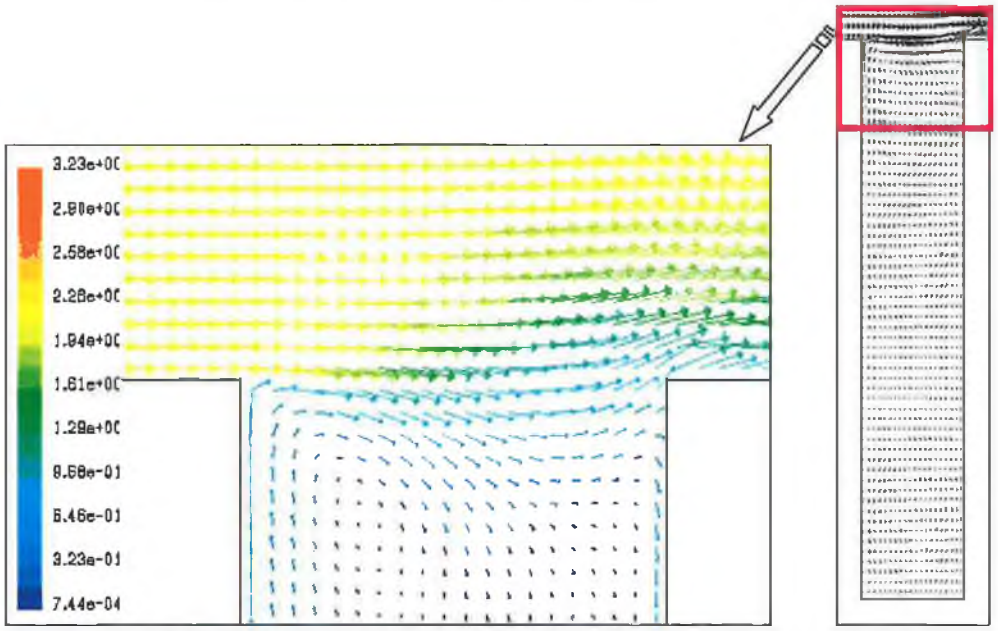

Figure 3. 78:Velocity vectors for a 6DL sharp tee at 2m/s and 3D extension

General lack of penetration into the branch with a recirculation zone noted along the downstream wall. Length of the dead-leg prevents penetration of the mainstream flow.

3.4.13 Velocity plots for 1DL, 2DL, 4DL and 6DL with 1D extension and velocity of 0.5&2 m/s

High flowrates noted on both the upstream and downstream walls. At this particular depth a maximum velocity was noted using 4D configuration. Higher penetration into the branch as compared to 1D extension (figure 3.64)

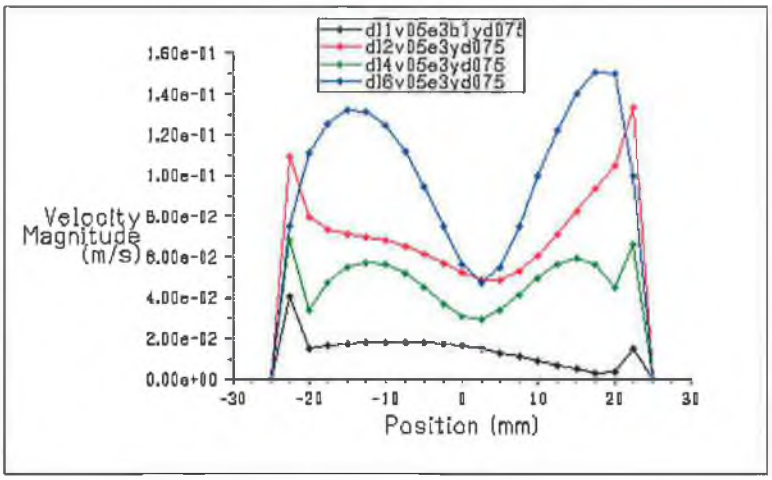

Figure 3. 79:y-Velocity plots at y/D=0.75, 3D extension and 2m/s for1D, 2D, 4Dand6D dead-leg length

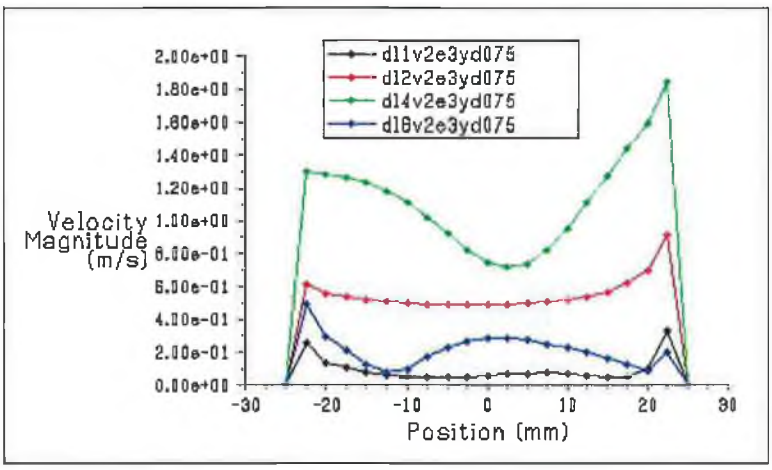

Figure 3. 80:y-Velocity plots at y/D=0.75, 3D extension and 2m/s for1D, 2D, 4Dand6D dead-leg length

3.4.14 Velocity plots for 1DL, 2DL, 4DL and 6DL sharp tee with bend and 1D extension

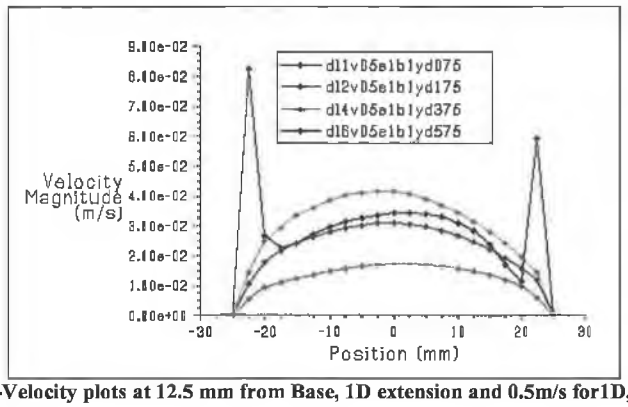

Figure 3. 81:y-Velocity plots at 12.5 mm from Base, 1D extension and 0.5m/s for1D, 2D, 4Dand6D

Dead-leg	Velocity (m/s)	
	Max	Min
1D	0.083	0.015
2D	0.018	0.005
4D	0.042	0.018
6D	0.03	0.016

Table 3. 1:Max and min velocity at 12.5 mm from Base, 1D extension and 0.5m/s for1D, 2D, 4Dand6D

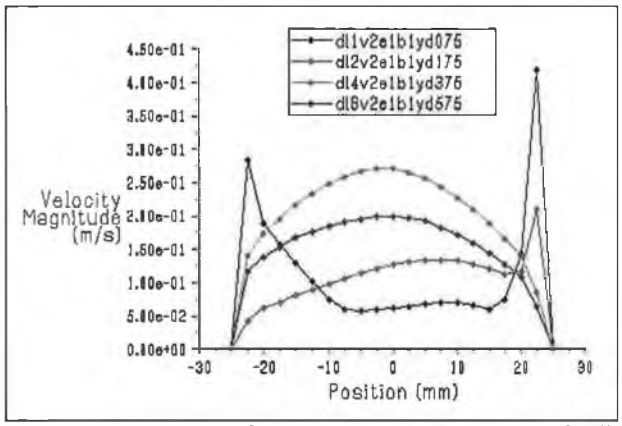

Figure 3. 82:y-Velocity plots at 12.5 mm from Base, 1D extension and 2m/s for1D, 2D, 4Dand6D

Dead-leg	Velocity (m/s)	
	Max	Min
1D	0.42	0.055
2D	0.2	0.04
4D	0.255	0.1
6D	0.2	0.055

Table 3. 2:Max and min velocity at 12.5 mm from Base, 1D extension and 2m/s for1D, 2D, 4Dand6D

3.4.15 Velocity plots for 1DL, 2DL, 4DL and 6DL sharp tee with bend and 3D extension

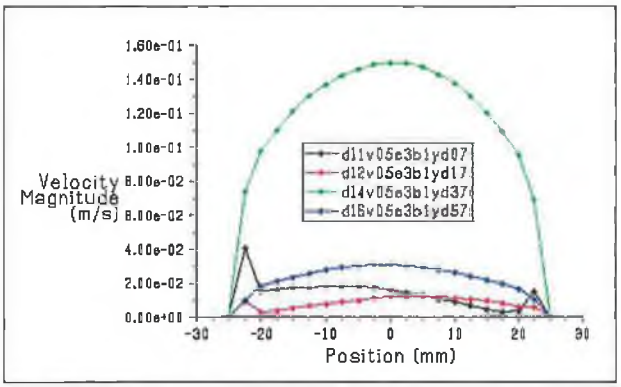

Figure 3. 83:y-Vclocity plots at 12.5 mm from Base, 3D extension and 0.5m/s for1D, 2D, 4Dand6D

Dead-leg	Velocity (m/s)	
	Max	Min
1D	0.04	0.055
2D	0.01	0.025
4D	0.15	0.005
6D	0.027	0.01

Table 3. 3:Max and min velocity at 12.5 mm from Base, 3D extension and 0.5m/s for1D, 2D, 4Dand6D

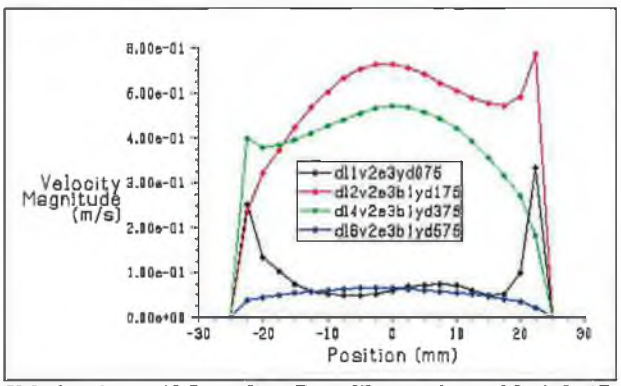

Figure 3. 84:y-Velocity plots at 12.5 mm from Base, 3D extension and 2m/s for1D, 2D, 4Dand6D

Dead-leg	Velocity (m/s)	
	Max	Min
1D	0.35	0.05
2D	0.6	0.025
4D	0.45	0.2
6D	0.05	0.02

Table 3. 4:Max and min velocity at 12.5 mm from Base, 3D extension and 2m/s for1D, 2D, 4Dand6D

3.4.16 Velocity plots for 1DL, 2DL, 4DL and 6DL sharp tee with bend and 6D extension

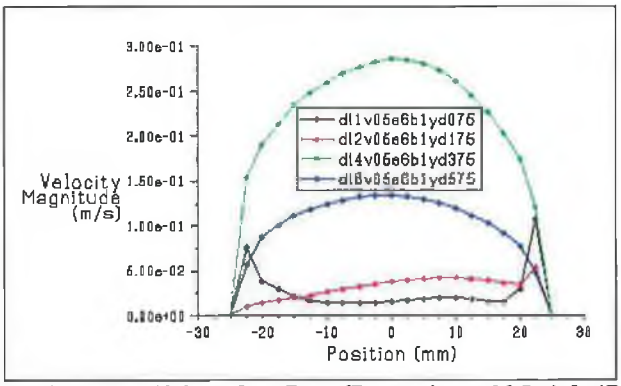

Figure 3. 85:y-Velocity plots at 12.5 mm from Base, 6D extension and 0.5m/s for1D, 2D, 4Dand6D

Dead-leg	Velocity (m/s)	
	Max	Min
1D	0.12	0.02
2D	0.06	0.02
4D	0.257	0.125
6D	0.13	0.05

Table 3. 5:Max and min velocity at 12.5 mm from Base, 6D extension and 0.5m/s for1D, 2D, 4Dand6D

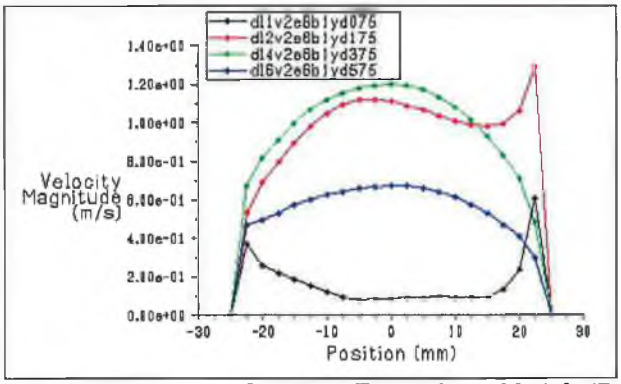

Figure 3. 86:y-Velocity plots at 12.5 mm from Base, 6D extension and 2m/s for1D, 2D, 4Dand6D

Dead-leg	Velocity (m/s)	
	Max	Min
1D	0.04	0.055
2D	0.1	0.025
4D	0.12	0.005
6D	0.027	0.01

Table 3. 6:Max and min velocity at 12.5 mm from Base, 6D extension and 2m/s for1D, 2D, 4Dand6D

3.4.17 Velocity plots for 1DL, 2DL, 4DL and 6DL sharp tee with a bend and 9D extension

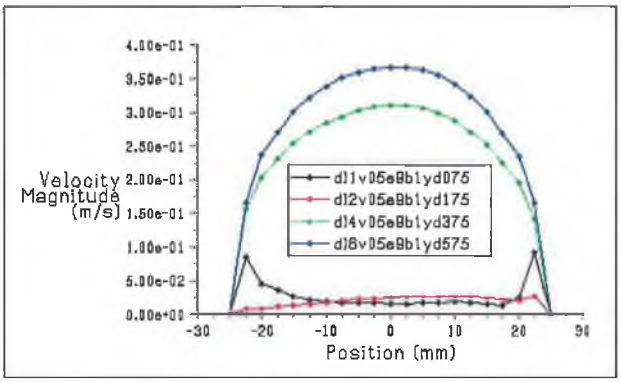

Figure 3. 87:y-Velocity plots at 12.5 mm from Base, 9D extension and 0.5m/s for1D, 2D, 4Dand6D

Dead-leg	Velocity (m/s)	
	Max	Min
1D	0.1	0.02
2D	0.03	0.01
4D	0.32	0.15
6D	0.355	0.154

Table 3. 7:Max and min velocity at 12.5 mm from Base, 9D extension and 0.5m/s for1D, 2D, 4Dand6D

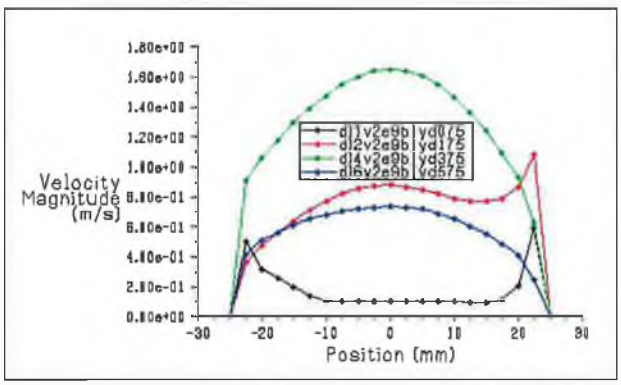

Figure 3. 88:y-Velocity plots at 12.5 mm from Base, 9D extension and 2m/s for1D, 2D, 4Dand6D

Dead-leg	Velocity (m/s)	
	Max	Min
1D	0.6	0.1
2D	1.1	0.38
4D	1.65	0.6
6D	0.7	0.3

Table 3. 8:Max and min velocity at 12.5 mm from Base, 9D extension and 2m/s for1D, 2D, 4Dand6D

EFFECT OF DEAD-LEG LENGTH ON THE FLOW VELOCITY

The main requirement in relation to dead-legs is to encourage movement within each branch configuration. The effect of upstream extension before a range of dead-leg branch sizes (1D-6D) was analysed for mainstream velocities of 0.5-2 m/s

To examine the effect of extension length on 1, 2, 4 and 6D dead-leg length, some velocity plots have been analysed at the base of each dead-leg branch, where usually the lowest flow velocity occurs.

In this section, each extension of 1D, 3D, 6D and 9D is studied with the 1, 2, 4 and 6 dead-leg lengths at 0.5m/s and 2m/s mainflow velocities.

1-1D extension

Figure 3.81 shows the velocity plots at 12.5mm from the dead-leg base at 1D extension with a bend and 0.5m/s for 1DL, 2DL, 4DL and 6DL. It can be observed that the peak velocity occurs near the upstream wall with 1DL, and along the centre of the branch with 4DL. Maximum and minimum velocities were 0.083m/s and 0.015 respectively for 1DL, and 0.04m/s and 0.016m/s respectively for 4DL (table 3.1).

At 2m/s mainflow velocity the highest velocity was obtained near the downstream wall with 1DL, however the greatest flow velocity in the middle of the pipe was found with 4DL (figure 3.82). The author noted that 1D extension has similar flow behaviour at high and low mainflow velocities except the peak velocity of 1DL was found near the upstream wall at 0.5m/s mainflow velocity where as greatest velocity at 2m/s mainflow was found near the downstream wall, irrespective of magnitudes.

2-3D extension

When the entrance of the tee pipe was extended to 3D, a noticeable difference in flow behaviour at 4DL extension and 0.5m/s mainflow velocity occurs. The largest flow recorded in the branch was 0.15m/s, with the lowest of 0.01m/s occurring with 2DL (figure 3.83, table 3.3).

At 2DL the highest flow velocity recorded was 0.6m/s at downstream wall. With 4DL, the maximum velocity recorded was 0.45m/s. 6DL had the lowest flow velocity with a maximum velocity of 0.05m/s occurring as shown in figure 3.84 and table 3.4.

3-6D extension

The trend is very similar to that obtained in 3D extension at 0.5 m/s mainflow velocity. However the velocity flow with 6DL in this case (with 6D extension) is higher than the previous case with an extension of 3D. At 2m/s mainflow velocity with 6D extension, the greatest overall velocity was found with 4DL, however the peak velocity occurs with 2DL near the downstream wall as shown in figure 3.86

4-9D

At mainflow velocity of 0.5m/s 6DL has the greatest flow in the branch while the best flow movement occurred at 4DL when the mainflow velocity is 2m/s (figures 3.87, 3.88)

Summary:

The overall results in relation to extension upstream of dead-leg is that irrespective of extension length a 4D branch offers the best result for the range of velocities examined. Therefore in industrial application a 4D branch should be used insteadly of the FDA 6D-Rule.

3.4.18 Velocity plots for 4DL sharp tee with bend and 9D extension

As the largest velocities were found at 4DL with 9D extension, figure 3.89 shows the velocity plots of 4DL dead-legs at different mainflow velocities of 0.5, 1, 1.5 and 2 m/s. The figure revealed that the higher velocities occurred at 4DL in all of the mainflow velocities, compared to their counterpart at 1DL, 2DL and 6DL.

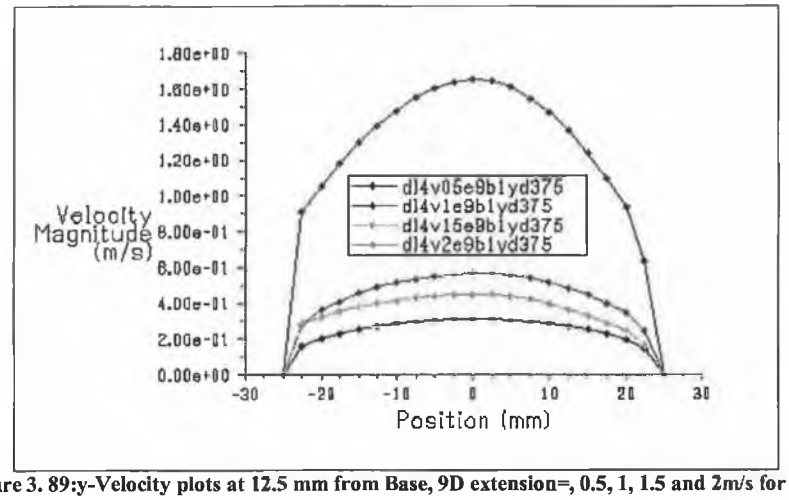

Figure 3. 89:y-Velocity plots at 12.5 mm from Base, 9D extension=, 0.5, 1, 1.5 and 2m/s for 4DL

Velocity Magnitude m/s	4DL	
	Max	Min
0.5	0.3	0.15
1	0.55	0.28
1.5	0.4	0.2
2	1.65	0.65

Table 3. 9:Max and min velocity at 12.5 mm from Base, 9D extension, 0.5, 1, 1.5 and 2m/s for 4DL

We can conclude the following:

1. Increase the entrance length of tee reflects an improvement in the flow of all dead leg length branches (1DL, 2DL, 4DL and 6DL).
2. High velocity in the mainstream flow gives better flow movement in 2DL and 4DL while the low mainstream velocity results in better flow at 6DL with different length extension.
3. At low mainflow velocities, 4DL and 6DL are preferred flow movement compared with 2DL, where as at high velocities 2DL and 4DL have a more improved flow than 6DL
4. 2DL leads to a good flow movement of the dead leg only at high main flow velocities.
5. 4DL shows a reasonable flow velocity of the branch in both high and slow main flow velocities.

Chapter Four
Rig Design & Flow Visualisaion

CHAPTER 4. RIG DESIGN & FLOW VISUALISATION

4.1 Experimental Rig

A test rig was modified to allow flow visualisation studies on various dead-leg test sections to be investigated. The rig consists of a recirculation loop, glass dead-leg test section, pump, flow regulating valve, flowmeter and storage tank.

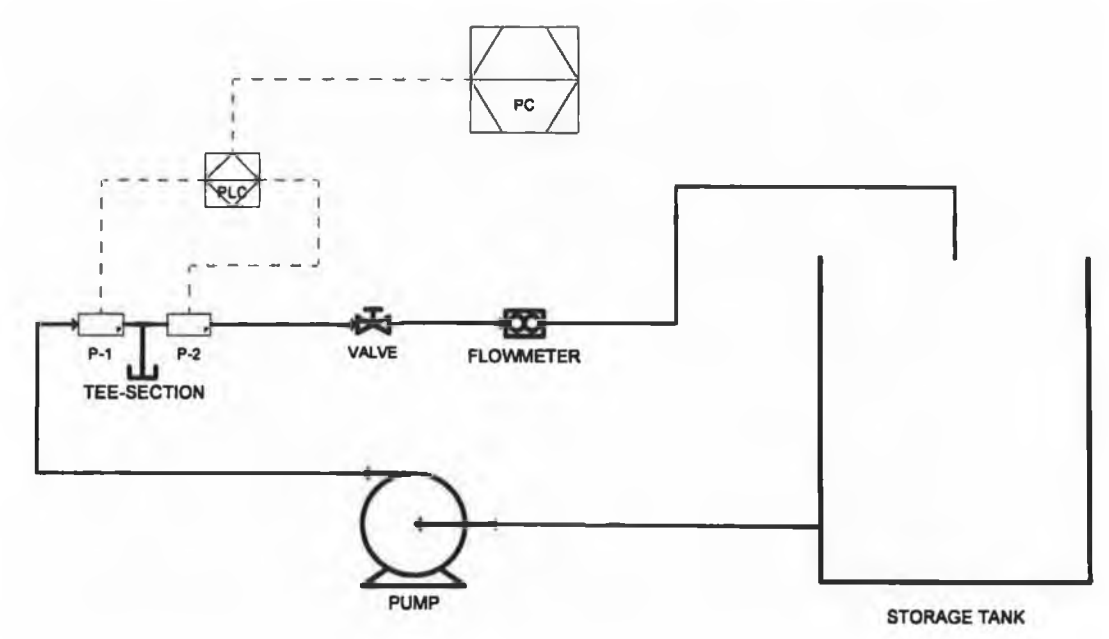

Figure 4. 1:Experimental Fluid Work

A schematic of the fluid rig used is shown in figure (4.1) and a description of the equipment is given in table 4.1

Item	Description	Manufacturer	Model
PUMP	Centrifugal Pump	Grundfos	CHI 12-10
STORAGE TANK	Open tank	DCU Workshop	n/a
VALVE	Globe Valve	Crane	D921

Table 4. 1: Equipment list

Water was pumped from a large stainless steel storage tank. From the pump, water flowed through a series of 90° bends before entering a straight length of pipe upstream of the glass test section.

Calculating a suitable entrance length using equation (1) to ensure fully developed turbulent flow upstream of the test section.

$$\ell_e = 4.4D\,(Re)^{1/6} \qquad (1)$$

$$Re = \frac{\rho v D}{\mu} = \frac{1000\ kg/m^3(0.5m/s)(0.05m)}{0.0008\ \ kg/m\text{-}s} = 31\times 10^4$$

$$\ell_e = 4.4(0.05)\,(31\times 10^4)^{1/6}$$

$$\ell_e = 1.23\ m$$

The 3m straight pipe length approaching the tee installed on the fluid rig will ensure fully developed flow. Following the straight length upstream of the test section another length measuring 1.5m was placed after the tee section.

After another series of 90° bends the fluid past a flowmeter. Flowrates were regulated via a control valve. Pressure transducers positioned upstream and downstream of the tee-section recorded pressure at entry and exit.

Item	Description	Manufacturer	Model
FLOWMETER	Metal tube Variable area flowmeter	InFlux	FloTrak
P-1	Pressure Transducer	Gem Sensors	2200B9A2501A3UA
P-2	Pressure Transducer	Gem Sensors	2200B9A2501A3UA
PC	Desktop Compute	Elonex	PC-6200/I
PLC	High resolution data logger	PICO	ADC-16

Table 4. 2: Instrumentation list

The glass section used for flow visualisations studies is displayed in figure 4.2 and figure 4.3 with attached septum ports. The section was manufactured by Allied Glass Blowers (AGB), Glasnevin, Dublin. The flanged or ferrule edges of the section were mated with the flanges/ ferrules on the stainless steel tee-section and held with tri-clamps. Restriction of flow from the tee-section served to create a dead-leg scenario within the branch-leg. Tee-sections used in the experiment are described in table 4.3

Tee Size	Manufacturer	Dimension	Material
2D	AGB Scientific	100mm length	Tempered Glass
4D	AGB Scientific	200mm length	Tempered Glass

Table 4. 3: Tee-section specifications

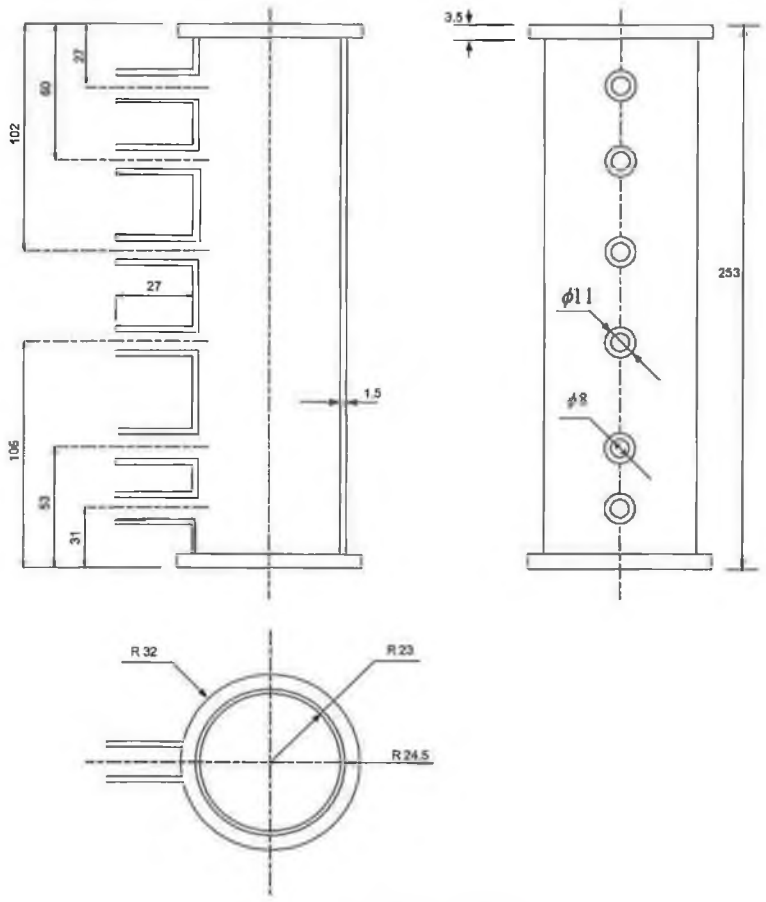

Figure 4. 2:Glass Section

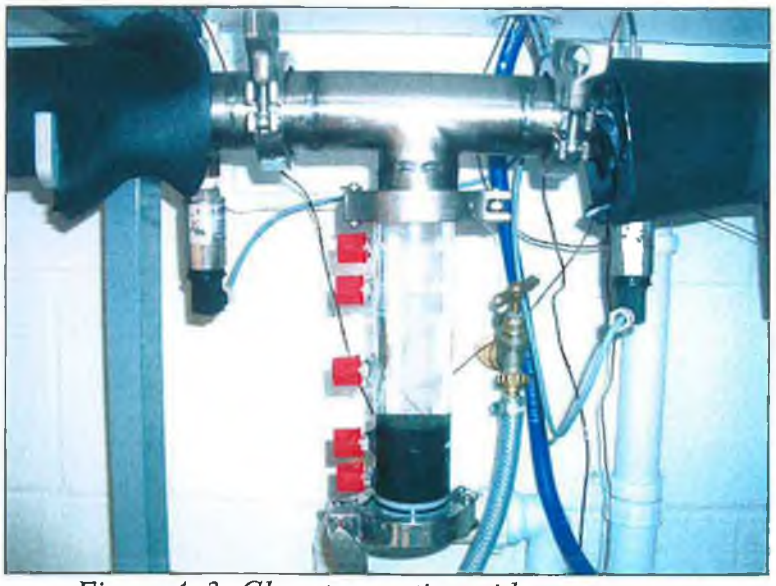

Figure 4. 3: Glass tee-section with septum ports

4.2 Rig Flowrates

The rig was operated at different flowrates to fully demonstrate flow patterns within a dead-leg for turbulent flows. Flowrates are shown in table 4.5. An expression (2) is required to convert rig flowrate into volumetric flowrate (see fig 4.4). The equation to calculate fluid velocity is given by equation (3).

Figure 4. 4:Flowmeter

$$1 \frac{L}{min} \left(\frac{10^{-3}}{60}\right) = 1 \text{ m}^3/\text{s} \quad (2)$$

$$A = V.\ v \quad (3)$$

The cross sectional area for flow is given by (4) for a pipe section radius r

$$A = \pi r^2 \quad (4)$$

Fluid velocity, v (m/s)	Rig flowrate (L/min)
0.5	**58.9**
1.5	**176.7**

Table 4. 4: Experimental flowrates

4.3 Die Injection Procedure

This section explains the experimental procedure used for flow visualization studies. By adhering to such experimental procedures, the author aims to insure consistency

of test conditions. The experimental procedure for injecting dye into the dead-leg is as follows:

1. Adjust flow valve to required flowrate
2. Attach digital camera to tripod and position recording equipment a suitable distance in front of tee section.
3. Fill syringe with 0.5 ml of prepared dye.
4. Inject dye via septum points. Record images of flow pathlines and start the stopwatch.
5. Wait until the tee section becomes completely clean from the dye, and then record the time.
6. Repeat for various injection points and flowrates.

4.4 Results

Using a PENTAX Optio S digital camera 3.2 Megapixels 3x optical zoom with tripod stand the flow pattern of dye is recorded. Images are taken as a series of pictures over period of seconds (unless otherwise stated) apart to illustrate the flow pattern. Streakline images within the dead-leg are presented with descriptions of the flow they represent. Dye is injected with the same amount (0.5ml) in a slow consistent manner to avoid unnatural over-mixing with the water, ensure clearer visuals and compare the time needed to clear branch from the dye.

4.5 Tee Inlet Velocity 0.5 m/s

Operating the system rig at a flow rate of 0.5 m/s, dye was injected at the base via septum points into the dead-leg. Image 4.1 shows the flow pattern of dye injected at the base of the tee-section, 4D depth. The dye has begun to disperse immediately with the water. The dye flows across the base of the dead-leg towards the downstream wall.

Image 4.2 shows the dye flow pattern along the downstream wall. The dye was found to slowly travel up the downstream wall of the dead-leg. Very little dye traveled above 2D indicating a capping of the flow by fast flowing fluid above this zone. Fluid in this 2D zone was slowly rotating fluid. After 2 or 3 seconds the dye continue swirling where image 4.3 is taken.

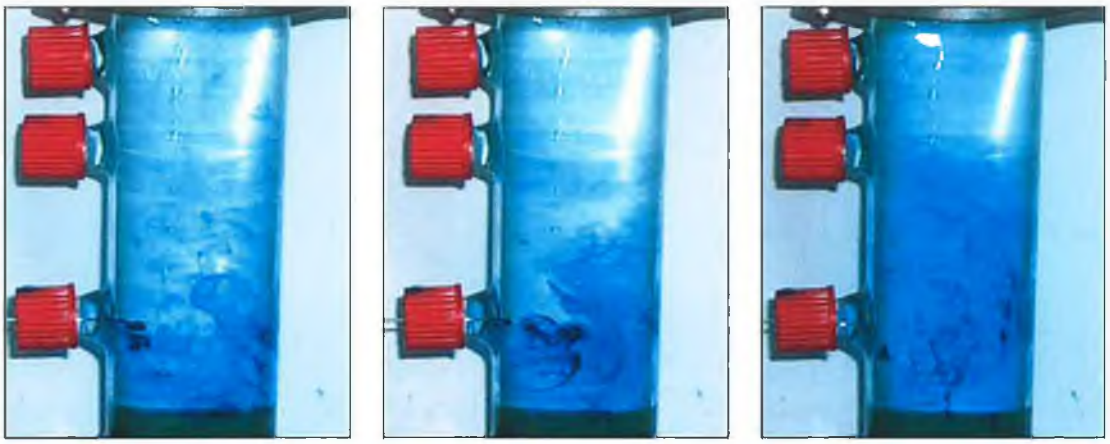

Image 4.1 **Image 4.2** **Image 4.3**

Figure 4. 5: Dye injection images for a 4D dead-leg at 0.5m/s

Image 4.4 displays that as dye is injected at 2D a separation of the fluid in the dead-leg is taking place. The dye is drawn down the upstream wall of the tee by a secondary circulation region. Injecting slightly higher as in image 4.5 a noticeable primary re-circulation zone occurs where the dye moves up to the mouth of the tee suggesting dye has been injected in between the two re-circulations zones, movement in the primary zone (2D and above) is clockwise and below this zone is anti-clockwise as shown in image 4.6.

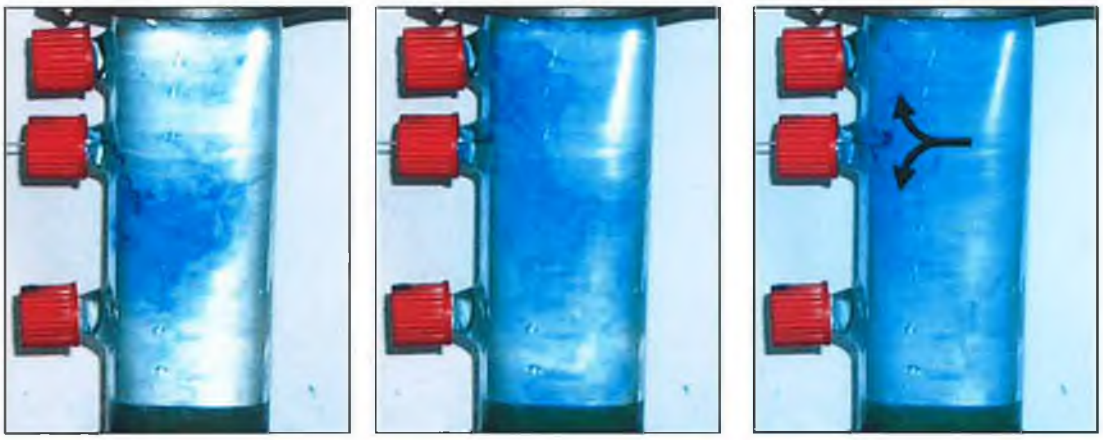

Image 4.4 **Image 4.5** **Image 4.6**

Figure 4. 6: Dye injection images for a 4D dead-leg at 0.5m/s

Images 4.7 – 4.9 highlight flow patterns when dye is injected close to the mouth of the dead-leg. The dye immediately dispersed across the tee to the downstream wall, quickly coloring the primary zone. Dye penetration into the secondary zone is at a slow rate, the secondary zone is not completely exposed to dye at any point.

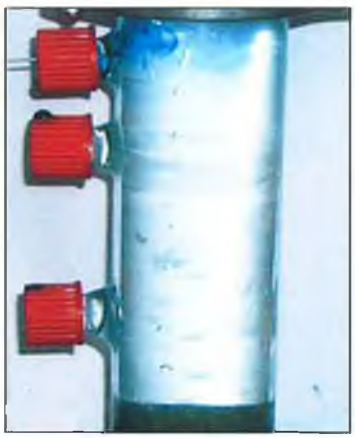
Image 4.7


Image 4.8


Image 4.9

Figure 4. 7: Dye injection of the top of 4D dead-leg at 0.5m/s.


Image 4.10


Image 4.11


Image 4.12

Figure 4. 8: Dye injection along the downstream wall of a 4D dead-leg at 0.5m/s.

Injecting close to the downstream wall highlights further the gradual movement of the fluid up the downstream wall of the dead leg (Images 4.10 – 4.11). It should be noted that it is possible for some exchange of fluid between the primary and secondary zone as highlighted by dye penetration shown in image 4.12. Dye injected towards the base of the tee has colored the primary zone.

4.6 Tee Inlet Velocity 1.5 m/s

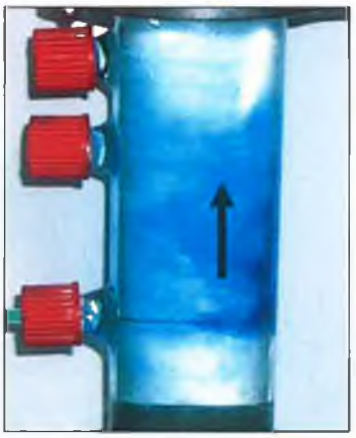
Image 4.13


Image 4.14


Image 4.15

Figure 4. 9: Dye injection at 4D at 1.5m/s.

An increase in velocity from 0.5 m/s to 1.5 m/s resulted in a very different flow pattern in the branch. The dye was found to rapidly disperse indicating higher flow velocities with the dead-leg (Image 4.13). Images 4.14-4.15 show the test section colored by the dye indicating an exchange of fluid between the primary and secondary zone. Dye concentrates at the base indicating a slower motion in the secondary zone.


Image 4.16


Image 4.17


Image 4.18

Figure 4. 10: Dye injection at the base of a 4D dead-leg at 1.5m/s.

Injecting dye close to the base resulted in dye immediately dispersed across the tee to the downstream wall as shown in images 4.16-4.17, where at low velocity the dye is drawn towards the base of the tee section. It is clear that the circulations are faster and more turbulent at high velocity.



Image 4.19 **Image 4.20** **Image 4.21**

Figure 4. 11: Dye injection at 2D into a 4D dead-leg at 1.5m/s.

Image 4.19-4.21 highlighted flow pattern in the primary zone. Once injected the dye flows up along the upstream wall. As it approached the top of the tee it is immediately mixed by fast flowing fluid and dispersed throughout the primary zone. This indicates very high velocity in this region.

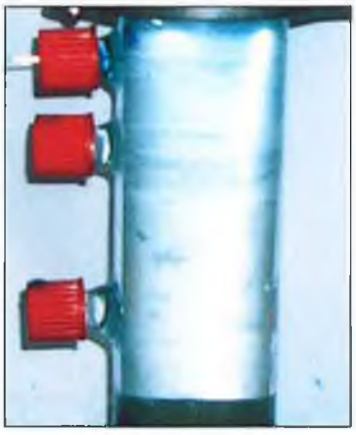

Image 4.22 **Image 4.23** **Image 4.24**

Figure 4. 12: Dye injection of the top of a 4D dead-leg at 1.5m/s.

This is also highlighted by injection close to the top of the branch, the dye is rapidly dispersed throughout the primary zone.

4.8 Tee Inlet Velocity 0.5 m/s

To analyse the effect of reducing dead-leg length on flow patterns, a stopper was designed and installed into the glass branch to reduce the dead-leg length to 2D. As series of tests at 0.5 – 1.5 m/s were evaluated and the flow pattern presented in the following images. The following set of results highlight the flow pattern for a 2D dead-leg configuration this was achieved by moving the stopper to a position of 2D within the glass test section & preventing flow beyond that depth.

Image 4.25 **Image 4.26** **Image 4.27**

Figure 4. 13: Dye injection at the base of a 2D dead-leg at 0.5m/s.

As the dye injected in at the base of the 2D dead-leg, it immediately dispersed coloring the glass section (images 4.25, 4.26, 4.27). this highlights the rapid mixing and motion within a branch of this length.

Image 4.28 **Image 4.29** **Image 4.30**

Figure 4. 14: Dye injection of the top of a 2D dead-leg at 0.5m/s.

When the dye was injected in the middle of the dead-leg, it dispersed immediately coloring the glass section indicating high swirling and moving towards the mouth of the tee as shown in images 4.28, 4.29, 4.30. Image 4.29 highlights a swirl region that was evident in some of the CFD studies at 2D.

4.9 Tee Inlet Velocity 1.5 m/s

Image 4.31 **Image 4.32** **Image 4.33**

Figure 4. 15: Dye injection along the downstream wall of a 2D dead-leg at 1.5m/s.

The effect of increasing velocity to 1.5 m/s is shown in the above images.

Images 4.31- 4.33 show a high motion in the glass section, as the dye injected towards the base of the tee colored the whole zone. The dye disappears quickly indicating fluid replacement from the branch as shown in image 4.33. Water in this zone (2D) and at this velocity (1.5 m/s) is quickly replaced by water from the mainstream flow. This results in no stagnation zones with the dead-leg at this velocity.

Image 4.34 **Image 4.35** **Image 4.36**

Figure 4. 16: Dye injection of the top of a 2D dead-leg at 1.5m/s.

Image 4.34 highlights the highly turbulent mixing conditions of the dead-leg. The dye disperses very quickly as obvious in images 4.34, 4.35, 4.36, where the dispersion of the dye at low velocity in their counterpart images 4.25, 4.26, 4.27 is slower.

At 0.5 m/s dye injected at the base of the dead-leg moved back towards the upstream wall before climbing the wall towards the top of the branch the flow pattern was similar to that found during the CFD studies (image 4.25-4.27). Mixing throughout the branch was faster than that of a 4D dead-leg and no secondary zone of flow was identified.

Dye injection near the top of the branch resulted in flow pattern highlighted in image 4.28 – 4.30. These results highlight a flowing region near the top left hand corner of the dead-leg (image 4.29). This region is not visible at higher flowrates (image 4.34). The move to a velocity of 1.5 m/s highlights the rapid mixing that takes place within a 2D dead-leg. Dye is rapidly dispersed. Image 4.31 shows the dye while is injecting to the base of the dead-leg. However the dye was injected at the base, it dispersed rapidly (images 4.32-4.33). When the dye was injected at the middle of the upstream of the dead-leg (image 4.34) is not visible indicating very high turbulence near the mouth of the branch.

A key requirement of a dead-leg system is to exchange fluid between the branch and the mainstream flow. To analyse this 0.5 m/s of dye was quickly injected into the branch of a 4D and 2D dead-leg and the time noted for the dye to fully disperse from the branch and be replaced by mainstream fluid.

Dead-Leg (1DL=50mm)	**Dye (ml)**	**Velocity (m/s)**	**Time of dispersion (sec)**
4DL	0.5	0.5	91
4DL	0.5	1.5	39
2DL	0.5	0.5	26
2DL	0.5	1.5	15

Table 4. 5: Dispersion time

Table 4.6 reveals that the mainflow velocity is inversely proportional to the time of dispersion, and the length of the dead-leg is directly proportional to the time of dispersion.

Chapter Five
Conclusion & Future Work

CHAPTER 5. CONCLUSION AND FUTURE WORK

5.1 Conclusion

This Thesis has examined high purity water systems-tee junction pipes. Analysis of extension length and bend highlights the effect of each configuration on flow within the dead-leg branch. The following conclusion can be drawn from the results discussed earlier:

1. For different mainflow velocities at varying dead-leg lengths,

- High velocity in the mainstream flow gives better flow movement in 2DL and 4DL compared with 6DL.
- At high main flow velocities, good flow movement only occurs at 2DL dead leg length.
- At low mainflow velocities, 4DL and 6DL are preferred flow movement compared with 2DL. While increasing the length extension results in better flow pattern in 6DL.
- At both high and low mainflow velocities, 4DL shows a reasonable flow velocity throughout the branch.

2. Entry length upstream of a pipe dead-leg has little effect on the flow velocity within the dead-leg branch.

3. With a bend incorporated into the system, an increase in entrance length reflects an improvement in the flow of all dead-leg branches.

4. Flow visualization studies performed confirmed CFD results for 4DL dead-leg length. However accelerated dye dispersion was observed at 2DL suggesting differences between experimental and simulated results at this dead-length.

5.2 Future Work

Some key areas in the investigation of pipe dead-leg have been highlighted by this work. However additional areas of investigation include:

1. Investigation the flow configuration in 3DL and 5DL branch.
2. Examination of the fluid exchange between the mainflow and dead-leg branch for various dead-leg lengths using accurate instruments such as Laser Doppler and PIV

3. Studying the flow motion in the dead-leg branch with different branch diameter sizes.

4. Comparison the flow configuration of fluid in the dead-leg branch between two positions, when the branch is horizontal or placed in a vertical position.

5. Investigation of a flushing time model for suitable dead-legs to ensure exchange of fluid with the branch and reduce contamination.

6. Design of an insert with the tee to encourage exchange of fluid between the mainstream and the dead-leg.

Chapter Six
List of References

CHAPTER 6. LIST OF REFERENCES

1. Elga Labwater, "The Pure Water Guide – A Practical User's Guide to Modern Water Purification Technology", p.1. (2001)

2. Fessenden, B., (1996), "A Guide to Water for the Pharmaceutical Industry – Part 1: Basic Chemical, Physical and Dynamic Concepts", Journal of Validation Technology, Vol. 1 (4). p. 30.

3. Meltzer, T.H., (1997), "Pharmaceutical Waters", *Pharmaceutical Water Systems*, Tall Oaks Publishing, Littleton USA., p.1.

4. Meltzer, T.H., (1997), "Pharmaceutical Waters", *Pharmaceutical Water Systems*, Tall Oaks Publishing, Littleton USA., p.2.

5. Elga Labwater, "The Pure Water Guide – A – A Practical User's Guide to Modern Water Purification Technology", pp. 3 – 5. (2000)

6. R. O. Consumables, (online), http://www.roconsumables.com/USP.html (Accessed 30 October 2004).

7. Martyak, J.E. "Reverse Osmosis/Deionized Water Bacterial Control at the Central Production Facility", *Microcontamination* 6(1), pp. 34-37, 55 (1988).

8. USP National Formulary – The Official Compendia of Standards (27th Revision).

9. Meltzer, T.H., (1997), "Pharmaceutical Waters", *Pharmaceutical Water Systems*, Tall Oaks Publishing, Littleton USA., p. 657.

10. Celeste, "Operation of the FDA: A Summary", Chapter in *"Filtration in the Pharmaceutical Industry"*, 2nd Edition, New York.

11. Food and Drug Administration – Code of Federal Regulations.

12. Nelson Laboratories, (online), http://www.nelsonlabs.com/chemistry/uspwater.html (Accessed 12 November 2004).

13. Pharmaceutical Engineering Guides for New and Renovated Facilities Volume 4 – Water and Steam Systems.

14. Goozner, R.,; Comstock, D. "Field for the Reduction of SDI by Pre-RO Filters",*Ultrapure Water* 7(2),pp. 20-30 (1990).

15. Filters, Water & Instrumentation, Inc, (online), http://www.filterswater.com/svssch.html, (Accessed 4 November 2004).

16. Muraca, PW. (1990), "Disinfection of Water Distribution Systems for Legionella: Review of Application Procedure and Methodologies", *Infection Control and Hospital Epidemiology*, Vol. 11 (2), pp. 79 – 88.

17. Cruver, J.E. "Water Disinfection-Comparison of Clorine. Ozone, UV light, and Membrane Filteration", Eighth Annual Membrane Technology/Planning Conference & First High-Tech Separations Symposium, Newton, MA (October 15-17, 1990).

18. Chapman, K.G.; Alegnani, W. C.; Heinze, G.E.; Flemming, C.W.: Kochling, J.; Croll, D.B.; Fitch, M.W.; Kladko, M.; Lehman, W.J.; Smith, D.C.; Adair, F.W.; Amos, R.L.; Enzinger, R.M.; Soli, T.E."Protection of Water Treatment Systems-Part IIB-Potential Solutions", Pharmaceutical Technology 7(9), pp. 38-49 (1983b).

19. HydroFlo Technologies, Inc., (online), http://www.hydroflotech.com/Sand%20Filter.htm, (Accessed 3 December 2004).

20. Windsor System Saver Water Softeners, (online), http://www.systemsaver.com/windsor-website/product-list/product-list/specifications/service.html, (Accessed 26 November 2004).

21. Weitnauer, A.K., :A Practical Approach to Controlling Growth in USP Purified Water", *Ultrapure Water* 13(3), pp. 26-30 (1996).

22. Watersolve International, (online), http://www.watersolve.com/USP%20technical.html, (Accessed 9 December 2004).

23. Anderson, R.L. "Ion-Exchange Separations", Section 1-12, pp. 1-359 to 1-414, in Handbook of Separation Techniques for Chemical Engineers, P.W> Schweitzer, ed., McGraw-Hill Book Company, New York (1979).

24. La Habra Welding Inc., (online), http://www.lhwinc.com/images/ion%20exchange.jpg , (Accessed 16 December 2005).

25. Havapure Water Systems, (online), http://www.havapure.com/clean.html, (Accessed 10 February 2005).

26. Weitnauer, A.K. (1996), "Two – Pass RO for Pharmaceutical Grade Purified Water". *Ultrapure Water*, Vol. 13 (2), PP. 42 – 45.

27. PHOENIX Process Equipment Co, (online), http://www.dewater.com/images/eq/revosmosis- lg.jpg, (Accessed 10 February 2005).

28. Bukay, M., "Dead Legs: A Widespread Threat to DI Water Systems", *Ultrapure Water* 4(3), pp. 66-70 (1987).

29. Michigan State University, (online), http://web1.msue.msu.edu/msue/imp/mod02/visuals/wq22v1.jpg, (Accessed 17 February 2005).

30. Saari, R. (1977), "Production of Pryogen-Free Distilled Water for Pharmaceutical Purposes", *Bulletin of the Parenteral Drug Association*, Vol. 31 (5), pp. 248 – 253.

31. Nebel, C.; Nebel, T. "The Process Water Sterilant", Pharmaceutical Manufacturing 1(2), pp. 16-22 (1984).

32. GE Water Technologies, (online), http://www.gewater.com/library/tp/1104_Disinfection_of.Jsp, (Accessed 16 February 2005).

33. Edstrom Industries Inc., (online), http://www.edstrom.com/Resources.efm?doc_id=149 (Accessed 19 February 2005).

34. Characklis, W.G. (1990), *Biofilms*, John Wiley & Sons, Inc., New York.

35. InPharm Internet Services Ltd, (online), http://www.inpharm.com/static/intelligence/pdf/MAG_146222.pdf (Accessed 24 February 2005).

36. Edstrom Industries Inc., (online), http://www.edstrom.com/Resources.cfm?doc_id=143, (Accessed 19 February 2005).

37. Edstrom Industries Inc., (online), http://www.edstrom.com/Resources.efm?doc_id=147 , (Accessed 19 February 2005).

38. Pittner, GA, Bertler, G, (1998). "Point of Use Contamination Control of Ultrapure Water Systems", Ultrapure Water, Vol. 5 (4), pp. 16-23.

39. McCoy, WF,; Costerton, JW., (1982). "Fouling Biofilm Development in Tubular Flow Systems", *Developments in Industrial Microbiology*, Vol. 23, pp. 551-558.

40. Corcoran B.G. and Foley G., (1996). "Fouling of Plate Heat Exchangers by Cheese Whey Solutions", *MSc thesis*, Dublin City University, Ireland.

41. Mittelman, MW (1985). "Biological Fouling of Purified Water Systems, Pat 1", *Microcontamination*, Vol. 3 (10), pp. 51-55.

42. Patterson, M K, Husted, GR, Rutkowshi A, (1991). "Isolation, Identification and Microscopic Properties of Biofilms in High Purity Water Distribution Systems", *Ultrapure Water*, Vol. 8 (4), pp. 18-24.

43. Corcoran, B.G. (2002), "Investigation of Turbulent Flow in Pharmaceutical Pipe Tee-Junctions", Proceedings of the 1st International Conference on Heat Transfer, Fluid Mechanics and Thermodynamics, Kruger Park, South Africa, 8-10th April

44. Launder B.E., (1989). "Second-Moment Closure and Its Use in Modelling Turbulent Industrial Flows", *International Journal for Numerical Methods in Fluids*, Vol. 9, pp. 963-985.

45. Daly B.J. and Harlow F.H., (1970) "Transport Equations in Turbulence", *Phys. Fluids*, Vol. 13, pp. 2634-2649

46. Ferzieger J.L. and Peric . M., (1996). "Computational methods for Fluid Dynamics", Springer-Verlag, Heidelberg.

47. Launder B. E. and Spalding. D.B., (1974) "The Numerical Computation of Turbulent Flows", Computer Methods in Applied Mechanics and Engineering, Vol. 3, pp. 269-289.

48. Speziale, CG (1991). "Analytical Methods for the Development of Reynolds-Stress Closures in Turbulence", *Annu. Rev. Fluid Mech.*, Vol. 23, pp. 107-157.

49. Reynolds, WC, (1987). "Fundamentals of turbulence for turbulence modelling and simulation", *Lecture Notes for Von Karman Institute Agard* Report No. 755.

50. Abbott, M.B. and Basco, D.R., (1989). "Computational Fluid Dynamics – An Introduction for Engineers", Longman Scientific and Technical, Harlow, England.

51. Shih, TH, Liou, W, W Shabbir, A, and Shu, J. (1995). " A new k-Eddy-Viscosity Model for high Reynolds Number Turbulent Flows – Model Development and Validation", *Computers Fluids*, Vol. 24 (3), pp. 227-238.

52. Bradshaw, P., Cebeci, T. and Whitelaw, J.H., (1981). "Engineering Calculation Methods for Turbulent Flow", *Academic Press, London.*

53. Patel, VC, Rodi W, and Scheuerer, G (1985). "Turbulent Models for Near-Wall and Low Reynolds Number Flows", *A Review AIAA J.*, Vol. 23 (9), pp. 1308- 1319.

54. Launder, B.E., and Spalding, D.B, (1974) "Numerical Computation of Turbulent Flows", Computer Methods in Applied Mechanics and Engineering, Vol. 3, pp. 269-289.

55. Fluent Inc., [online], www.fluentusers.com (accesed 10 Jan 2005).

56. Versteeg, H. K. and Malalasekera, W., (1995), "Computational Fluid Dynamics – An Introduction to", Pearson, England.

57. FLUENT v6.1, *Help Guide.*